Introduction to the 2026 Summer fMRI Course
&
A Short History of Neuroimaging and fMRI

Peter A. Bandettini, Ph.D.

SFIM

Section on Functional Imaging Methods
Functional MRI Core Facility
Center for Multimodal Neuroimaging

National Institute of Mental Health

FMRIF

Lecture #	Day	Date	Time	Location	Topic	Speaker
1	Thursday	June 25	1:00 to 2:00 PM	FAES Room 3	Introduction to the Course & Short History of Neuroimaging and fMRI	Peter Bandettini
2	Tuesday	June 30	1:00 to 2:00 PM	FAES Room 4	The basics of fMRI: fMRI contrast, processing, hardware, applications	Peter Bandettini
3	Thursday	July 2	1:00 to 2:00 PM	FAES Room 4	The basics of MRI: Image contrast, reconstruction, and hardware	Vinai Roopchansingh
4	Tuesday	July 7	1:00 to 2:00 PM	FAES Room 4	The parts of an fMRI study from design to interpretation	Dan Handwerker
5	Thursday	July 9	1:00 to 2:00 PM	FAES Room 5	Multi-echo fMRI	Dan Handwerker
6	Tuesday	July 14	1:00 to 2:00 PM	FAES Room 4	Real time fMRI and neurofeedback	Javier Gonzalez-Castillo
7	Thursday	July 16	1:00 to 2:00 PM	FAES Room 4	Resting state fMRI	Javier Gonzalez-Castillo
8	Tuesday	July 21	1:00 to 2:00 PM	FAES Room 3	fMRI Connectivity and advanced processing strategies	Josh Faskowitz
9	Thursday	July 23	1:00 to 2:00 PM	FAES Room 4	AFNI, fMRI processing and quality control	Paul Taylor
10	Tuesday	July 28	1:00 to 2:00 PM	FAES Room 4	fMRI QA	Dan Handwerker
11	Thursday	July 30	1:00 to 2:00 PM	FAES Room 4	The use of peripheral measures in fMRI	Burak Akin
12	Tuesday	August 4	1:00 to 2:00 PM	FAES Room 4	Combining psychophysical measures and fMRI	Sharif Kronemer
13	Thursday	August 6	1:00 to 2:00 PM	FAES Room 4	Deep sampling and Individual Differences in fMRI	Tyler Morgan + Catherine Walsh
14	Tuesday	August 11	1:00 to 2:00 PM	NMR Conf. Room	EEG and simultaneous EEG and fMRI	Pete Molfese
15	Thursday	August 13	1:00 to 2:00 PM	FAES Room 7	Physiology in the time series signal	Burak Akin
16	Tuesday	August 18	1:00 to 2:00 PM	FAES Room 4	fMRI and MRI at 7 Tesla	Tyler Morgan
17	Thursday	August 20	1:00 to 2:00 PM	FAES Room 4	Layer and Column fMRI	Tyler Morgan
18	Tuesday	August 25	1:00 to 2:00 PM	FAES Room 1	Challenges, Mysteries, and Controversies of fMRI	Peter Bandettini

A Short History of Neuroimaging …and fMRI

Pre-imaging: Lesion Mapping

1848 **Phineas P. Gage…”**Became fitful, irreverent, impulsive, and prone to ‘the grossest profanity,’ with little respect for social norms, in contrast to his earlier reputation as a responsible, reliable foreman.

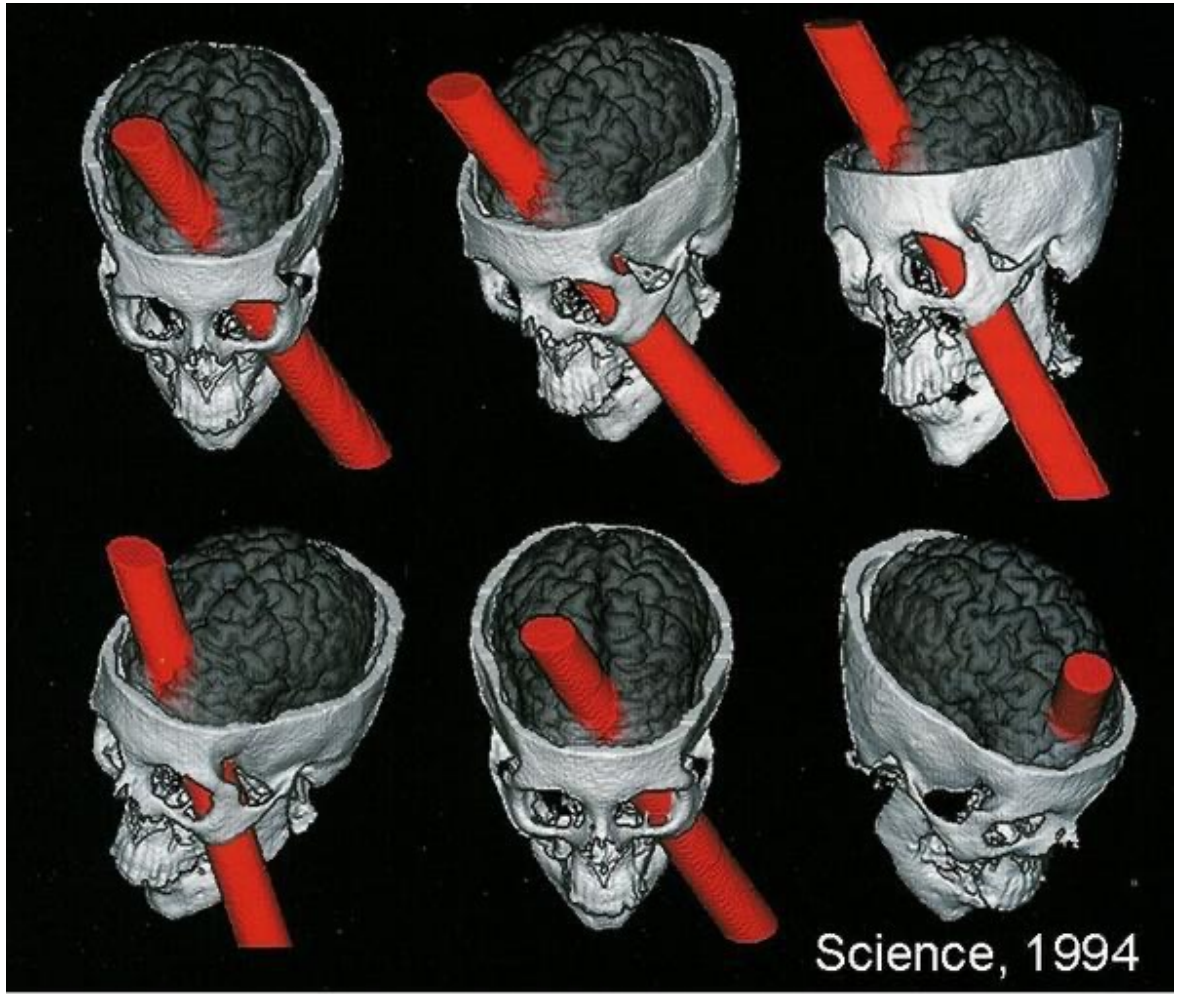

Lesion Mapping

1861 Paul Broca:

His patient could only produce the sound "tan" but understood words.

1874: Carl Wernicke

His patients could not understand or produce meaningful speech but could articulate words.

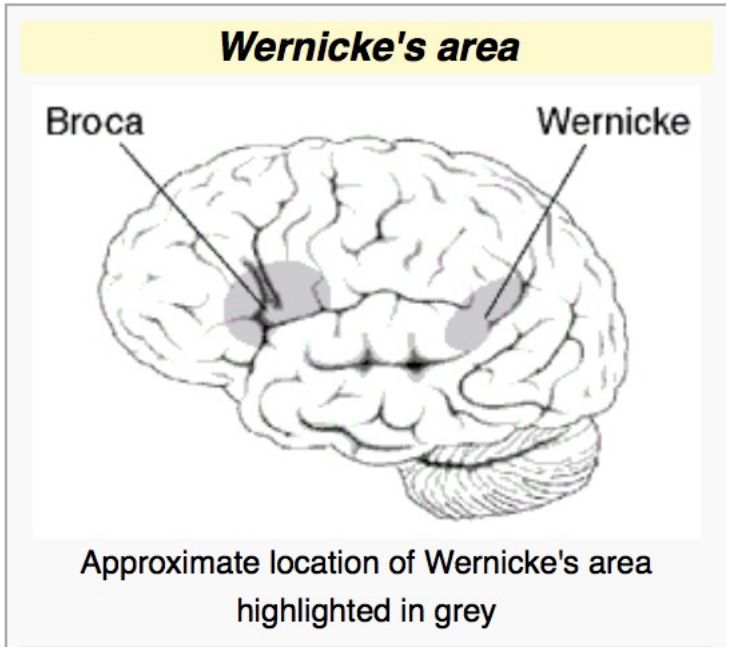

PHINEAS GAGE

- Frontal Aslant Tract
- Uncinate
- Frontal Superior Longitudinal
- Frontal Inferior Longitudinal
- Frontal Orbito Polar

LOUIS VICTOR LEBORGNE

- Arcuate
- Superior longitudinal fasc. III
- Superior longitudinal fasc. II
- Frontal Aslant Tract
- Frontal Inferior Longitudinal
- Frontal Orbito Polar

HENRY MOLAISON

- Uncinate
- Fornix
- Anterior commissure
- Cingulum

M. Thiebaut de Schotten, F. Dell'Acqua, P. Ratiu, A. Leslie, H. Howells, E. Cabanis, M. T. Iba-Zizen, O. Plaisant, A. Simmons, N. F. Dronkers, S. Corkin, M. Catani, From Phineas Gage and Monsieur Leborgne to H.M.: Revisiting Disconnection Syndromes, *Cerebral Cortex*, Volume 25, Issue 12, December 2015, Pages 4812–4827, https://doi.org/10.1093/cercor/bhv173

1880s – First experimental neuroimaging (Angelo Mosso) Development of the “human circulation balance,” that inferred changes in cerebral blood flow during mental activity - the first experimental neuroimaging technique.

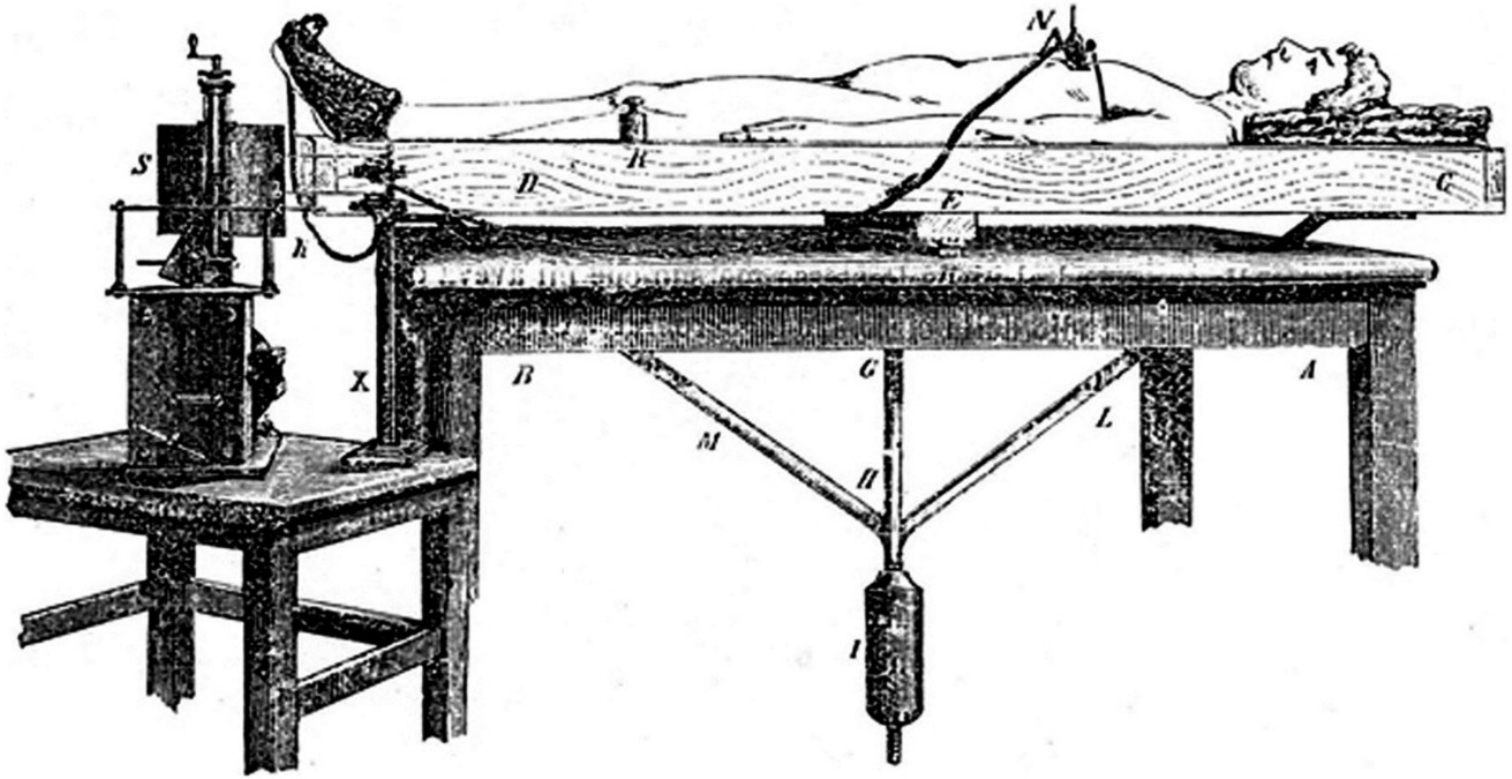

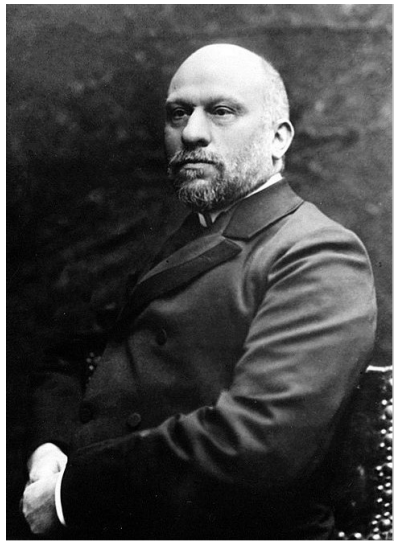

ON THE REGULATION OF THE BLOOD-SUPPLY OF THE BRAIN.

By C. S. ROY, M.D., F.R.S., *Professor of Pathology, University of Cambridge,* and C. S. SHERRINGTON, M.B., M.A., *Fellow of Gonville and Caius College. Lecturer on Physiology in the School of St Thomas's Hospital, London.*

Plates II., III. and IV.

From the Cambridge Pathological Laboratory.

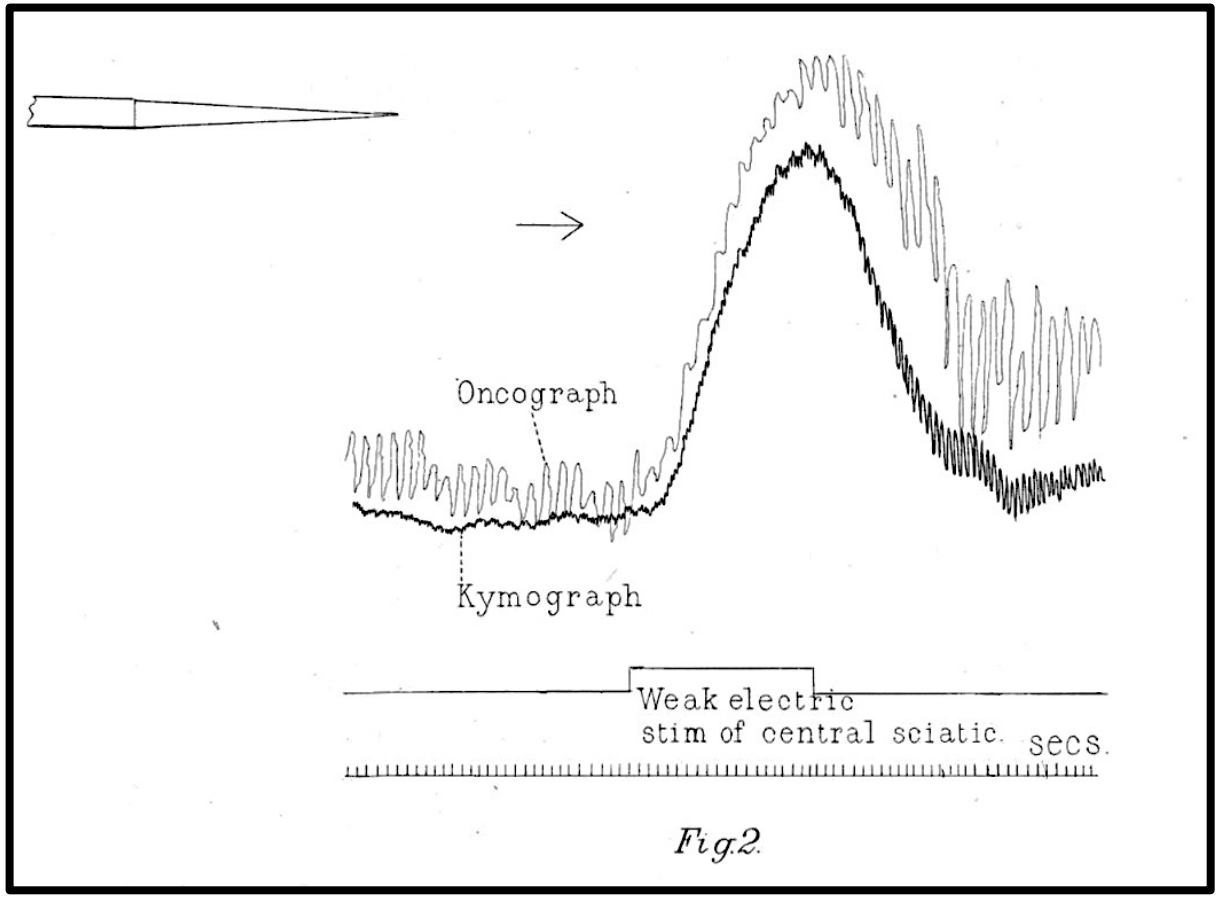

Fig. 2.

J. Physiol. **1890** Jan;11(1-2):85-158.17.
doi: 10.1113/jphysiol.1890.sp000321.

...and some quackery: **1905 - Phrenology**

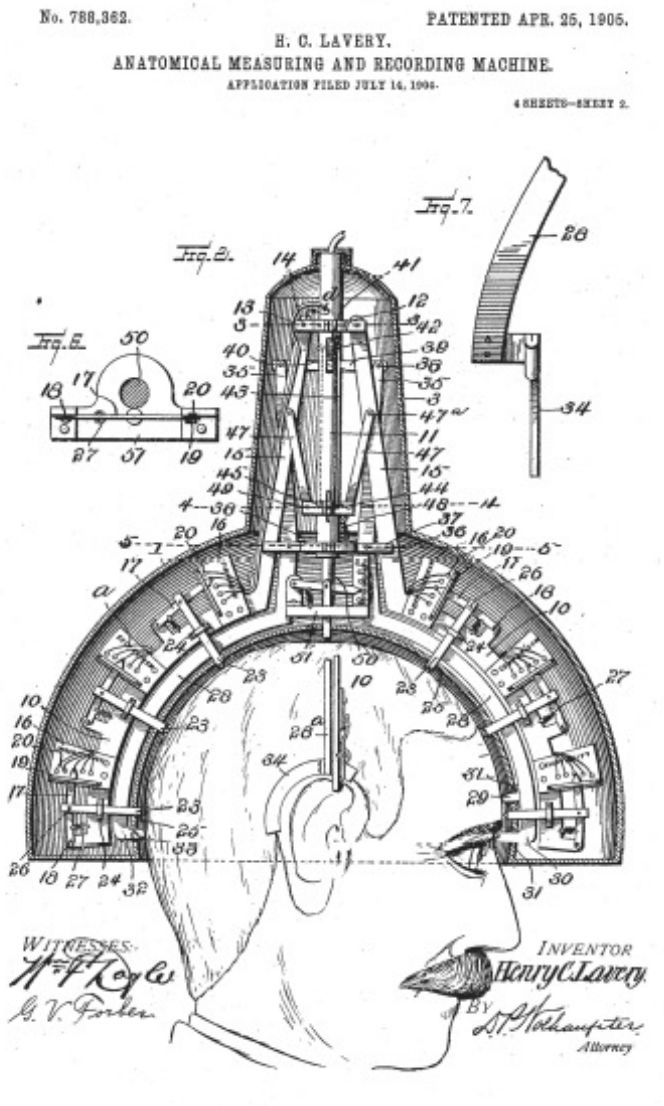
No. 788,362. PATENTED APR. 25, 1905.

H. C. LAVERY.

ANATOMICAL MEASURING AND RECORDING MACHINE.

APPLICATION FILED JULY 14, 1904.

4 SHEETS—SHEET 2.

Fig. 7.

Fig. 2.

Fig. 5.

WITNESSES:

INVENTOR

Henry C. Lavery

By

Attorney

* Not FDA-Approved

1895 – Discovery of X-rays (Wilhelm Röntgen) Röntgen's radiograph enabled visualization of internal structures, including the skull.

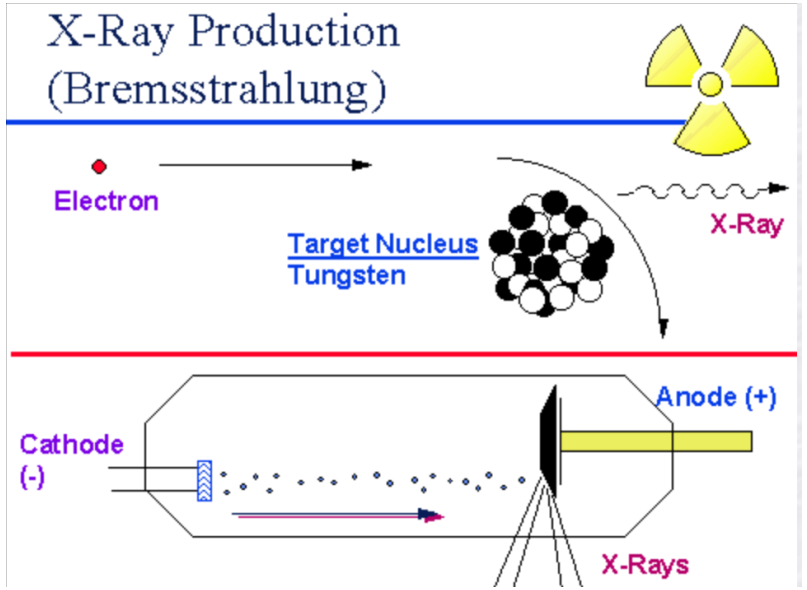

Crooke's tube

Early 1900's: Walter Dandy - Pneumoencephalography or Air Ventriculography

CSF drained from the brain to enhance contrast in x-rays

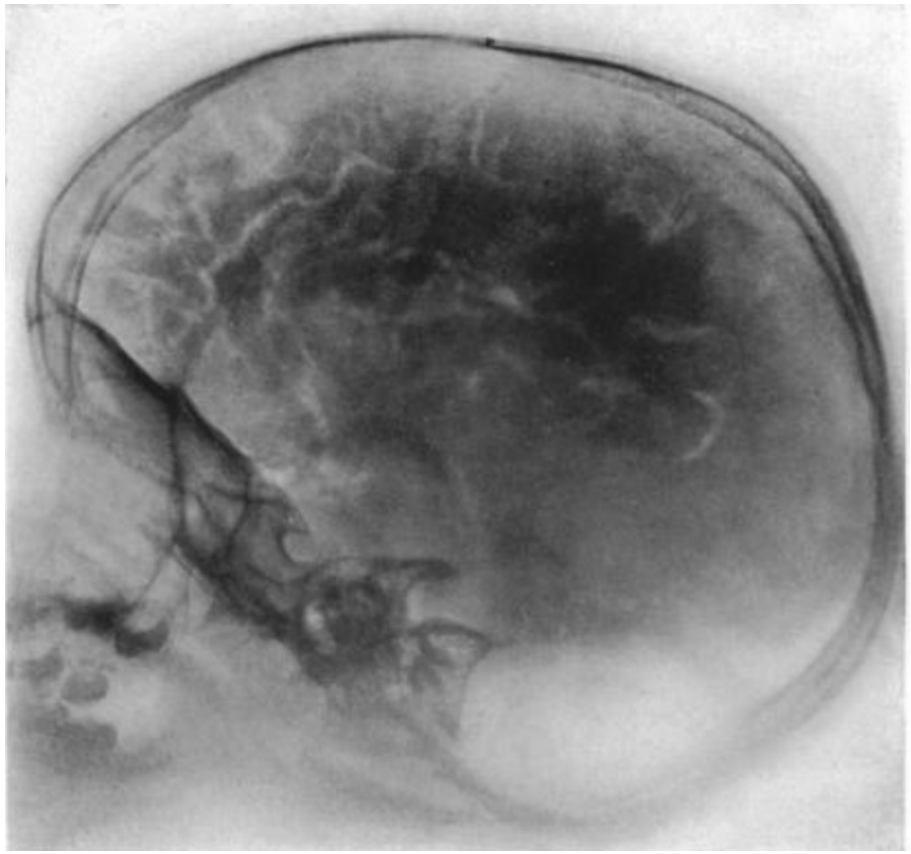

1927: Antonio Egas Moniz – first Arteriogram

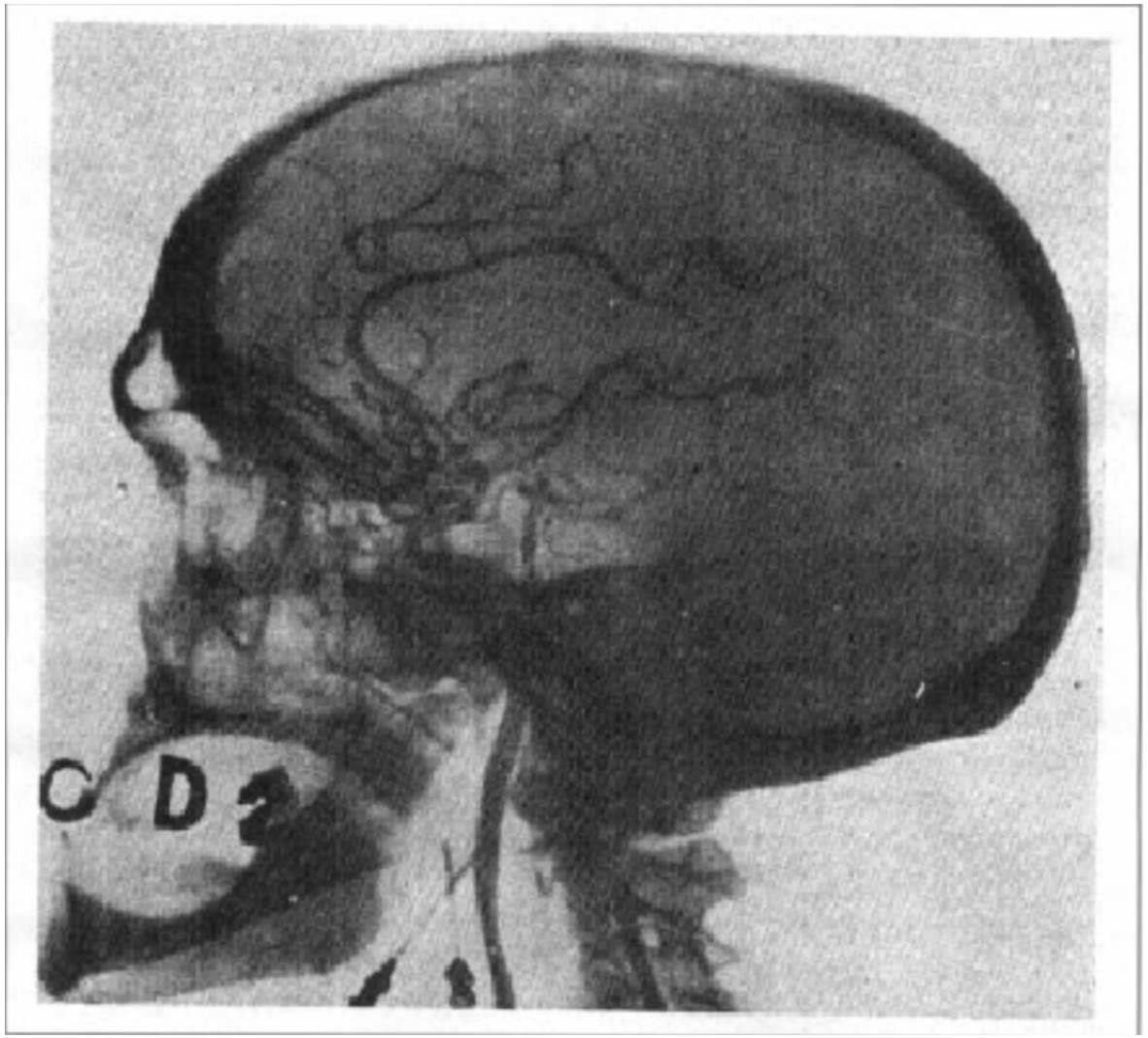

First used strontium and lithium bromide injections but those were toxic (one patient died). He switched to 25% sodium iodide. Today, iodine-based radiopaque contrast agents are used.

1924: Hans Berger– first Electroencephalogram (EEG)

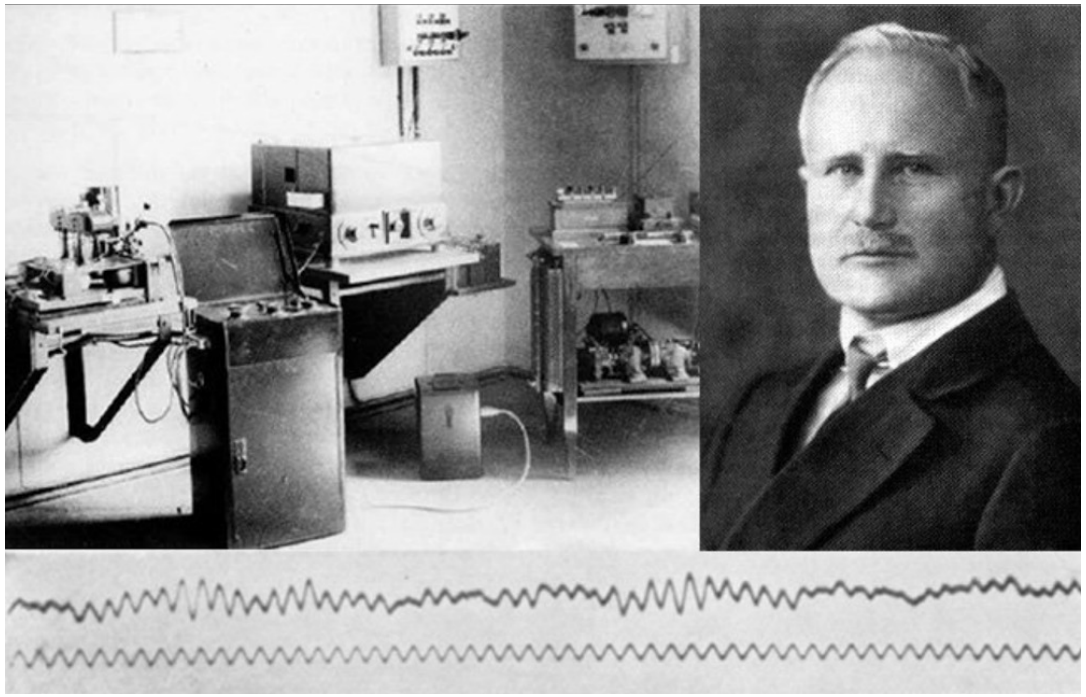

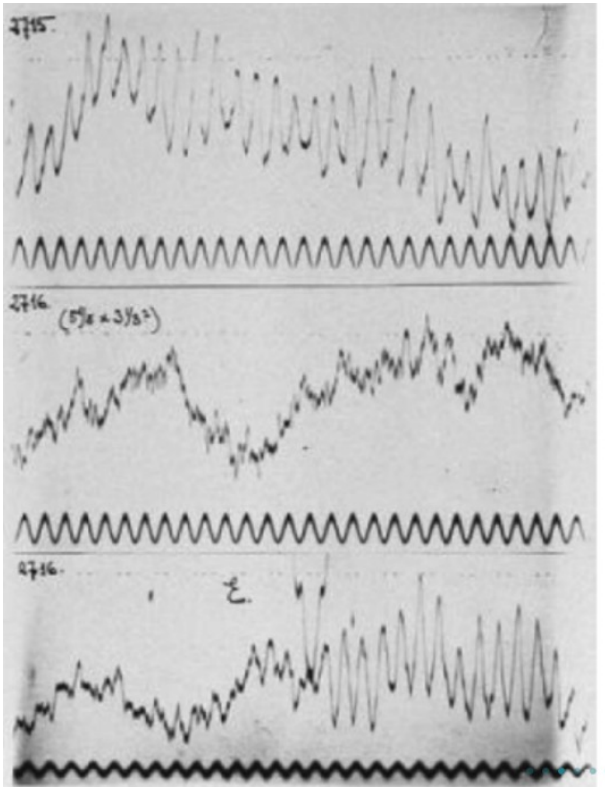

1950s – Conceptual foundations of PET and SPECT (William Sweet, David Kuhl) Work on radionuclide imaging and tomographic reconstruction laid the basis for Single Photon Emission Computed Tomography (SPECT) and Positron Emission Tomography (PET) as functional brain imaging tools.

- Framed imaging as tomographic mapping of function
- Formalized emission computed tomography as a quantitative technique using rotating detectors and reconstruction algorithms

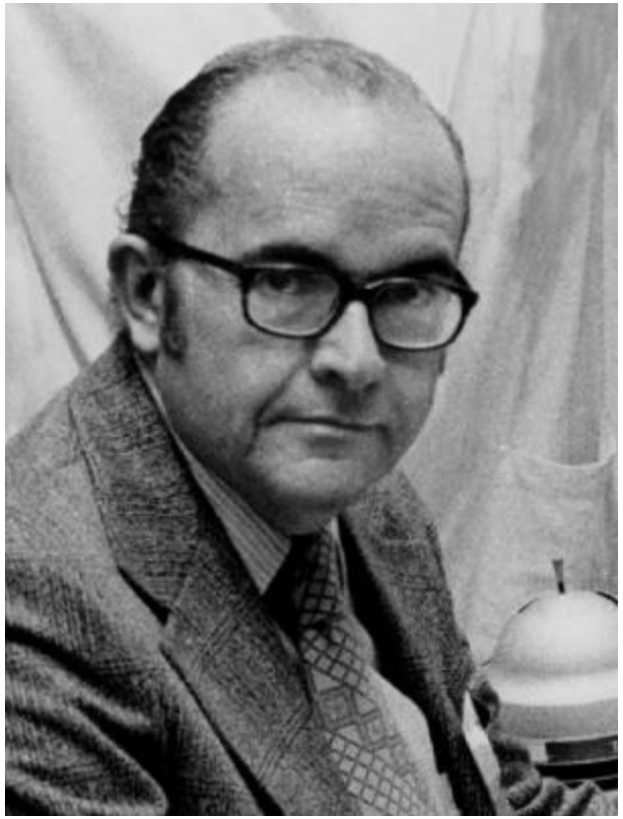

1960, William Oldendorf patented an electronically based device that could capture image slices continuously through a solid object – Computed Tomography

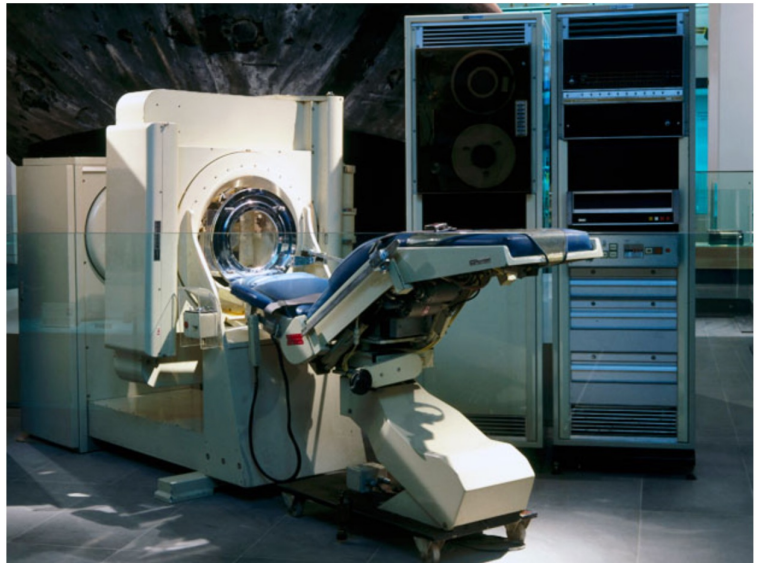

1971: Godfrey Hounsfield implemented the first CT scanner

Godfrey Hounsfield received the 1979 Nobel Prize in Medicine for his work in the development of computer assisted tomography (CAT) scanning.

Xenon-133 inhalation: developed in 1960's

Lassen, Ingval, Skinhoj, Scientific American, 239 (4): 50-59, 1978

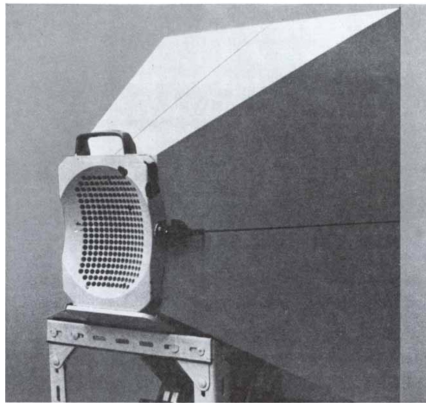

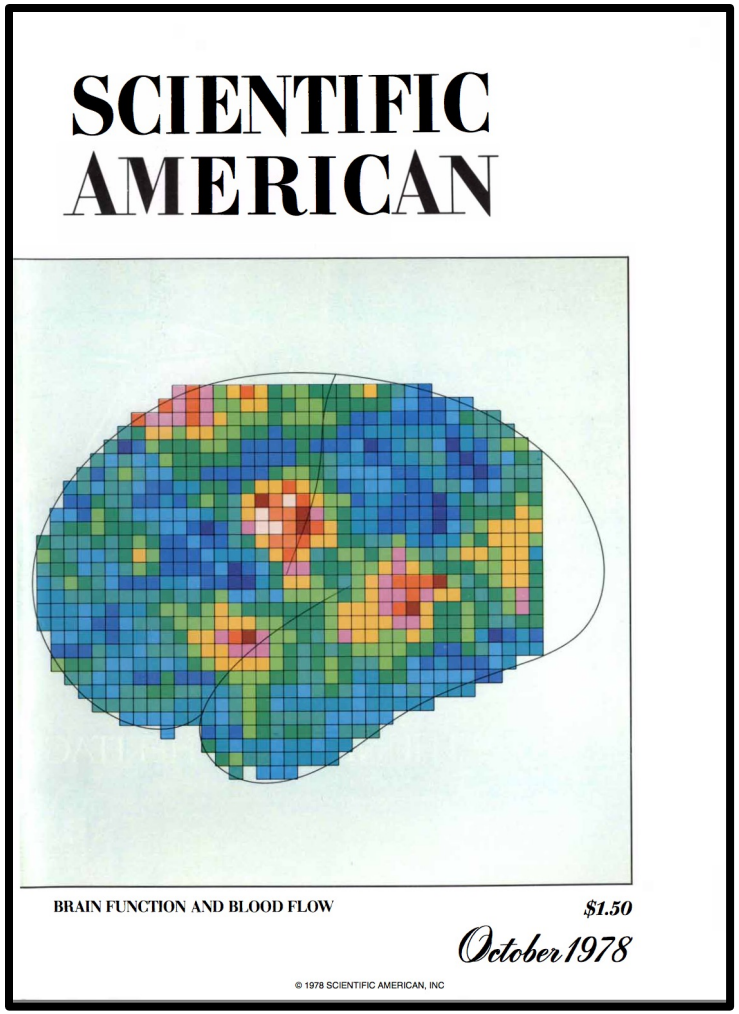

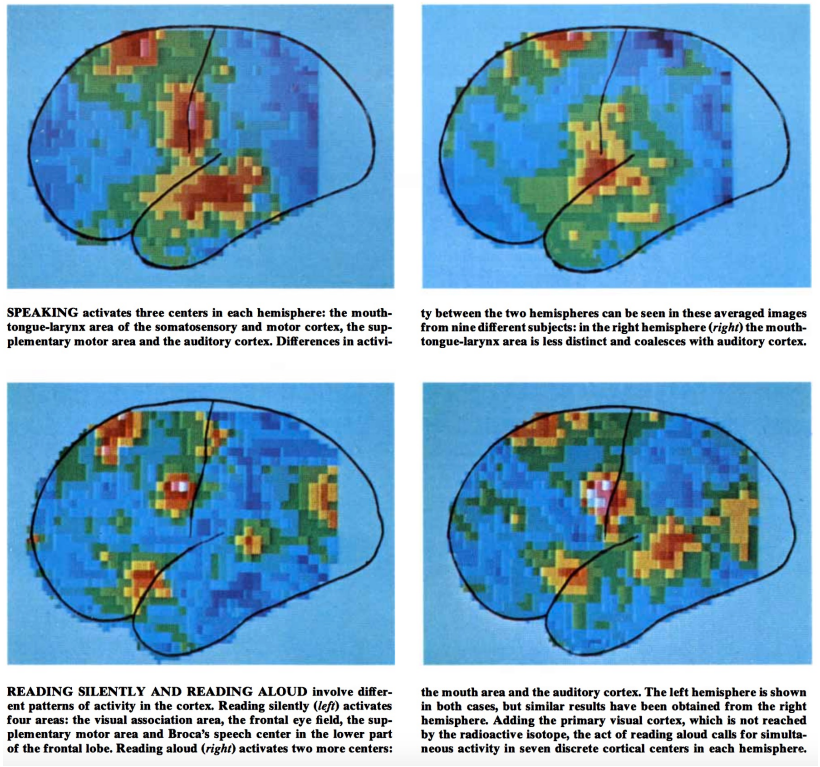

SPEAKING activates three centers in each hemisphere: the mouth-tongue-larynx area of the somatosensory and motor cortex, the supplementary motor area and the auditory cortex. Differences in activity between the two hemispheres can be seen in these averaged images from nine different subjects: in the right hemisphere (*right*) the mouth-tongue-larynx area is less distinct and coalesces with auditory cortex.

READING SILENTLY AND READING ALOUD involve different patterns of activity in the cortex. Reading silently (*left*) activates four areas: the visual association area, the frontal eye field, the supplementary motor area and Broca's speech center in the lower part of the frontal lobe. Reading aloud (*right*) activates two more centers: the mouth area and the auditory cortex. The left hemisphere is shown in both cases, but similar results have been obtained from the right hemisphere. Adding the primary visual cortex, which is not reached by the radioactive isotope, the act of reading aloud calls for simultaneous activity in seven discrete cortical centers in each hemisphere.

1950s – David Cohen. The first MEG. Initially a copper induction coil was the detector. After James Zimmerman developed SQUID magnetometers, Cohen built a single-channel SQUID MEG system in the 1970's.

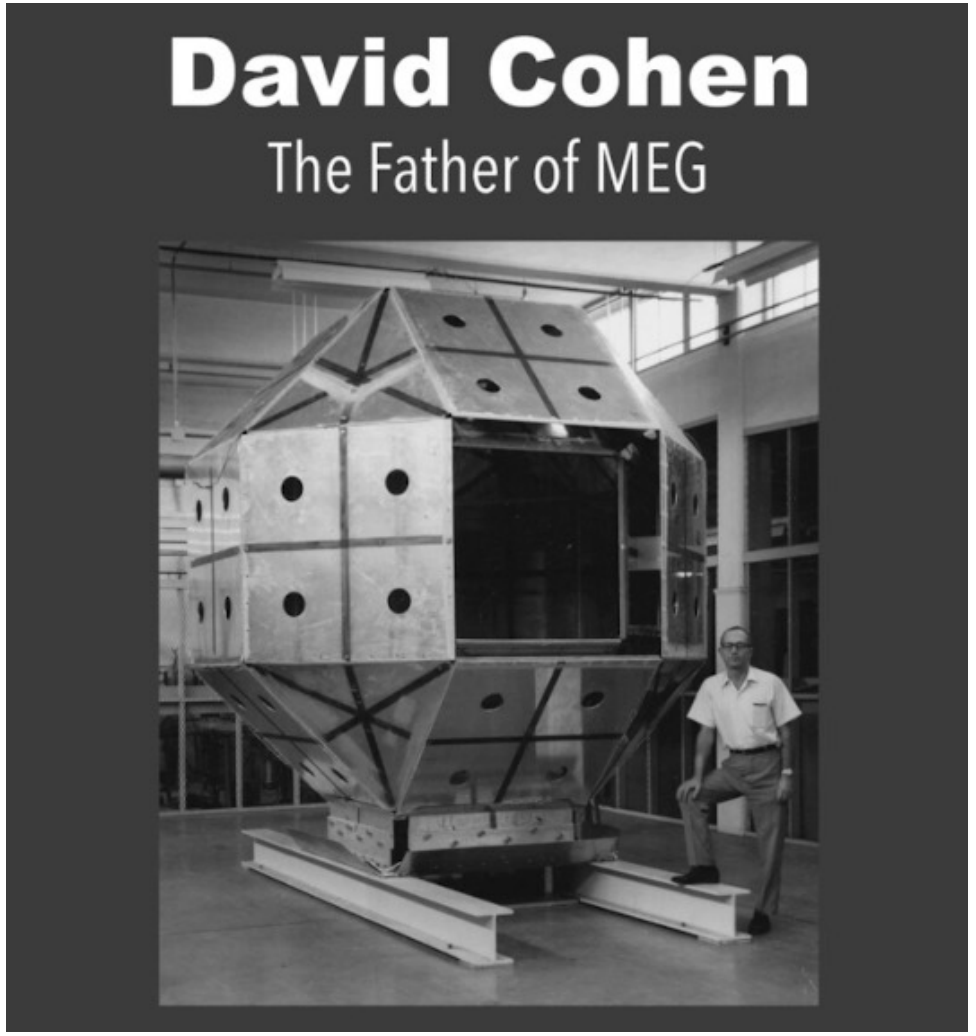

Magnetoencephalography (MEG)

Electroencephalography (EEG)

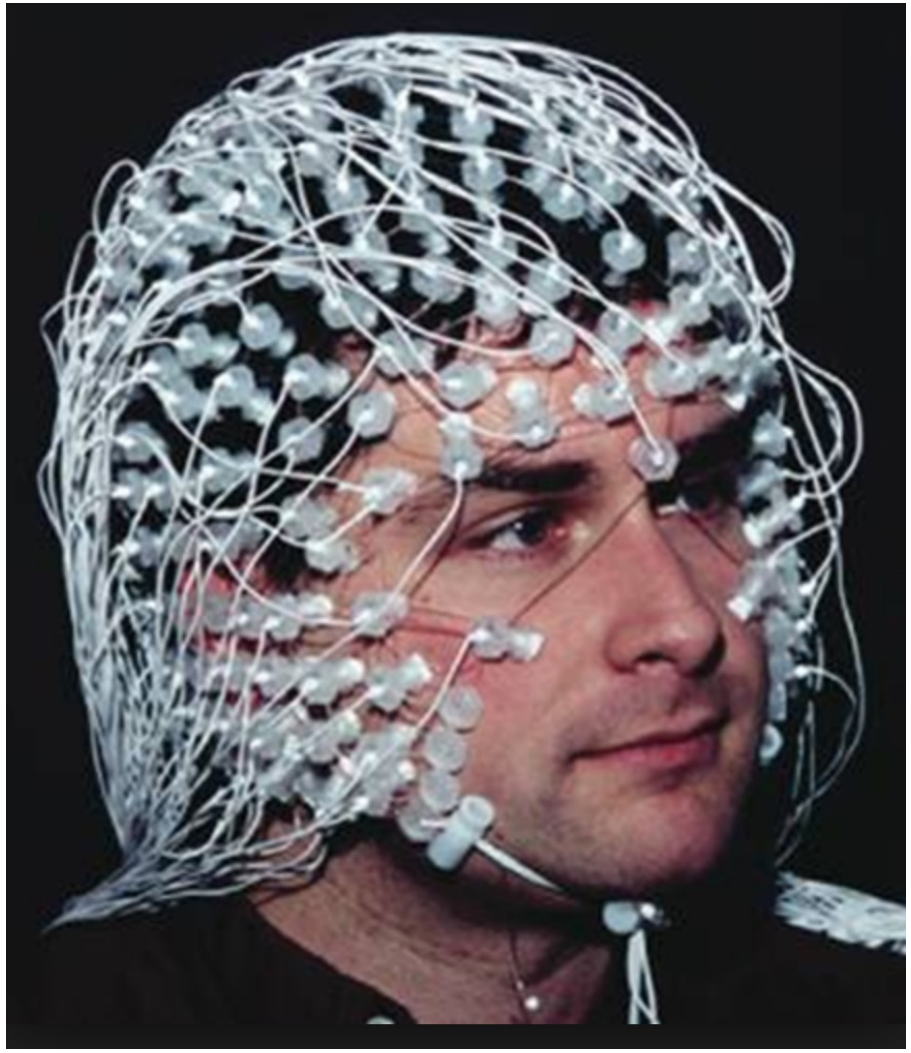

Optically Pumped Magnetometer (OPM) MEG

2006 – first demonstration
2010, 2012 –independent demonstrations

OPMs changes in magnetic field cause measurable changes in the quantum state and optical properties of a large ensemble of atoms, which can be read out with very high precision.

- In an OPM, a laser optically pumps an alkali vapor (such as rubidium or cesium) so that spins are aligned in a macroscopic spin polarization.
- These polarized spins precess at the Larmor frequency, - proportional to the magnetic field: if the field changes slightly, the precession frequency or orientation shifts.
- Changes in the magnetic field alter the spin precession and hence the optical signal.
- Modern OPMs can reach sensitivities in the Femtotesla

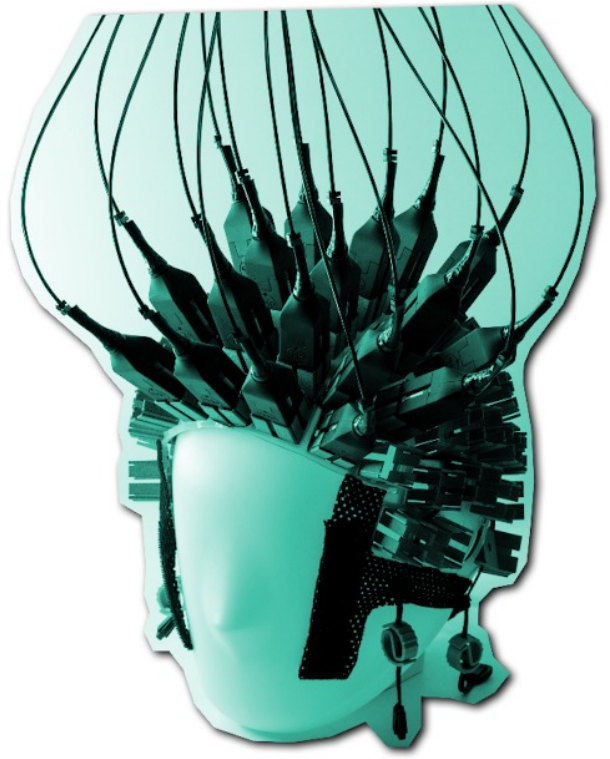

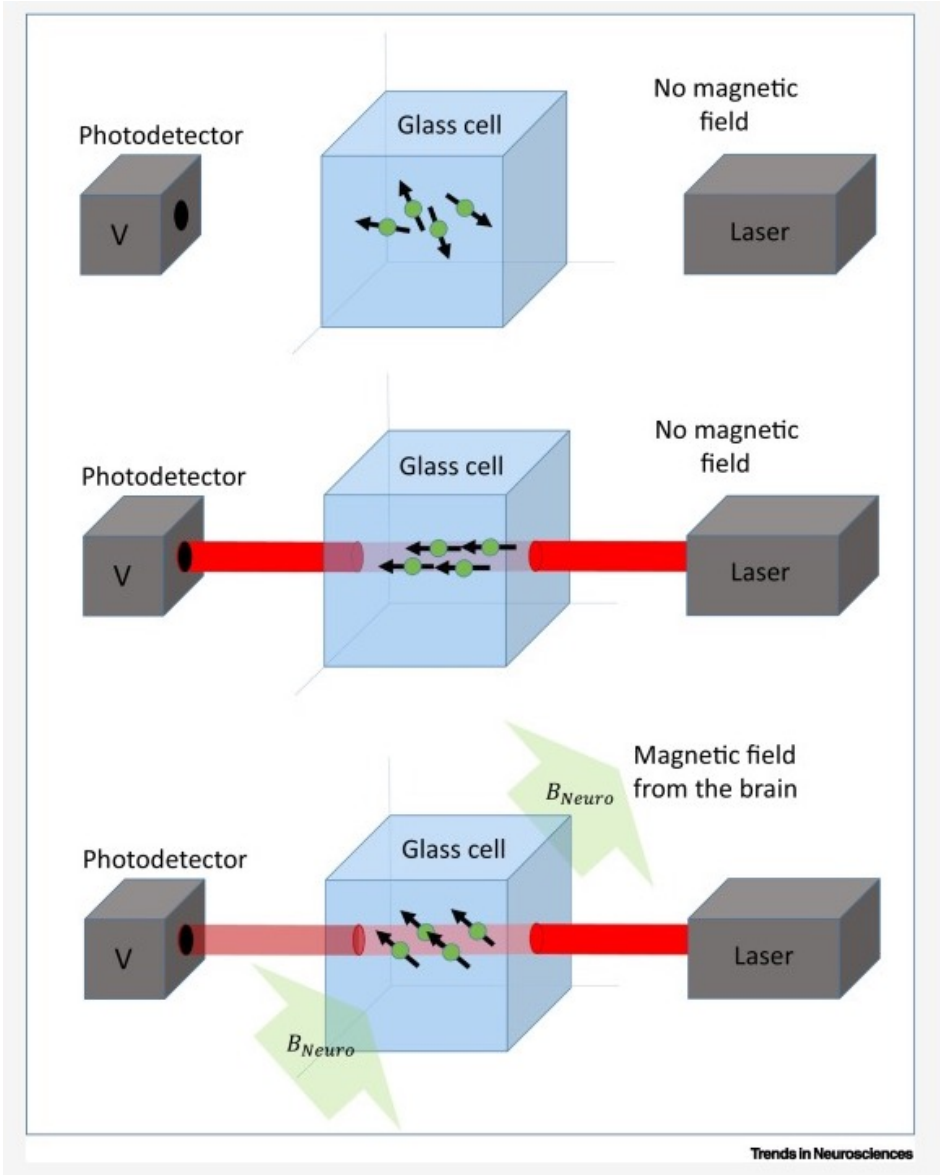

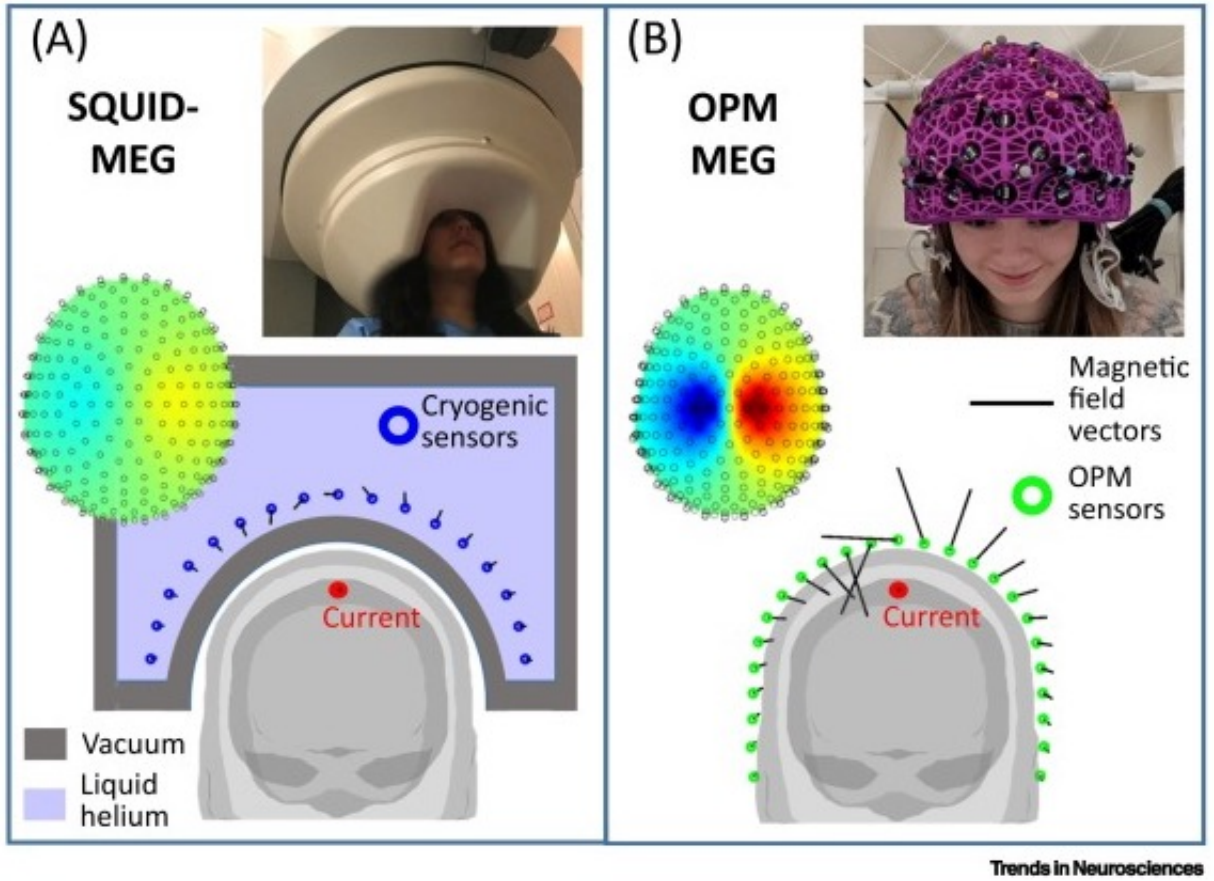

Matthew J. Brookes, James Leggett, Molly Rea, Ryan M. Hill, Niall Holmes, Elena Boto, Richard Bowtell, Magnetoencephalography with optically pumped magnetometers (OPM-MEG): the next generation of functional neuroimaging,
Trends in Neurosciences, Volume 45, Issue 8, 2022, Pages 621-634, https://doi.org/10.1016/j.tins.2022.05.008.

1950's – Erwin Hahn. Nuclear Magnetic Resonance

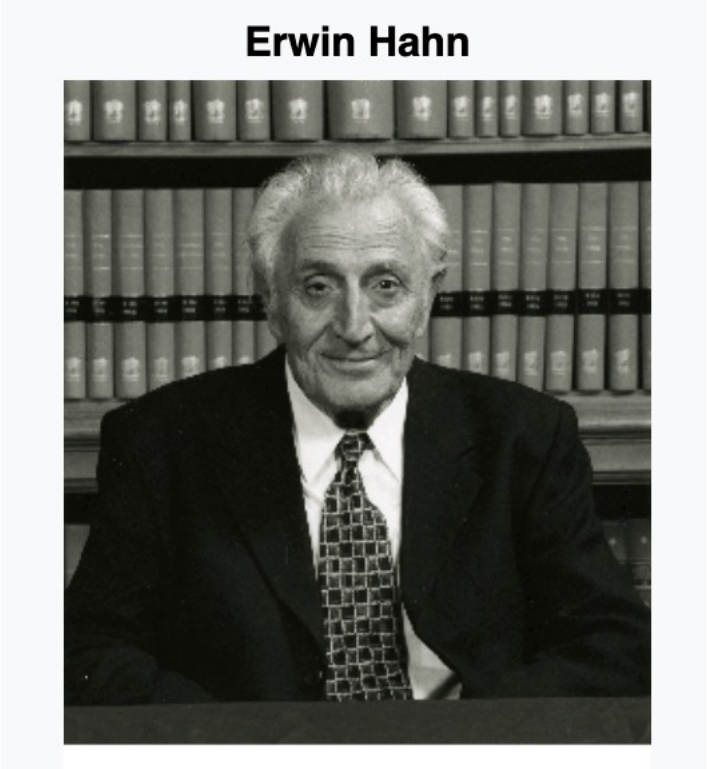

1950: Hahn discovered and theoretically explained the "spin-echo" and related pulsed NMR effects.

PHYSICAL REVIEW VOLUME 80, NUMBER 4 NOVEMBER 15, 1950

Spin Echoes*†

E. L. HAHN‡
Physics Department, University of Illinois, Urbana, Illinois
(Received May 22, 1950)

Intense radiofrequency power in the form of pulses is applied to an ensemble of spins in a liquid placed in a large static magnetic field H_0. The frequency of the pulsed r-f power satisfies the condition for nuclear magnetic resonance, and the pulses last for times which are short compared with the time in which the nutating macroscopic magnetic moment of the entire spin ensemble can decay. After removal of the pulses a non-equilibrium configuration of isochromatic macroscopic moments remains in which the moment vectors precess freely. Each moment vector has a magnitude at a given precession frequency which is determined by the distribution of Larmor frequencies imposed upon the ensemble by inhomogeneities in H_0. At times determined by pulse sequences applied in the past the constructive interference of these moment vectors gives rise to observable spontaneous nuclear induction signals. The properties and underlying principles of these spin echo signals are discussed with use of the Bloch theory. Relaxation times are measured directly and accurately from the measurement of echo amplitudes. An analysis includes the effect on relaxation measurements of the self-diffusion of liquid molecules which contain resonant nuclei. Preliminary studies are made of several effects associated with spin echoes, including the observed shifts in magnetic resonance frequency of spins due to magnetic shielding of nuclei contained in molecules.

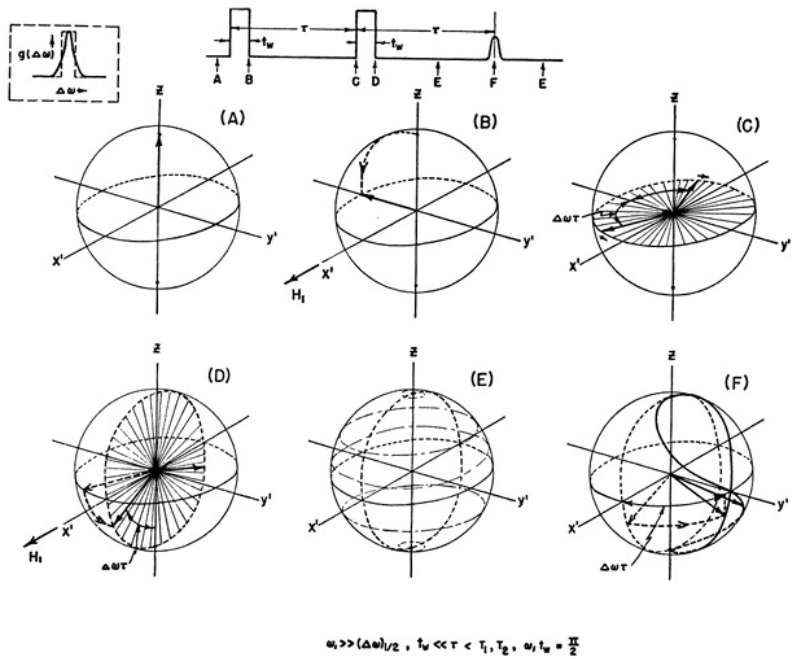

$\omega_1 >> (\Delta\omega)_{1/2}$, $t_w \ll \tau < T_1, T_2$, $\omega_1 t_w = \frac{\pi}{2}$

FIG. 1. For the pulse condition $\omega_1 t_w = \pi/2$, the formation of the eight-ball echo pattern is shown in the coordinate system rotating at angular frequency ω. The moment vector monochromats are allowed to ravel completely in a time $\tau \gg 1/(\Delta\omega)_{\frac{1}{2}}$ before the second pulse is applied. The echo gives maximum available amplitude at $\omega_1 t_w = 2\pi/3$.

1973 –Paul Lauterbur and Peter Mansfield: Magnetic Resonance Imaging

Sir Peter Mansfield and Paul Lauterbur, Winners of the Nobel Prize for Medicine, 2003

Lauterbur – spatial encoding with magnetic field gradients. ”zeugmatography”

Mansfield – formalism for gradient implementation, phase and frequency encoding, slice selection & conceived Echo Planar Imaging (1977) concept before it was possible.

Lauterbur's Contribution: Projectional NMR Tomography

Paul Lauterbur (1909-2007), a chemist working at the State University of New York at Stony Brook, published the first true MR image in *Nature* in March, 1973. His experimental setup involved two 1-mm-diameter tubes filled with water placed in an 1.4T magnet. Applying magnetic field gradients rotated successively by 45°, he was able to obtain four different 1-dimensional projections of the NMR signal. These data were then mathematically "back-projected" to form a 2-dimensional tomographic image. Because the result depended on the combined effects of two magnetic fields, Lauterbur named his technique "***zeugmatography***" after the Greek word, *zeugma*, meaning "that which is used for joining." Shortly thereafter, Lauterbur produced crude images of his first living subject: a tiny clam.

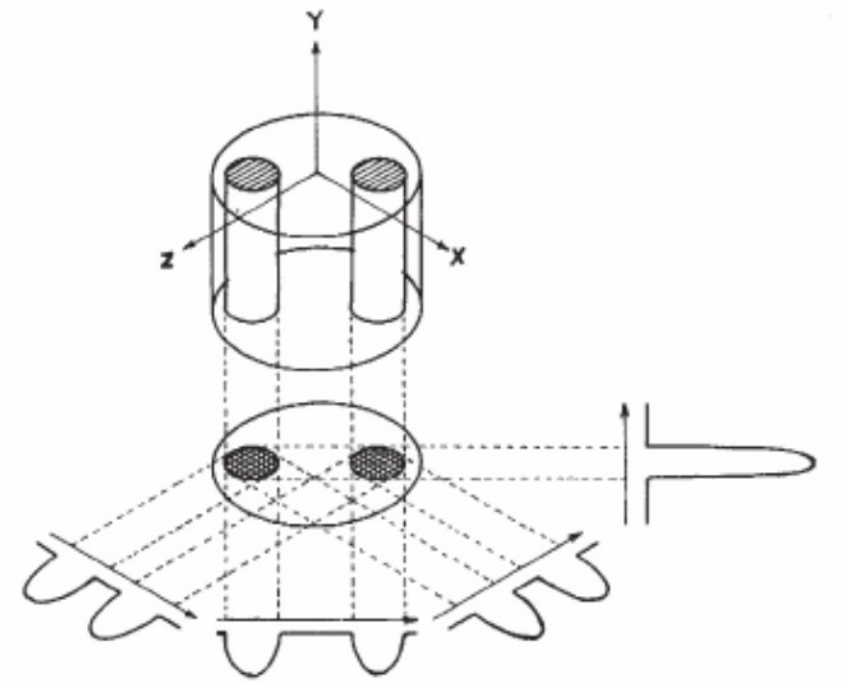

Fig. 1 Relationship between a three-dimensional object, its two-dimensional projection along the Y-axis, and four one-dimensional projections at 45° intervals in the XZ-plane. The arrows indicate the gradient directions.

Fig. 2 Proton nuclear magnetic resonance zeugmatogram of the object described in the text, using four relative orientations of object and gradients as diagrammed in Fig. 1.

Mansfield's Contribution: Use of a field gradient for slice selection

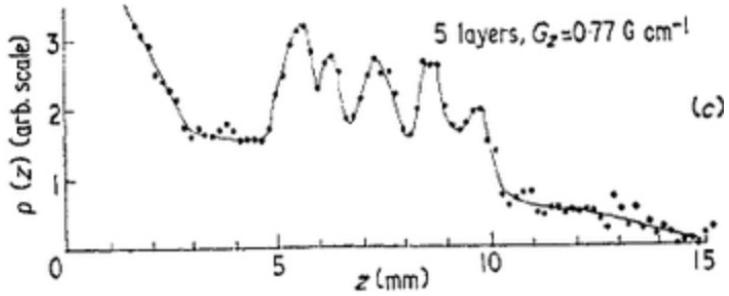

From Mansfield (1973). Five peaks corresponding to five stacked blocks of solid camphor.

Also in 1973, ***Peter Mansfield*** (b. 1933), a physicist working at the University of Nottingham, demonstrated how a linear field gradient could be used to localize the NMR signal on a slice-by-slice basis. Mansfield's experimental setup involved stacking multiple 1-mm-thick sheets of solid camphor into the bore of an NMR spectrometer. Applying a magnetic field gradient perpendicular to the sheets, Mansfield measured the transient NMR signal response to an applied RF-pulse. Interference peaks similar to those seen in x-ray diffraction were observed, which when inverse Fourier transformed revealed discrete layers of the camphor sample.

Later in the decade, Mansfield and his collaborator, Andrew Maudsley, further refined this method into a line-scan technique, producing the first image of a human body part, a finger, in 1977.

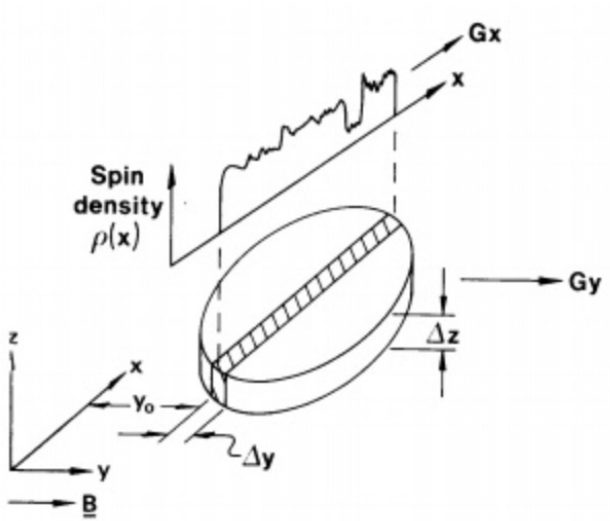

Line-scan technique, selectively irradiating a narrow strip with an isolated slice of magnetization.

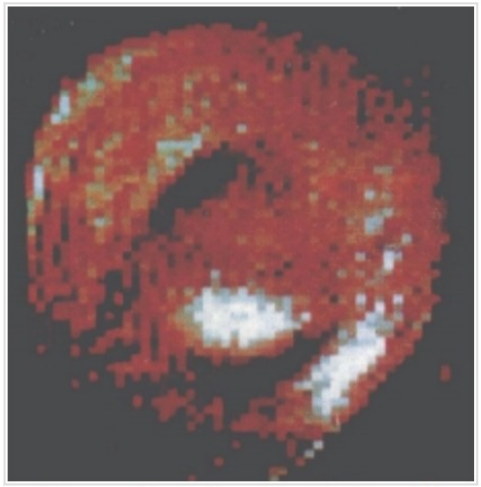

Image of human finger from Mansfield and Maudsley (1977) using line-scan technique obtained at 0.35T in 23 minutes. The white oval is marrow within the phalanx and the dark bands are tendons.

Damadian's Contribution: Vision of a human-sized scanner to detect disease

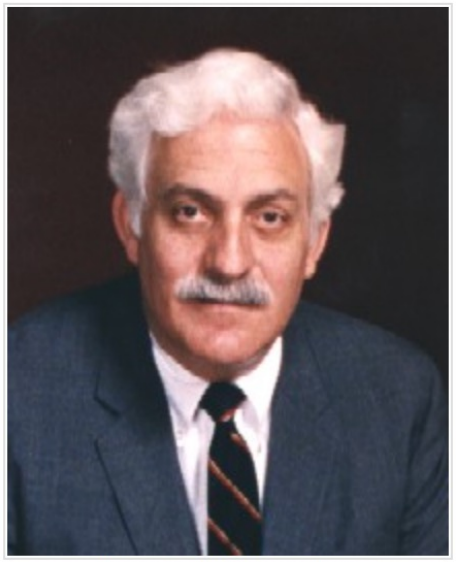

Raymond V. Damadian

Assistant Larry Minkoff in Indomitable

While Lauterbur and Mansfield were basic scientists, ***Raymond V. Damadian*** (b. 1936) was a physician, an Associate Professor of Medicine at the State University of New York - Brooklyn (Downstate). He looked at NMR from a different and original perspective — as a phenomenon that might be used to probe the body and diagnose human disease. In one of his landmark early papers (*Science*, 1971) Damadian demonstrated that cancer cells had longer T1 and T2 values than normal cells. In 1972 he filed a US patent application for an apparatus and method to detect cancer in tissue. Although the details of exactly how this 'apparatus" would produce images were not included in the application, Damadian and his team set out to build such a device which was named "***Indomitable***." By mid-summer, 1977, the first whole-body MR images were being produced, including the famous one shown below of his assistant's chest.

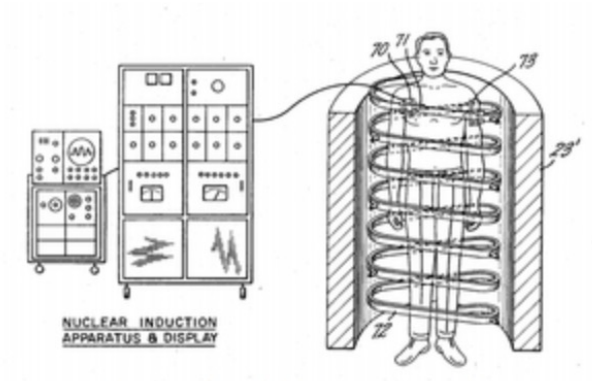

Damadian's 1972 patent application

Damadian used a "sensitive point" method for spatial localization of the NMR signal. This was based on a saddle-shaped magnetic field where only a small volume at the center matched the resonance frequency of the RF pulse. The patient's body was physically moved in a rectangular pattern until signals from all pixels were obtained.

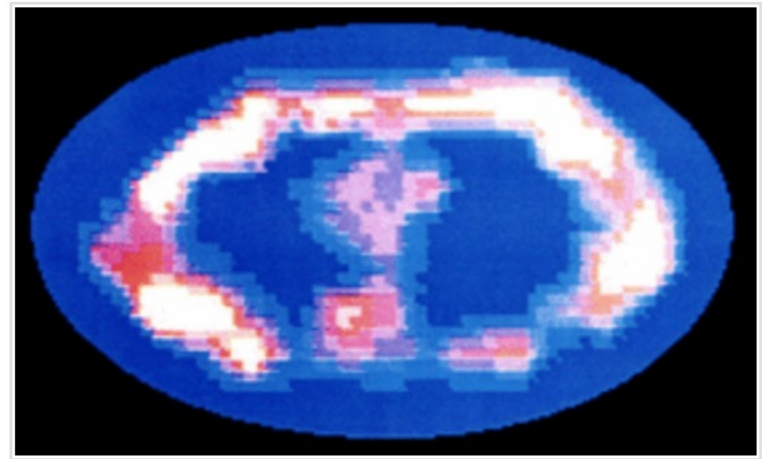

First whole body image (Minkoff's chest), obtained July, 1977. It required nearly 5 hours to produce.

Damadian called his imaging method "field-focused NMR" or FONAR. This became the name of his company, the first to manufacture clinical MR scanners commercially. It was soon recognized that the field-focused method was far too slow and clumsy for routine clinical imaging, and so it was abandoned in favor of the methods of Lauterbur and Mansfield in subsequent versions of the scanner.

When the 2003 Nobel Prizes for Medicine were announced, Damadian considered it a personal injustice that he was excluded. He placed full-page ads in several large world newspapers urging the Nobel committee to change its mind. The decision stood.

Positron Emission Tomography: Invented in 1975. Commercial use by 1980's

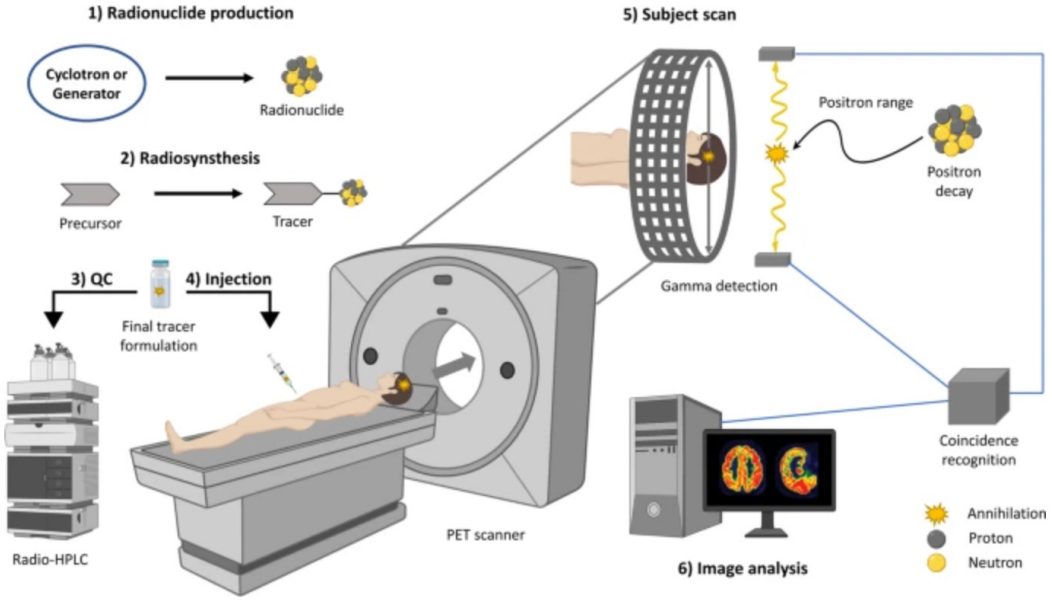

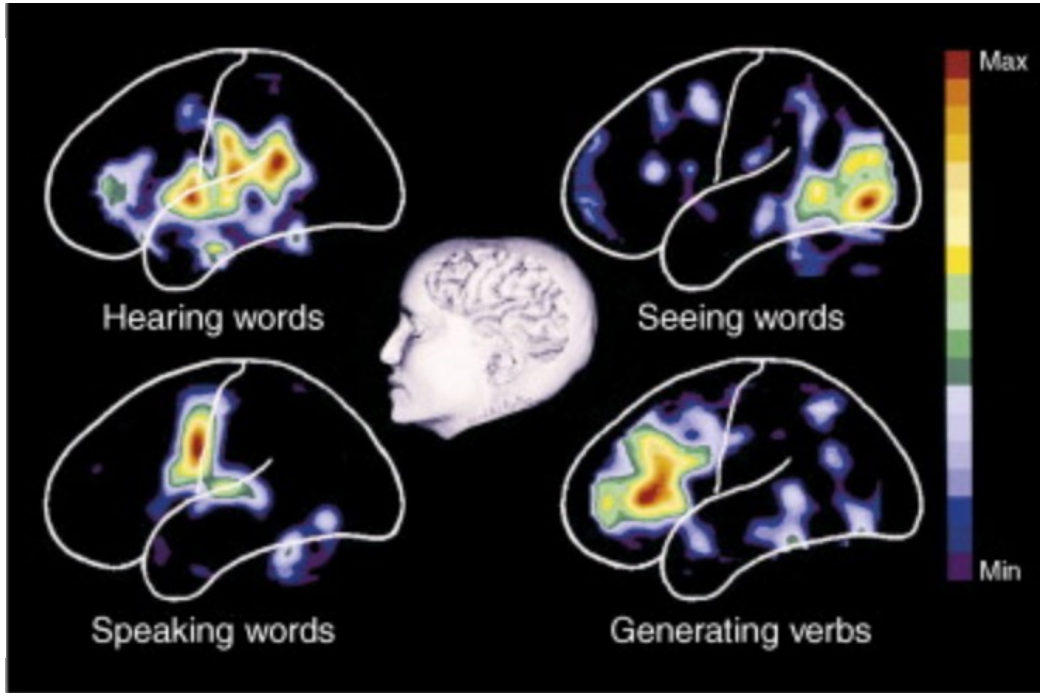

Positron emission tomographic studies of the cortical anatomy of single-word processing. Petersen, S.E. et al. Nature. 1988; 331: 585–589

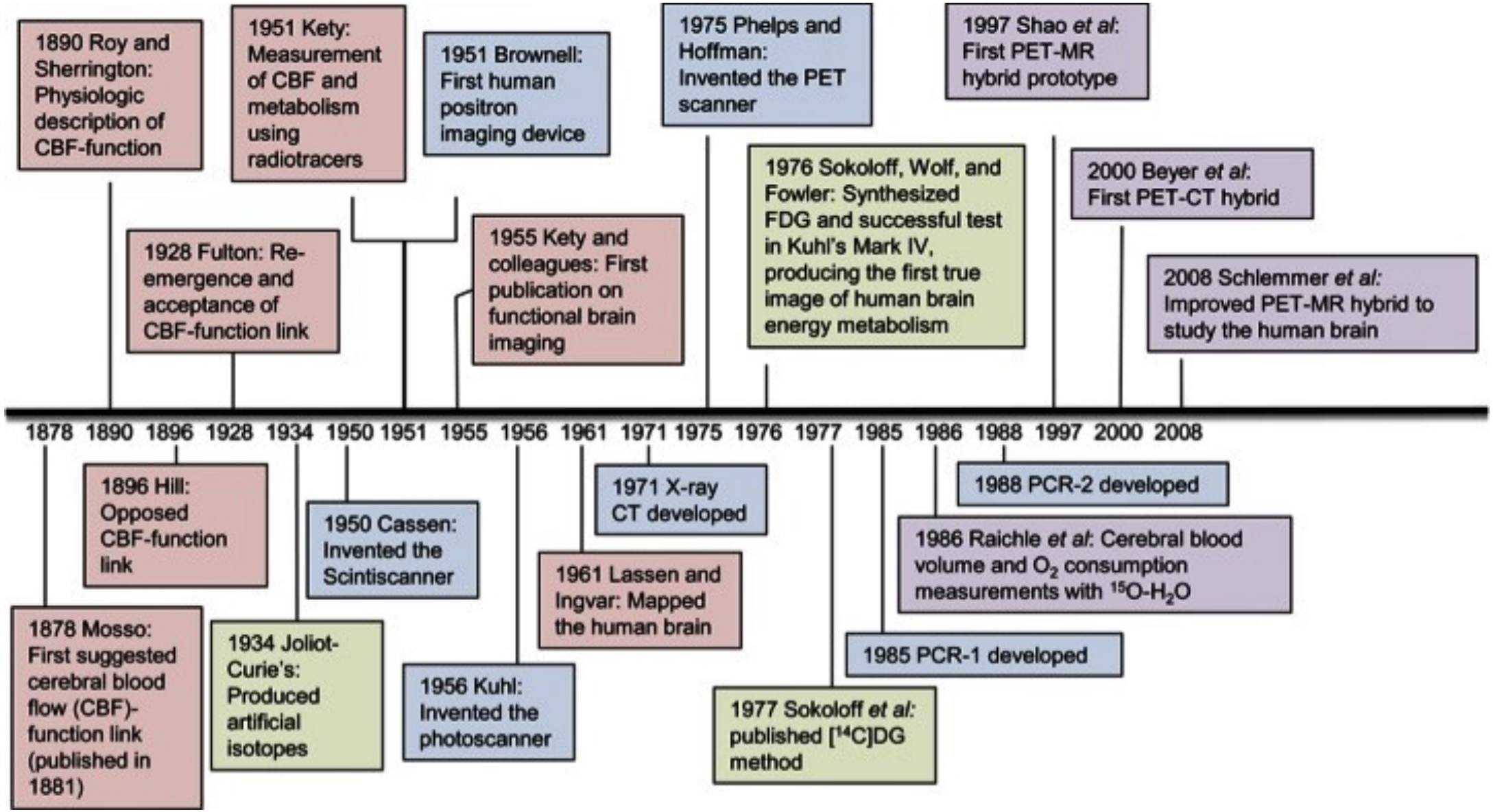

Portnow LH, Vaillancourt DE, Okun MS. The history of cerebral PET scanning: from physiology to cutting-edge technology. Neurology. 2013 Mar 5;80(10):952-6. doi: 10.1212/WNL.0b013e318285c135. Erratum in: Neurology. 2013 Oct 1;81(14):1275. doi: 10.1212/WNL.0b013e3182aa3d3a. PMID: 23460618; PMCID: PMC3653214.

Near Infrared Spectroscopy

Year	Major events
1977	Jöbsis demonstrates the possibility to detect changes of adult cortical oxygenation during hyperventilation by near-infrared spectroscopy.
1985	First NIRS clinical studies on newborns and adult cerebrovascular patients (Brazy; Ferrari)
1989	First commercial single-channel CW clinical instrument: NIRO-1000 by Hamamatsu Photonics, Japan
1991/1992	First fNIRS studies carried out independently by Chance, Kato, Hoshi, and Villringer by using single-channel instruments
1993	Publication of the first 6 fNIRS studies
	Simultaneous monitoring of different cortical areas by 5 single-channel instruments (Hoshi)
1994	First application of fNIRS on subjects affected by psychiatric disorders by using a single-channel system (Okada)
	Hitachi company (Japan) introduces a 10-channel CW system (Maki)
	First simultaneous recording of positron emission tomography and fNIRS data (Hoshi)
1995	First evidence of a fast optical signal related to neuronal activity (Gratton)
	First two-dimensional image of the adult occipital cortex activation by a frequency domain spectrometer (Gratton)

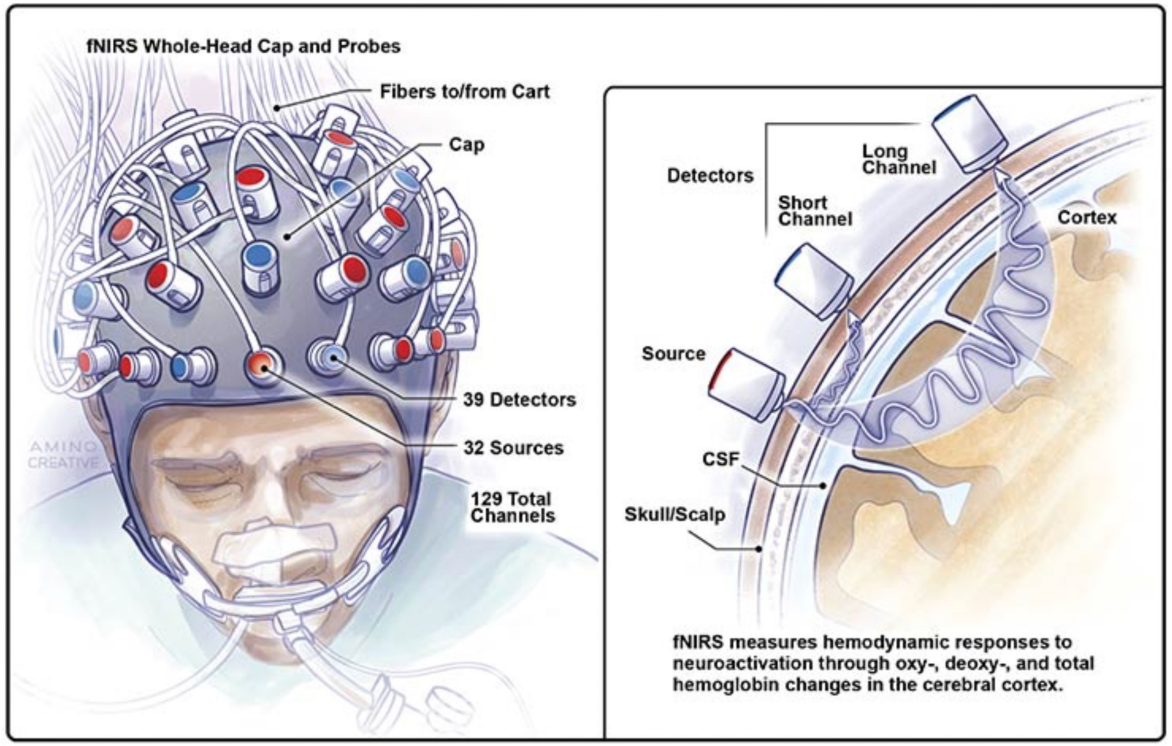

Marco Ferrari, Valentina Quaresima, A brief review on the history of human functional near-infrared spectroscopy (fNIRS) development and fields of application, NeuroImage, Volume 63, Issue 2, 2012, Pages 921-935,

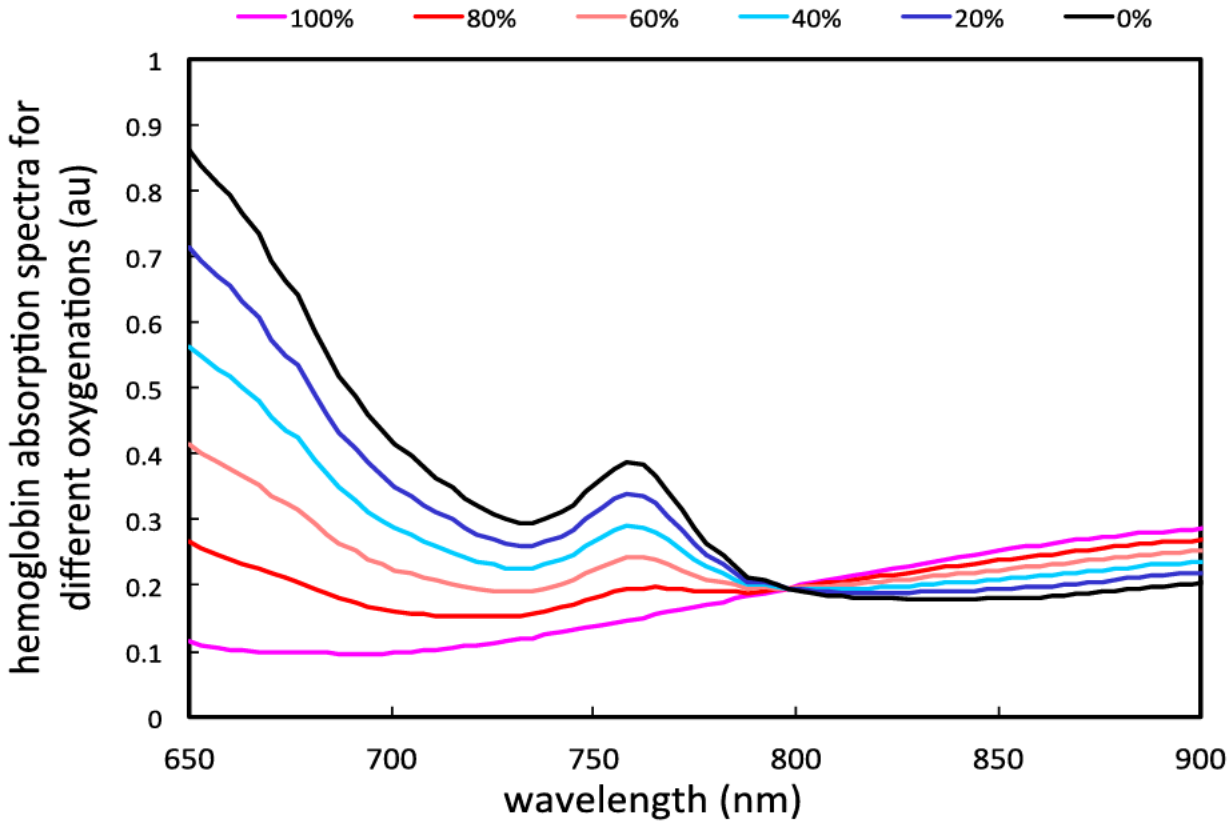

https://openfnirs.org/wp-content/uploads/2018/12/fNIRS_workshop2018_day1_NIRS_principles.pdf

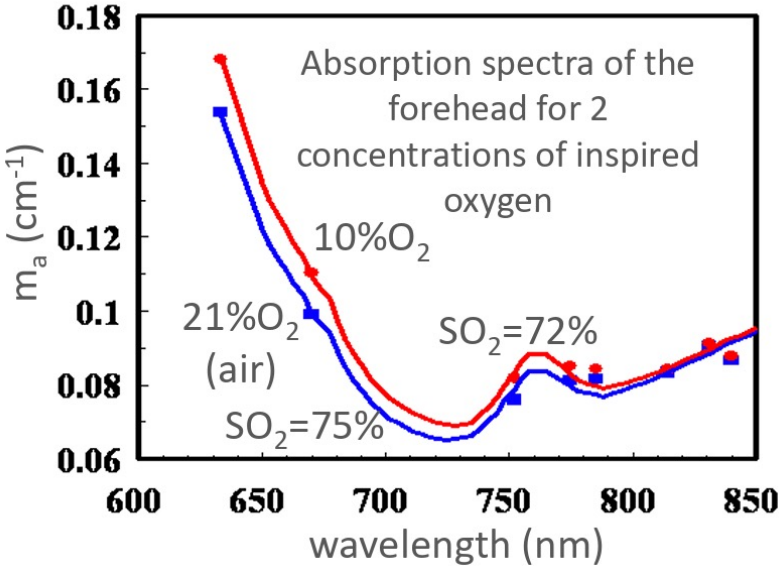

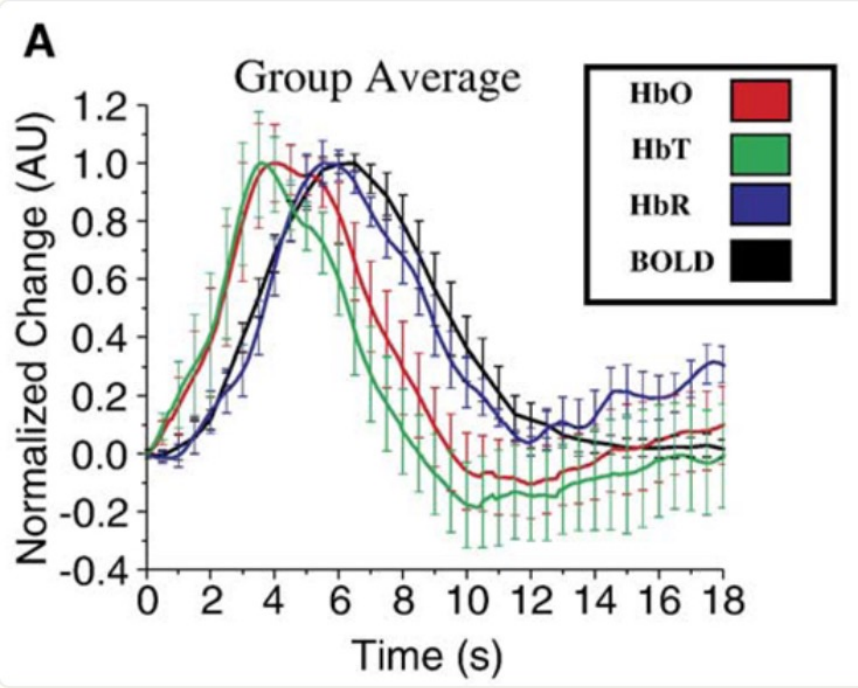

Huppert TJ, Hoge RD, Diamond SG, Franceschini MA, Boas DA. A temporal comparison of BOLD, ASL, and NIRS hemodynamic responses to motor stimuli in adult humans. Neuroimage. 2006 Jan 15;29(2):368-82. doi: 10.1016/j.neuroimage.2005.08.065. Epub 2005 Nov 21. PMID: 16303317; PMCID: PMC2692693.

fNIRS Commercial Systems

NIRx Medical Technologies

ETG 4000, Hitachi

Biopac fNIR

FLEX, MRRA Inc.

Oxymon, Artinis

LABNIRS, Shimatzu

CW6, TechEn

Brainsight NIRS, Rogue Research

NTS, Gowerlabs

https://openfnirs.org/wp-content/uploads/2018/12/fNIRS_workshop2018_day1_NIRS_principles.pdf

Magnetic Resonance Imaging:

Invented in 1977, Introduced clinically in 1984

Hydrogen "precesses" at 127.7 MHz at 3T

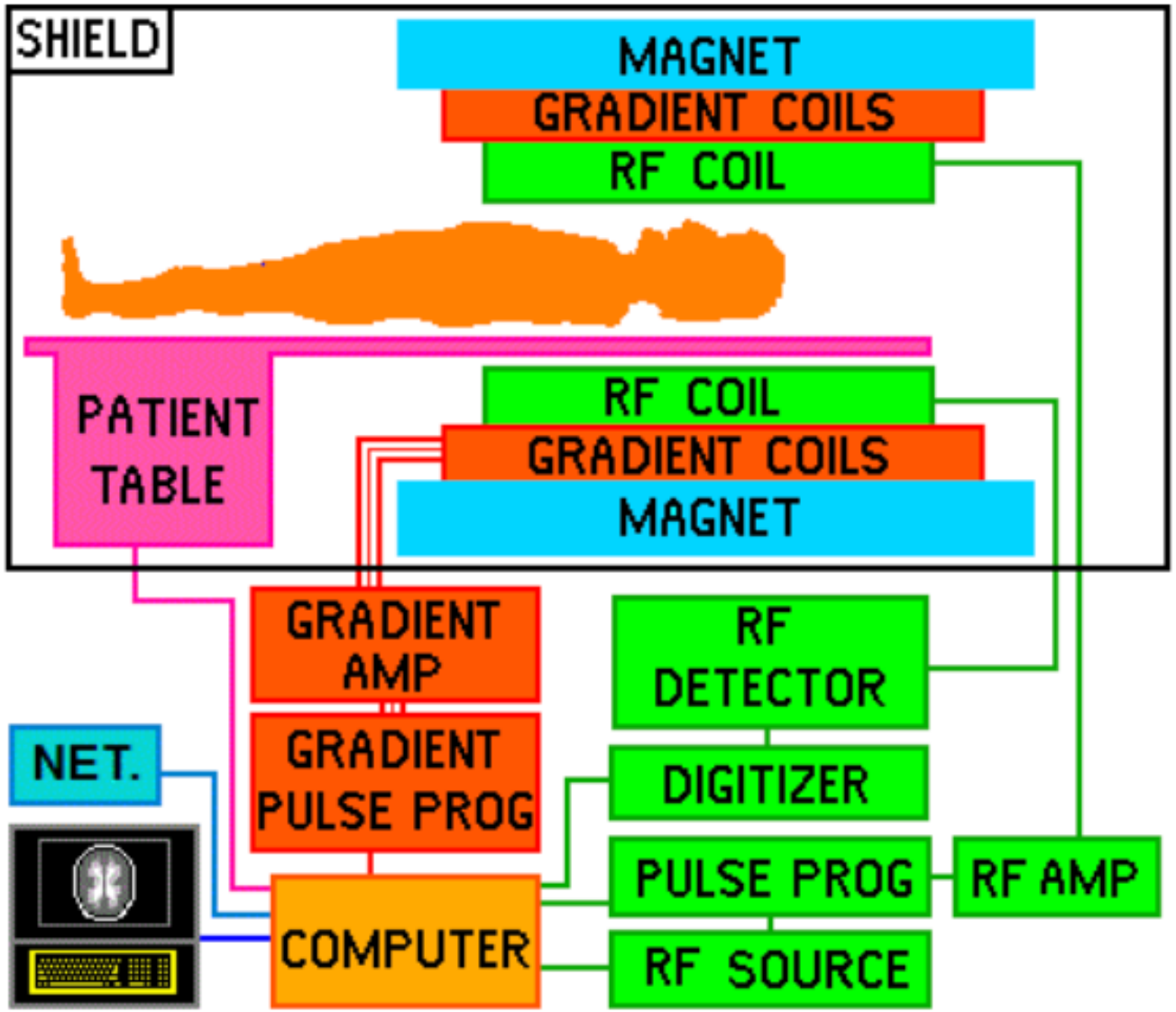
SHIELD
MAGNET
GRADIENT COILS
RF COIL
PATIENT TABLE
RF COIL
GRADIENT COILS
MAGNET
GRADIENT AMP
GRADIENT PULSE PROG
RF DETECTOR
DIGITIZER
PULSE PROG
RF AMP
RF SOURCE
NET.
COMPUTER

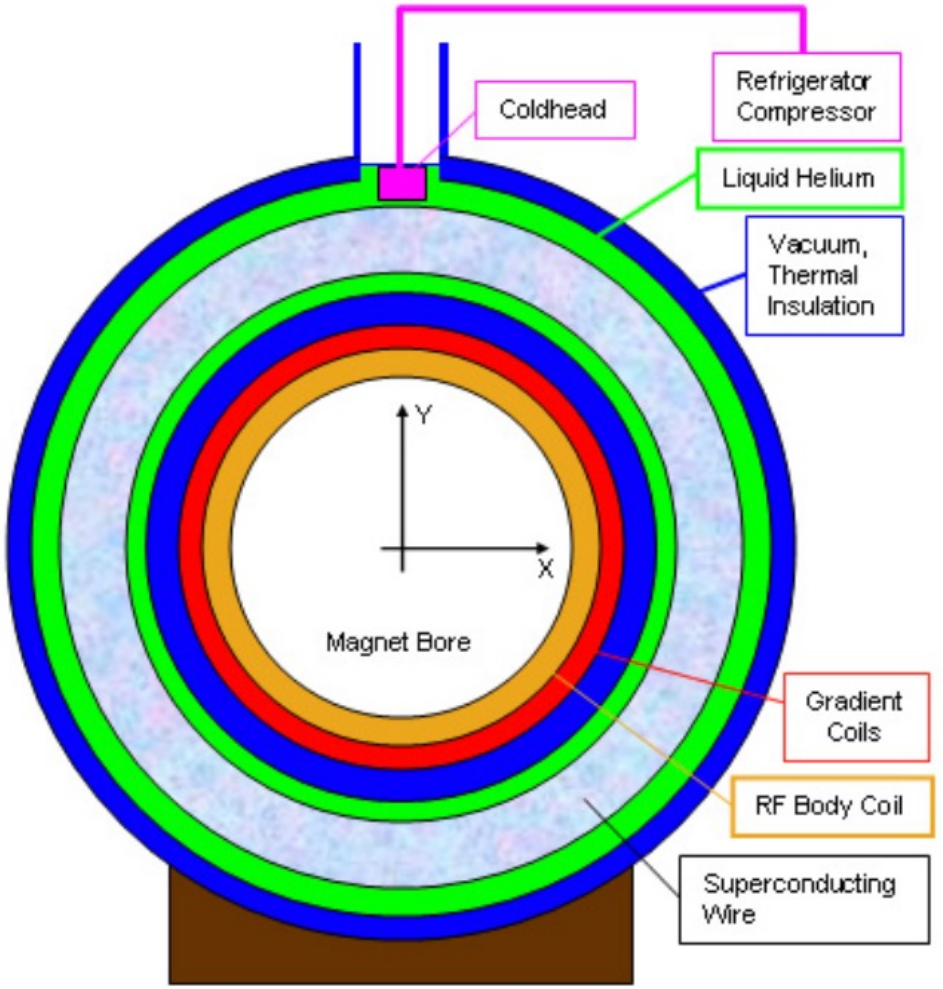
Coldhead
Refrigerator Compressor
Liquid Helium
Vacuum, Thermal Insulation
Y
X
Magnet Bore
Gradient Coils
RF Body Coil
Superconducting Wire

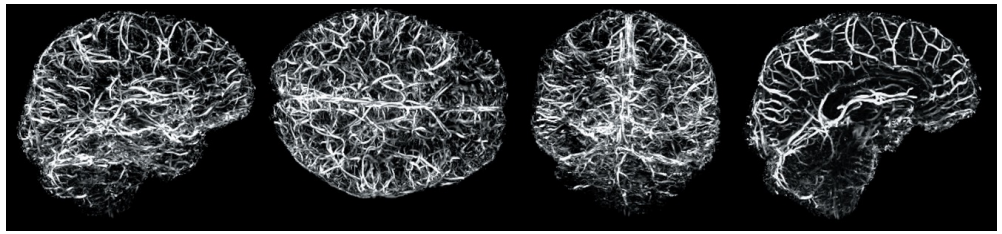

Venography

T1 weighted T2 weighted

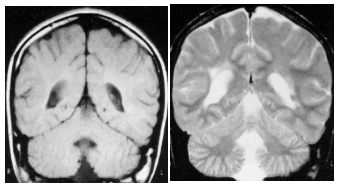

Fiber Track Imaging

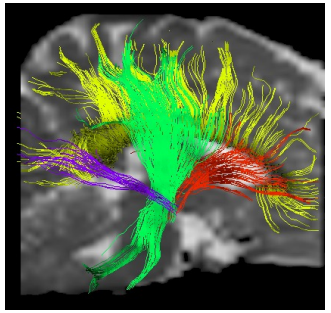

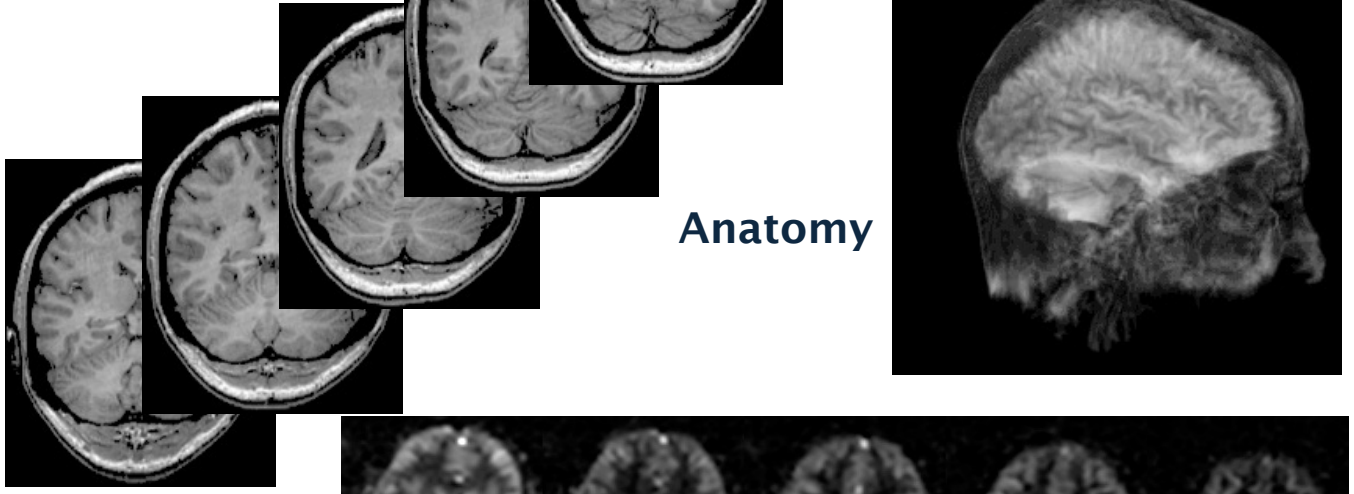

Anatomy

Angiography

Perfusion

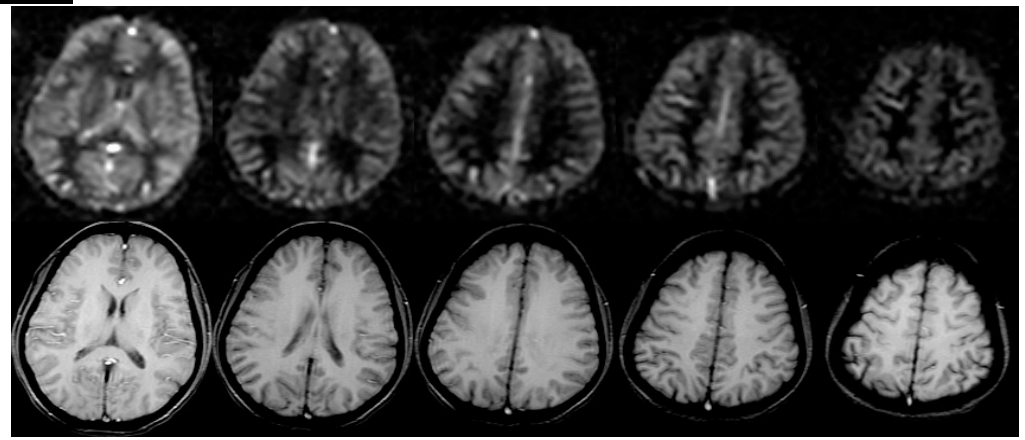

The First Successful Functional MRI Result

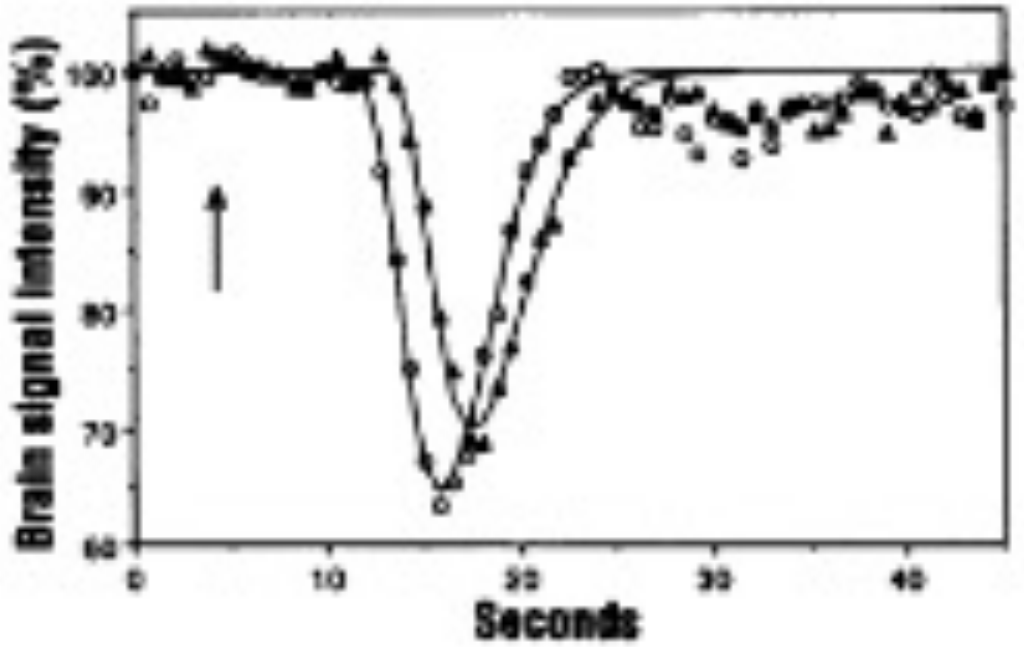

Functional Mapping of the Human Visual Cortex by Magnetic Resonance Imaging

J. W. Belliveau,* D. N. Kennedy, R. C. McKinstry, B. R. Buchbinder, R. M. Weisskoff, M. S. Cohen, J. M. Vevea, T. J. Brady, B. R. Rosen

Science, Volume 254, Issue 5032, Nov 1991

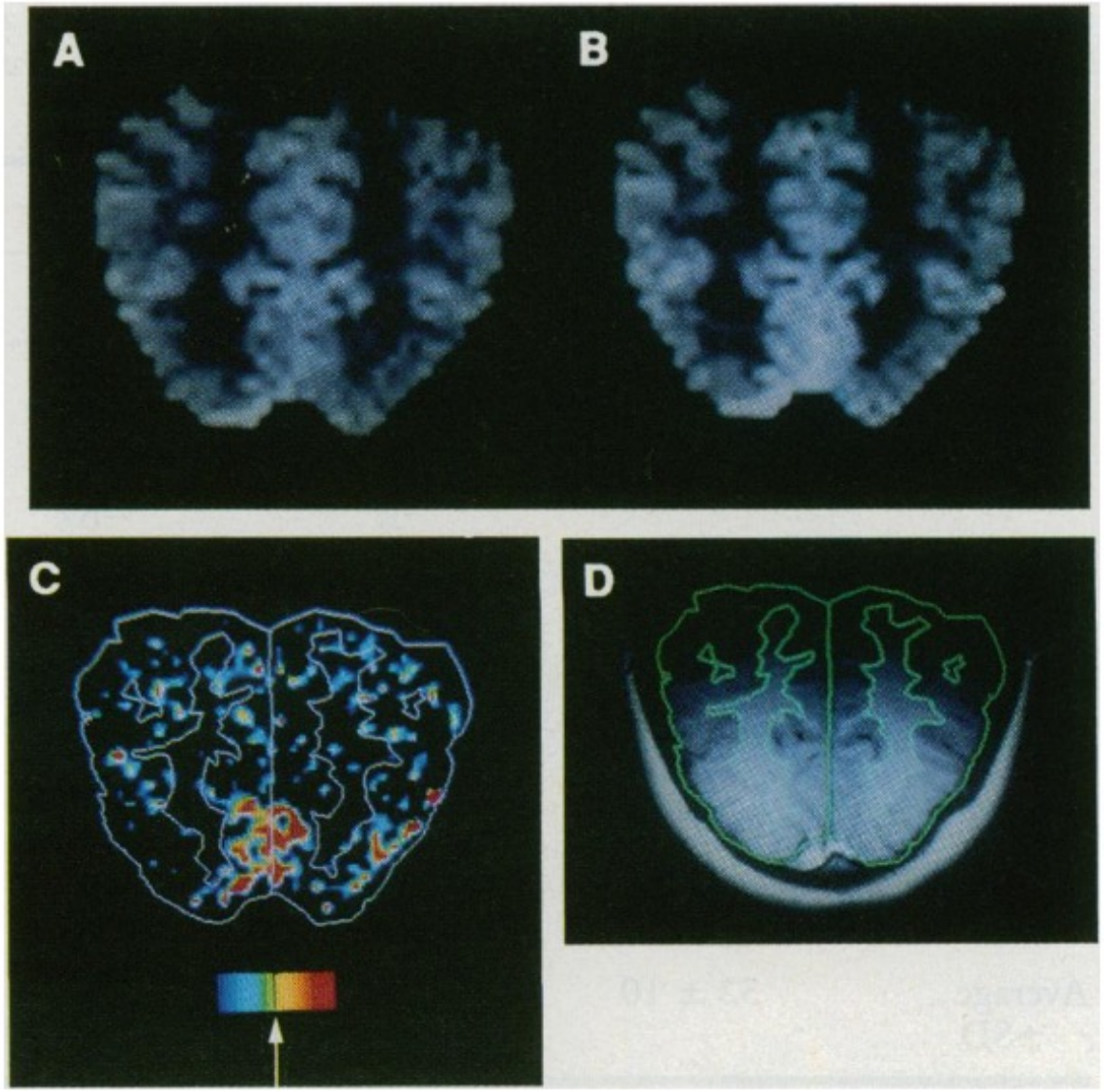

American Association for the Advancement of Science

SCIENCE

1 November 1991 $6.00
Vol. 254 ■ Pages 621–768

Blood Oxygen Level Dependent (BOLD) contrast

L. Pauling, C. D. Coryell, *Proc.Natl. Acad. Sci. USA 22, 210-216*, 1936.
(Blood susceptibility changes with oxygenation)

K.R. Thulborn, J. C. Waterton, et al., *Biochim. Biophys. Acta. 714: 265-270*, 1982.
(Blood T2 is proportional to oxygenation & mechanism is bulk susceptibility)

S. Ogawa, T. M. Lee, A. R. Kay, D. W. Tank, *Proc. Natl. Acad. Sci. USA 87, 9868-9872*, 1990.
(T2 and T2 modulation in vessels in living rat brains with oxygenation changes)*

Turner, R., Lebihan, D., Moonen, C. T. W., Despres, D. & Frank, J. *MRM,* 22, 159-166, 1991
(T2 modulation with cat brain with oxygenation changes)*

red blood cells

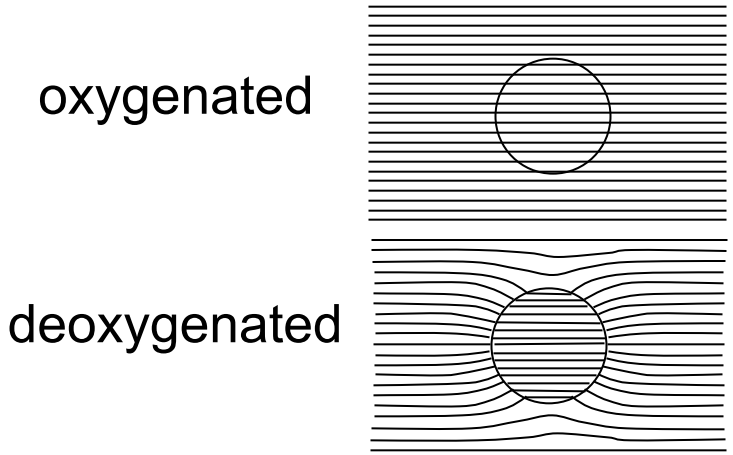

BOLD contrast investigation started in 1936…or even 1845.

THE MAGNETIC PROPERTIES AND STRUCTURE OF HEMOGLOBIN, OXYHEMOGLOBIN AND CARBONMONOXYHEMOGLOBIN

BY LINUS PAULING AND CHARLES D. CORYELL

GATES CHEMICAL LABORATORY, CALIFORNIA INSTITUTE OF TECHNOLOGY

Communicated March 19, 1936

Over ninety years ago, on November 8, 1845, Michael Faraday investigated the magnetic properties of dried blood and made a note "Must try recent fluid blood." If he had determined the magnetic susceptibilities of arterial and venous blood, he would have found them to differ by a large amount (as much as twenty per cent for completely oxygenated and completely deoxygenated blood); this discovery without doubt would have excited much interest and would have influenced appreciably the course of research on blood and hemoglobin.[1]

Continuing our investigations of the magnetic properties and structure of hemoglobin and related substances,[2] we have found oxyhemoglobin and carbonmonoxyhemoglobin to contain no unpaired electrons, and ferrohemoglobin (hemoglobin itself) to contain four unpaired electrons per heme. The description of our experiments and the interpretation and discussion of the results are given below.

Biochimica et Biophysica Acta, 714 (1982) 265–270
Elsevier Biomedical Press

BBA 20122

OXYGENATION DEPENDENCE OF THE TRANSVERSE RELAXATION TIME OF WATER PROTONS IN WHOLE BLOOD AT HIGH FIELD

KEITH R. THULBORN, JOHN C. WATERTON *, PAUL M. MATTHEWS and GEORGE K. RADDA

Department of Biochemistry, University of Oxford, South Parks Road, Oxford OX1 3QU (U.K.)

(Received August 4th, 1981)

Key words: Oxygenation dependence; Transverse relaxation time; Water proton; High field NMR; (Whole blood)

At high and medium magnetic field, the transverse NMR relaxation rate (T_2^{-1}) of water protons in blood is determined predominantly by the oxygenation state of haemoglobin. T_2^{-1} depends quadratically on the field strength and on the proportion of haemoglobin that is deoxygenated. Deoxygenation increases the volume magnetic susceptibility within the erythrocytes and thus creates local field gradients around these cells. From volume susceptibility measurements and the dependence of T_2^{-1} on the pulse rate in the Carr-Purcell-Meiboom-Gill experiment, we show that the increase in T_2^{-1} with increasing blood deoxygenation arises from diffusion of water through these field gradients.

Oxygenation Changes T2

Biochimica et Biophysica Acta, 714 (1982) 265–270
Elsevier Biomedical Press

BBA 20122

OXYGENATION DEPENDENCE OF THE TRANSVERSE RELAXATION TIME OF WATER PROTONS IN WHOLE BLOOD AT HIGH FIELD

KEITH R. THULBORN, JOHN C. WATERTON *, PAUL M. MATTHEWS and GEORGE K. RADDA

Department of Biochemistry, University of Oxford, South Parks Road, Oxford OX1 3QU (U.K.)

(Received August 4th, 1981)

Blood R2 proportional to Oxygenation

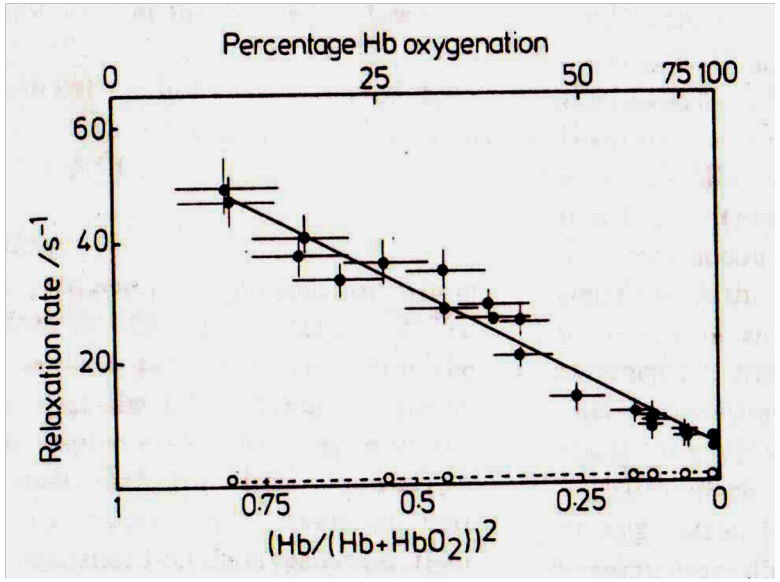

R2 effect is due to bulk susceptibility and not dipole-dipole interaction

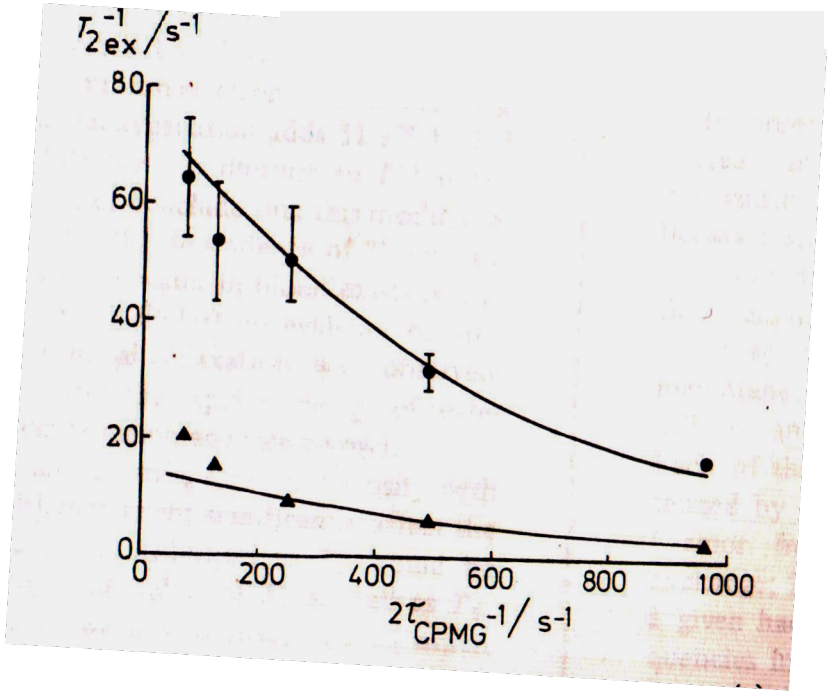

...Six years later...

Oxygenation-Sensitive Contrast in Magnetic Resonance Image of Rodent Brain at High Magnetic Fields

SEIJI OGAWA, TSO-MING LEE, ASHA S. NAYAK,* AND PAUL GLYNN

AT&T Bell Laboratories, Murray Hill, New Jersey 07974

Received November 30, 1988; accepted June 20, 1989

At high magnetic fields (7 and 8.4 T), water proton magnetic resonance images of brains of live mice and rats under pentobarbital anesthetization have been measured by a gradient echo pulse sequence with a spatial resolution of 65 × 65-μm pixel size and 700-μm slice thickness. The contrast in these images depicts anatomical details of the brain by numerous dark lines of various sizes. These lines are absent in the image taken by the usual spin echo sequence. They represent the blood vessels in the image slice and appear when the deoxyhemoglobin content in the red cells increases. This contrast is most pronounced in an anoxy brain but not present in a brain with diamagnetic oxy or carbon monoxide hemoglobin. The local field induced by the magnetic susceptibility change in the blood due to the paramagnetic deoxyhemoglobin causes the intra voxel dephasing of the water signals of the blood and the surrounding tissue. This oxygenation-dependent contrast is appreciable in high field images with high spatial resolution.

Seiji Ogawa

in vivo

in vitro

100% O_2

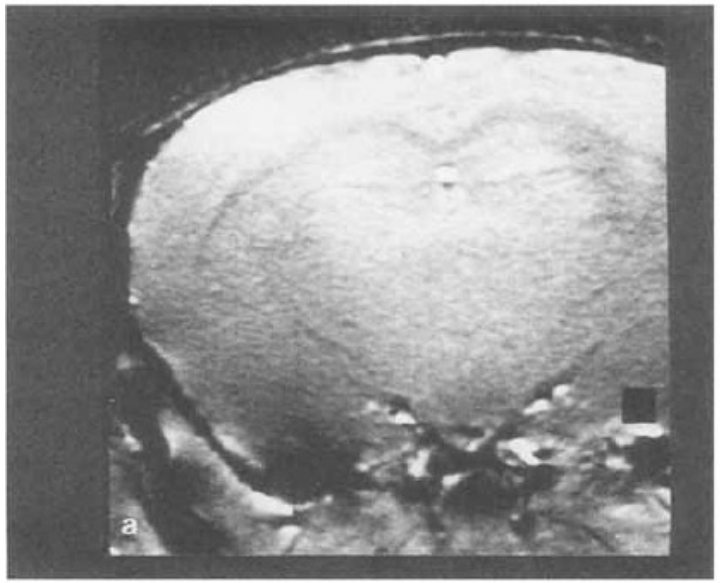

100% oxygenated blood

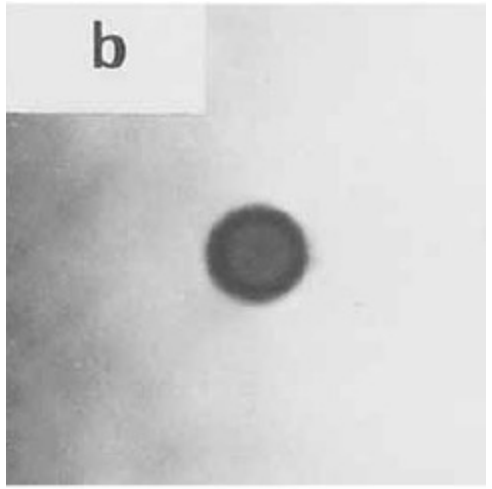

20% O_2

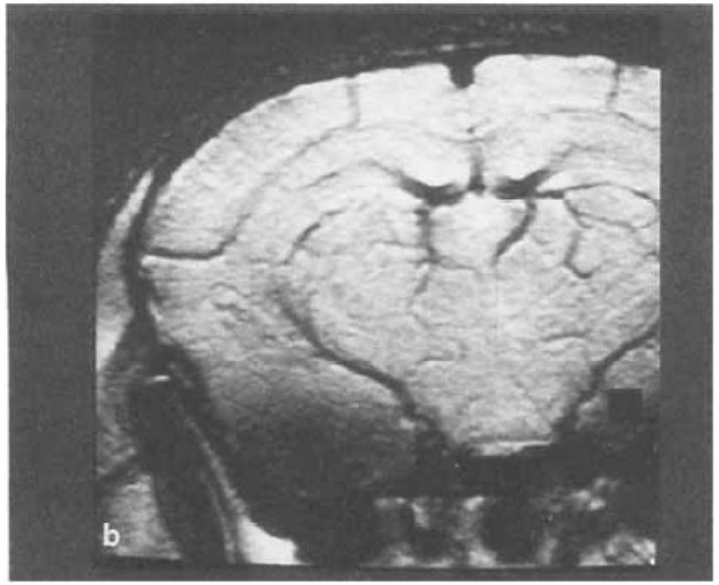

0% oxygenated blood

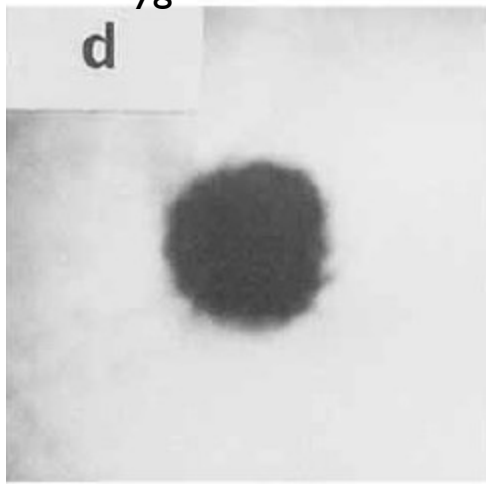

S. Ogawa, T.-M. Lee, A. S. Nayak, P. Glynn, Magn. Reson. Med, 14, 68-78 (1990)

Ogawa predicted fMRI but got the sign wrong…

"...we expect this oxygenation-sensitive contrast could be used to monitor regional oxygen usages in the brain. When some region in a brain is much more active than other regions, the active region could show darker lines in the image because of the increased level of deoxyhemoglobin resulting from higher oxygen consumption."

"Therefore, in addition to the anatomy of the brain, one aspect of its physiology can be studied by the MRI of water"

Oxygenation-Sensitive Contrast in Magnetic Resonance Image of Rodent Brain at High Magnetic Fields, Seiji Ogawa, Tso-Ming Lee, Asha S. Nayak, and Paul Glynn. Magnetic Resonance in Medicine 14, 68-78 (1990).

Susceptibility-Induced Field Distortion in the Vicinity of a Microvessel $\perp$ to B_o.

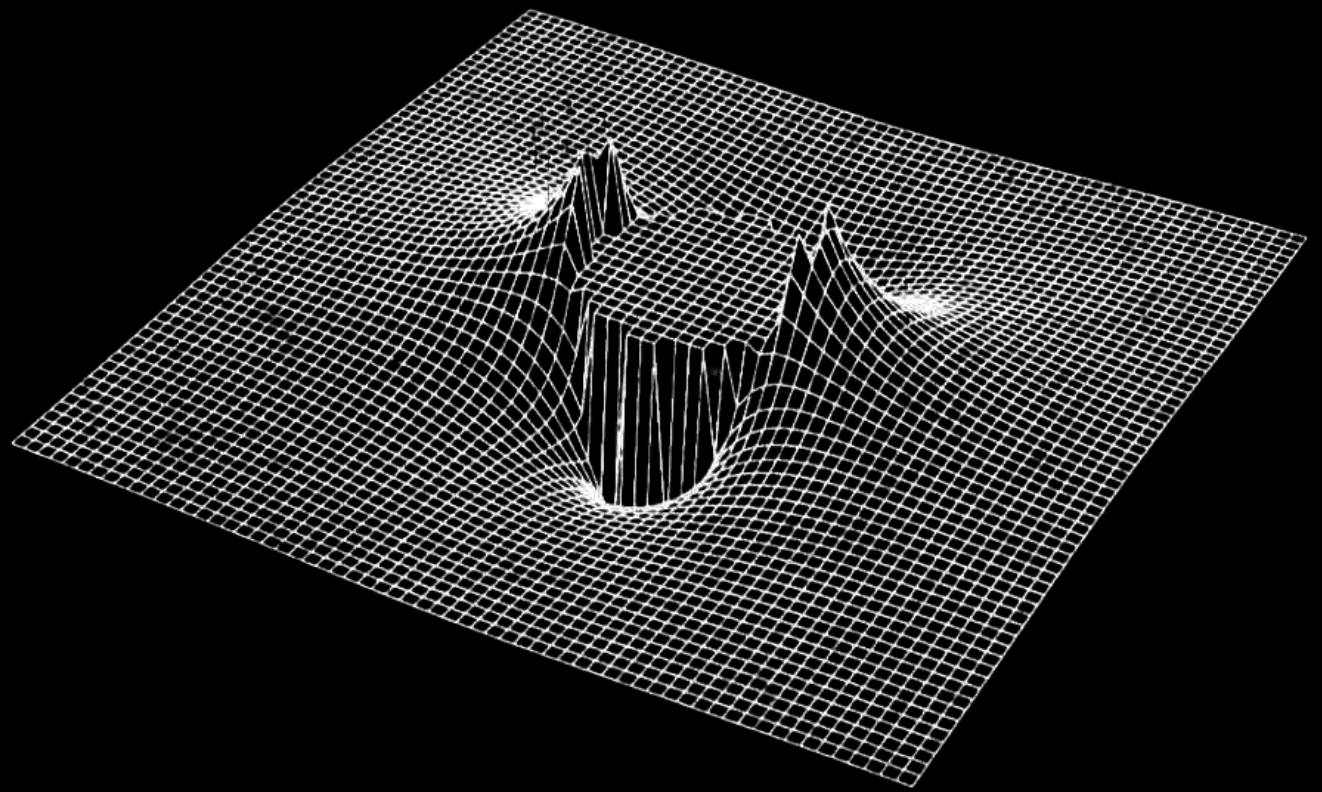

MAGNETIC RESONANCE IN MEDICINE 22, 159–166 (1991)

Echo-Planar Time Course MRI of Cat Brain Oxygenation Changes

ROBERT TURNER,*† DENIS LE BIHAN,‡ CHRIT T. W. MOONEN,§
DARYL DESPRES,§ AND JOSEPH FRANK‡

* *Laboratory of Cardiac Energetics,* ‡ *Diagnostic Radiology Department, and* § *In Vivo NMR Research Center, National Institutes of Health, Bethesda, Maryland 20892*

Received June 25, 1991; revised August 7, 1991

When deoxygenated, blood behaves as an effective susceptibility contrast agent. Changes in brain oxygenation can be monitored using gradient-echo echo-planar imaging. With this technique, difference images also demonstrate that blood oxygenation is increased during periods of recovery from respiratory challenge.

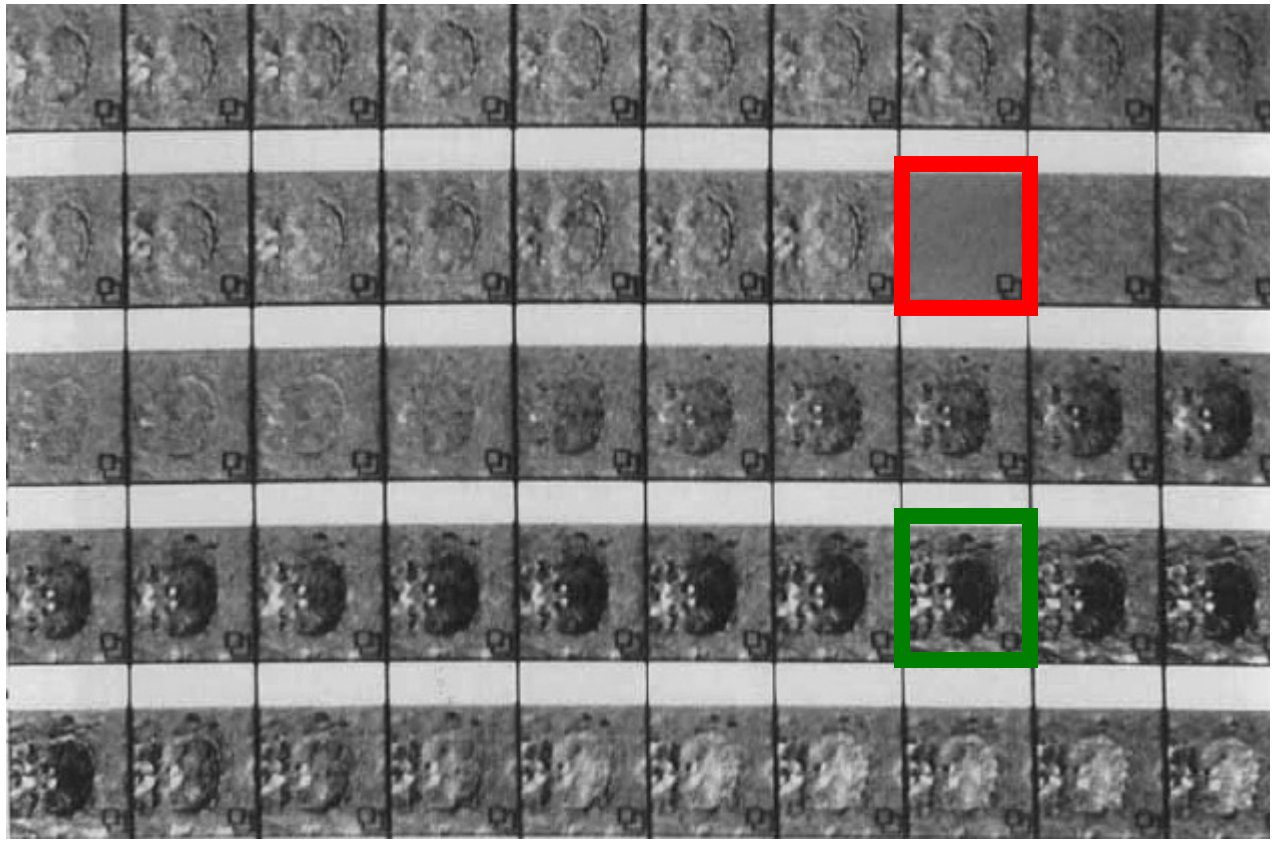

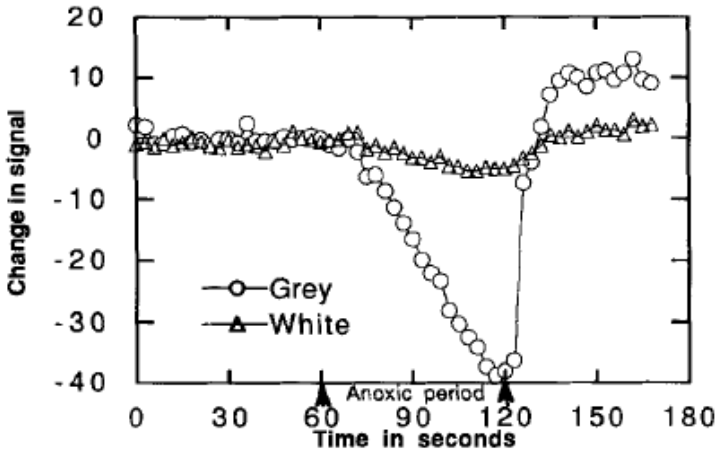

R. Turner, D. LeBihan, C.T.W. Moonen, D. Despres, J. Frank, Magn. Reson. Med, 22, 159-166 (1991)

The video that started it all.
Aug 12, 1991: Tom Brady Plenary Lecture at SMRM, San Francisco

Ken Kwong

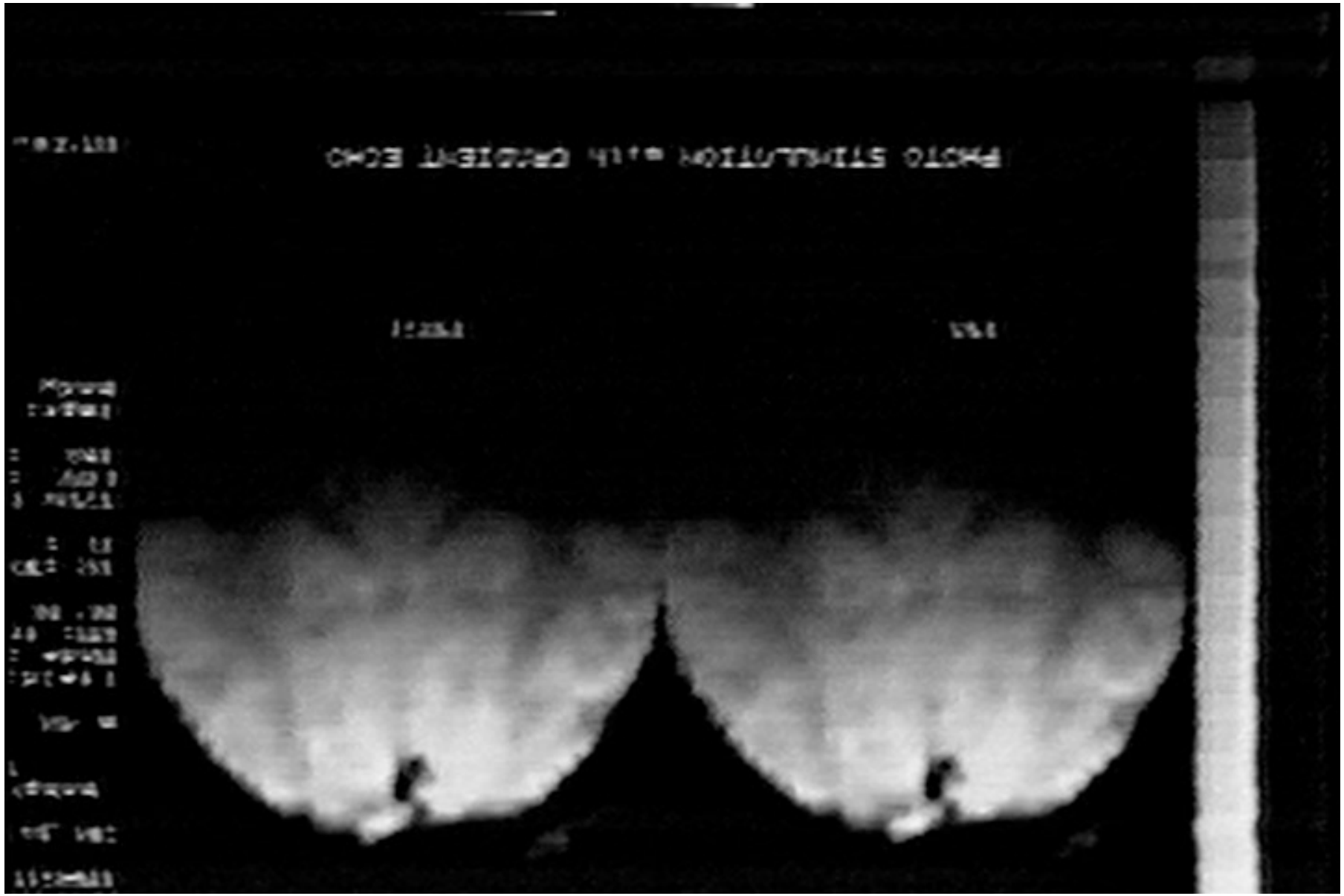

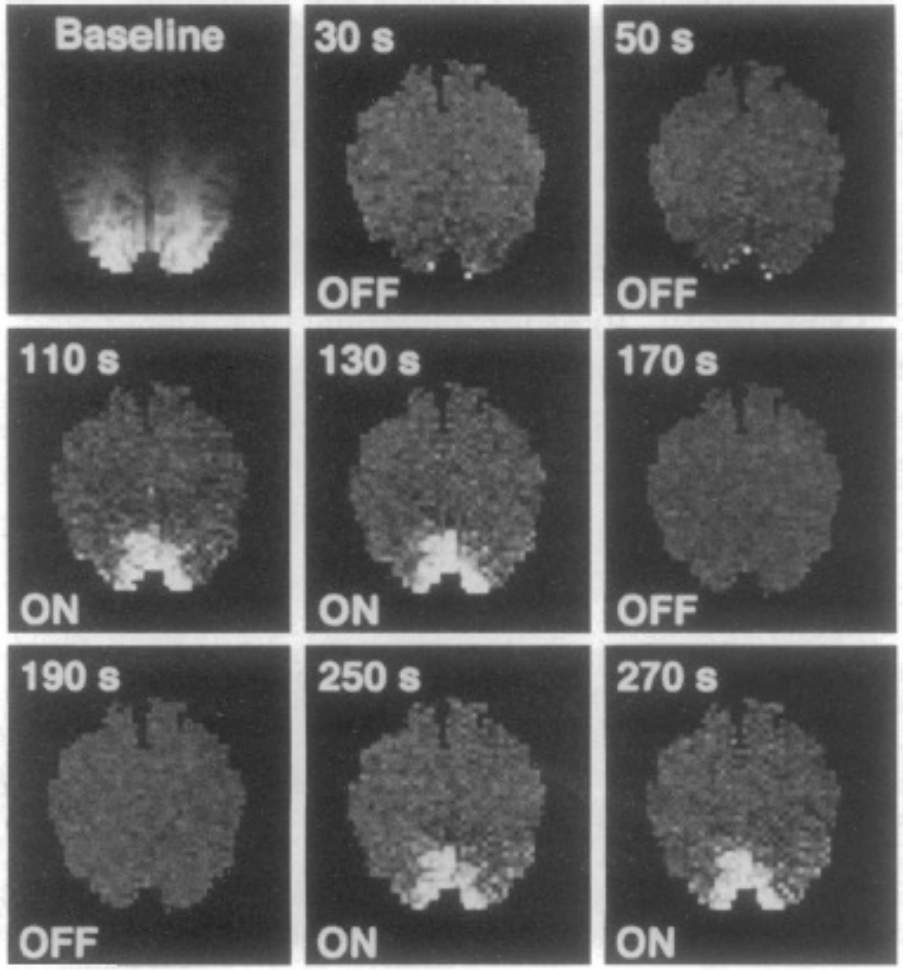

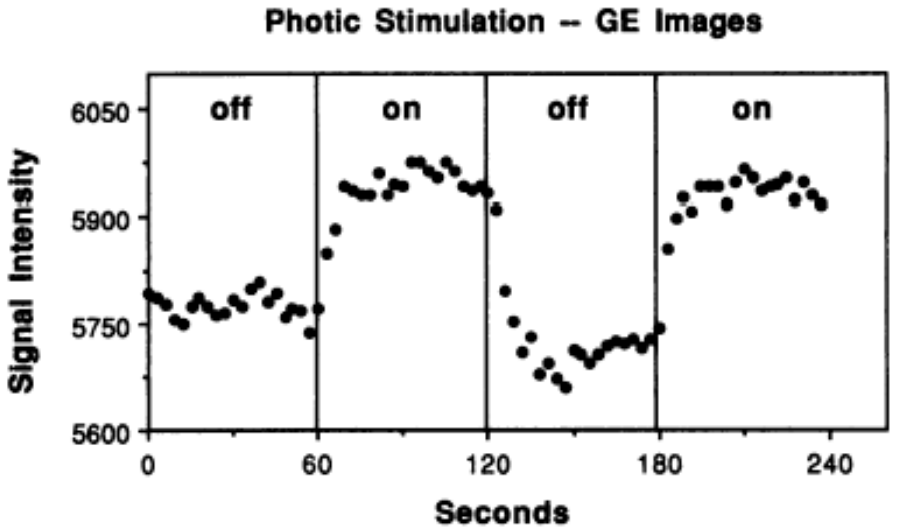

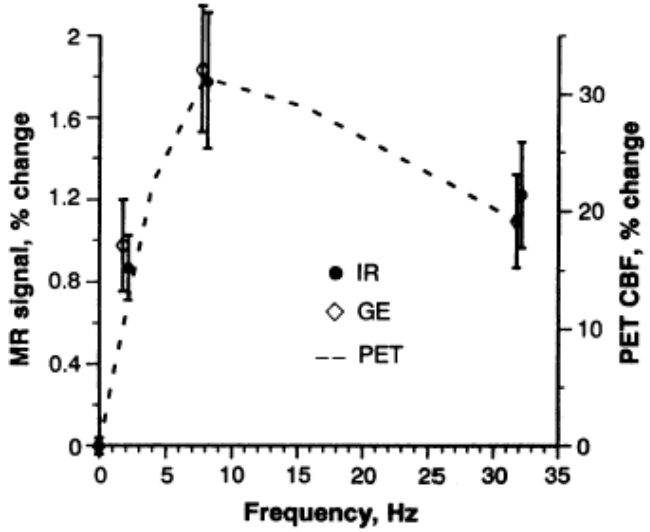

K. K. Kwong, et al, (1992) "Dynamic magnetic resonance imaging of human brain activity during primary sensory stimulation." Proc. Natl. Acad. Sci. USA. 89, 5675-5679.

photo stim. 5 in GP

~~GRE~~

IR

GE 350

70 sec skip

disdaq=2 30 pre 40 post

2.5

IR

disdaq 3.0 TR

=2 40 pre 40 post

TI = 1.05 s.

~~20~~ 30 50 20 80

90 sec

40 40 80

20 20 20

10 cm. slice cardiac.

rewing spikes

irstim. pre 2 3 5-8 13 14 16 18 19 25-29 (16 together)

irstim. post 34-38 40-47 49-65 67-80 (44 together)

Avg them (with sewing x5ir)

Get mirstim. avg (save them)

10 cm. slice cardiac

TR = 2.5 s TE = 4 ~~0~~

GE TA = 10 9

RA = 350

7106

MAY 9/91

Michelle

30 TR 40 on

GE-stim. dat

gestim. pre 3-30 (28)

gestim. post 33-70 (38) 30 30 2-3

~~post~~ gepre. avg

gepost. avg

7106

gestim. avg

gestim. sub 2d

	RA	TA
IR	370	10 2

TR = 3s TI = 1100 ms TE = 42

~~40~~ → 40

30 50

IR Image 66

jump up.

irstim. ~~p~~

irstim

irstim.

irstim. 74

irstim. s

irstim. s

~~irstim. sub (45 → include RC)~~

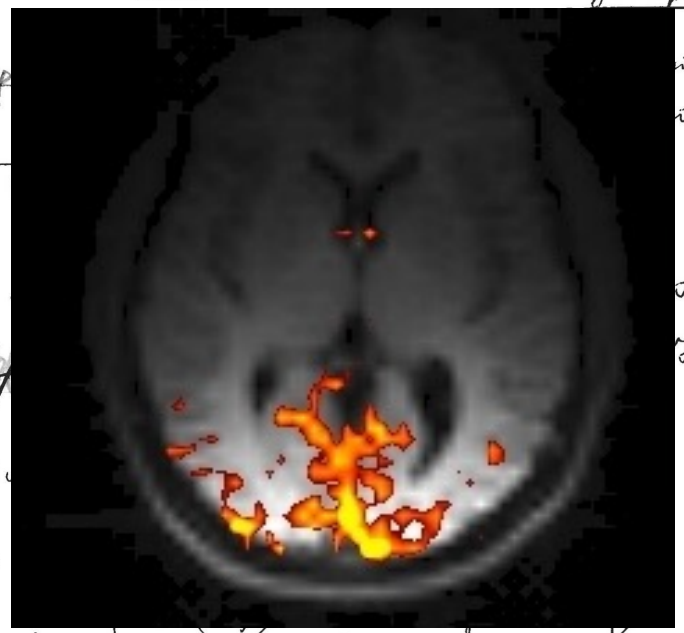

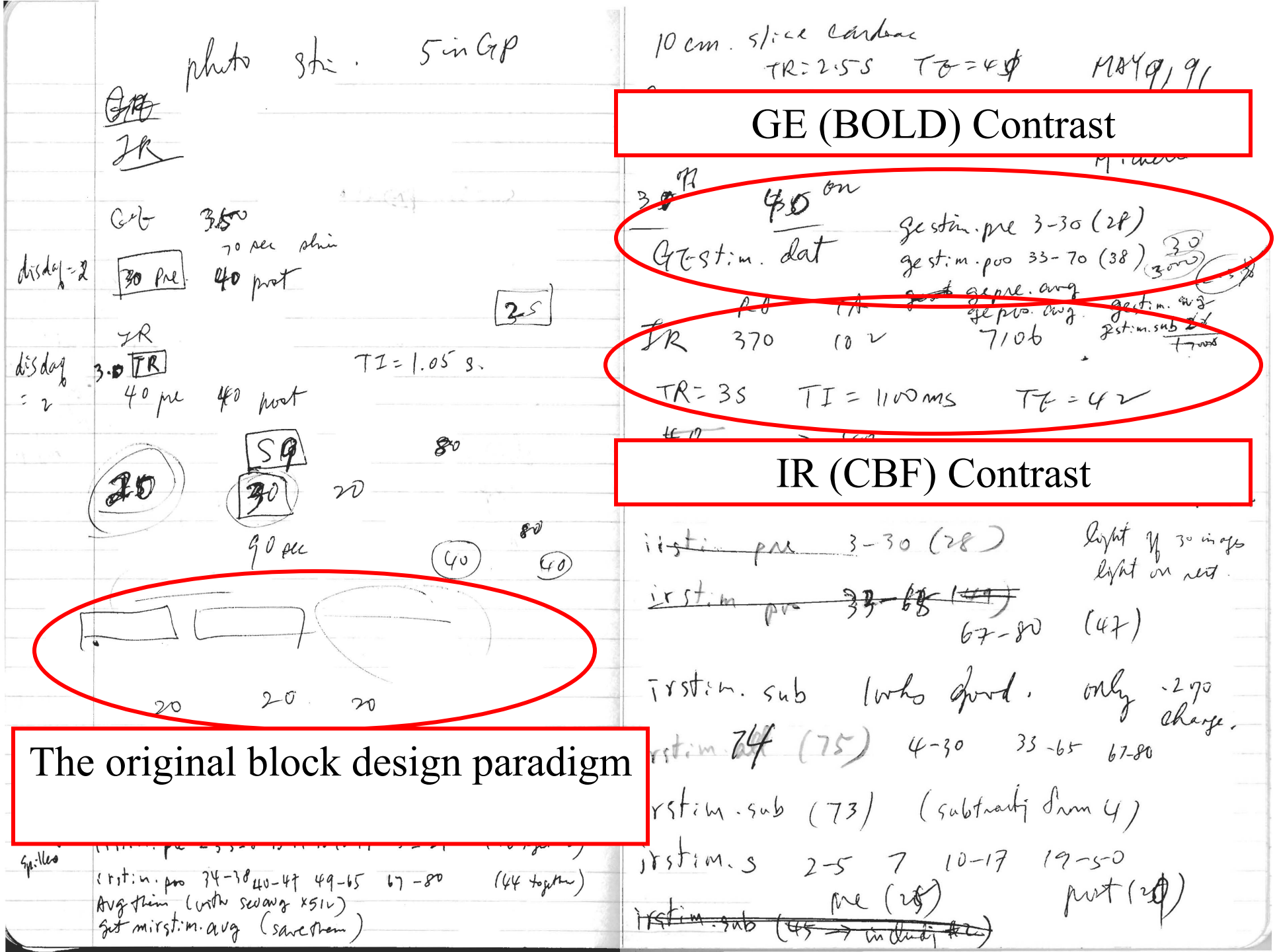
GE (BOLD) Contrast
IR (CBF) Contrast
The original block design paradigm

Multi-shot results at 4T, U. Minnesota.

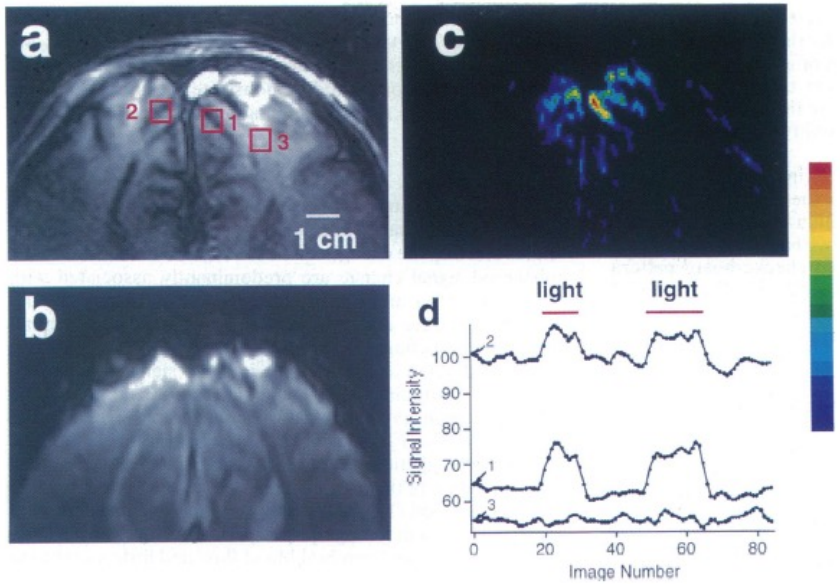

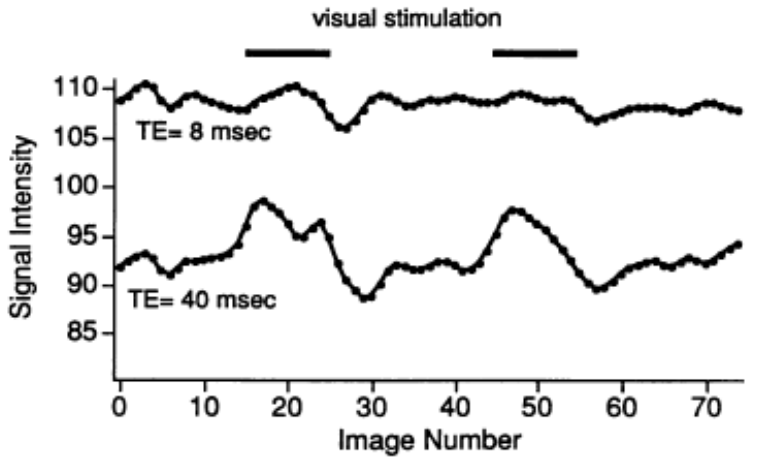

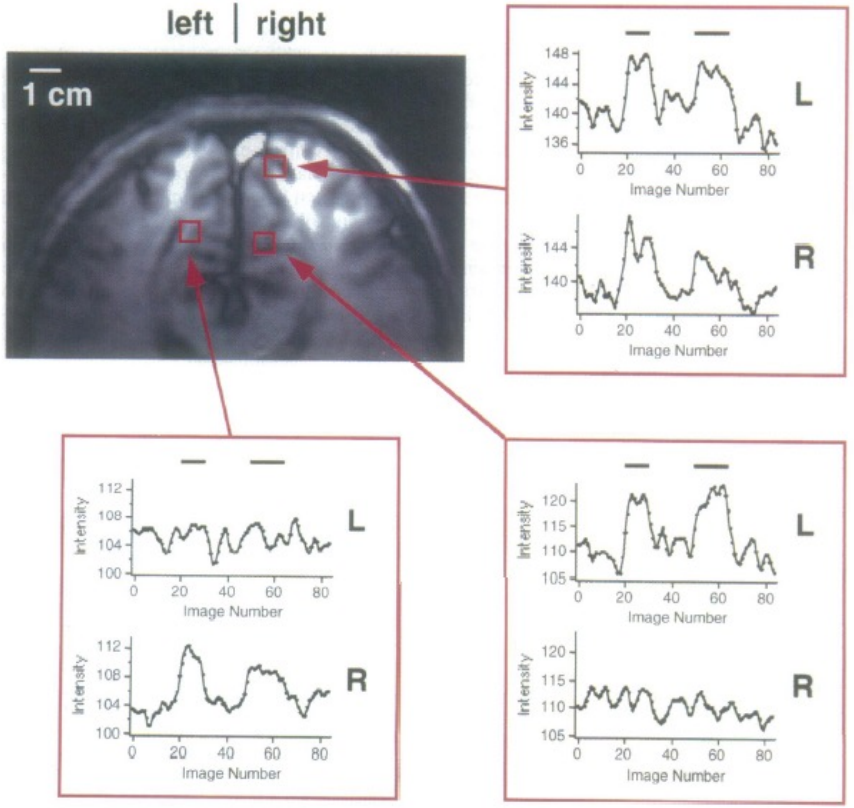

S. Ogawa, et al., (1992) “Intrinsic signal changes accompanying sensory stimulation: functional brain mapping with magnetic resonance imaging.” Proc. Natl. Acad. Sci. USA. 89, 5951-5955.

Single Shot Echo Planar Imaging (EPI)

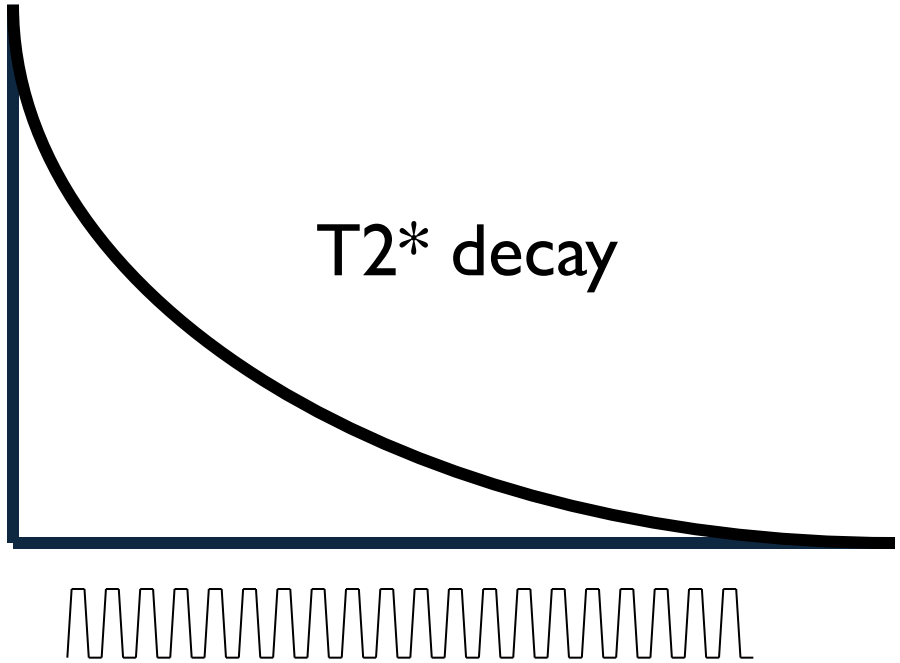

EPI Readout Window

≈ 20 to 40 ms

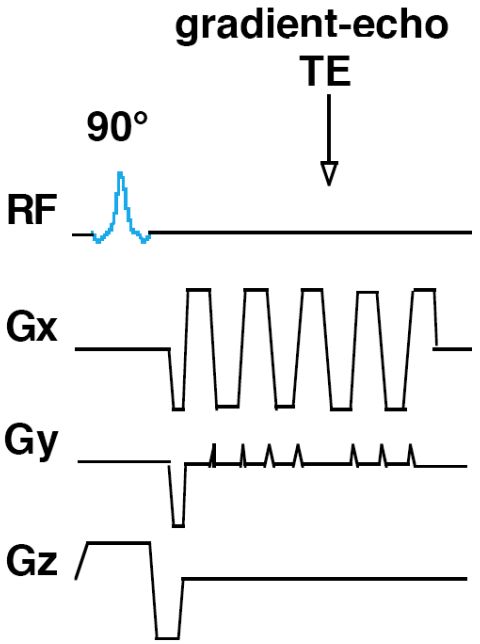

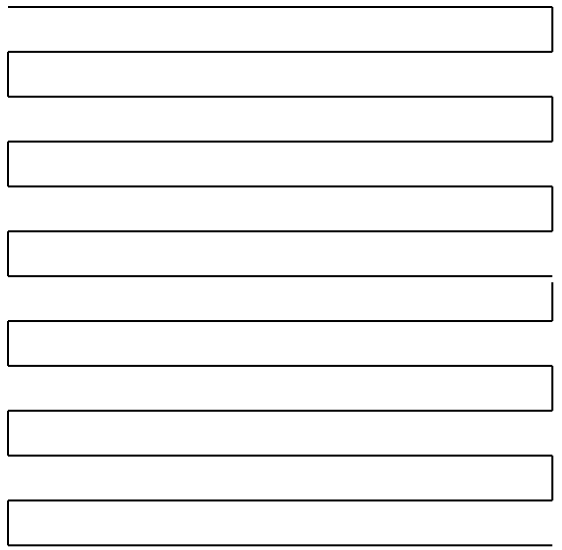

First Fast Imaging Approaches

1. MGH: ANMR retrofitted resonant gradient system with EPI (1.5T)

2. Minnesota: Standard gradients with Multi-shot with navigator echoes (4T)

3. MCW: local low-inductance gradient coil with EPI (1.5T)

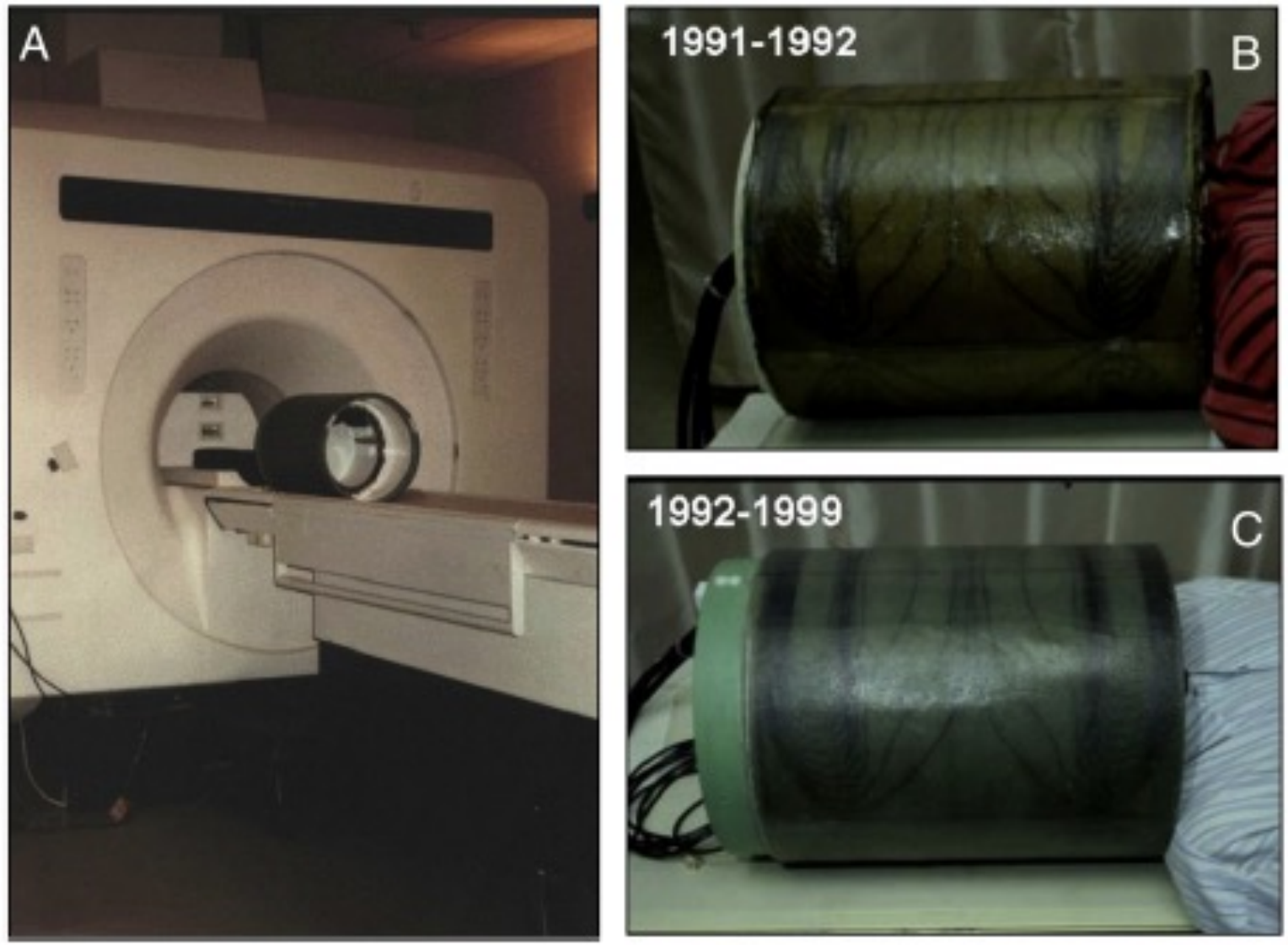

Setup at the Medical College of Wisconsin

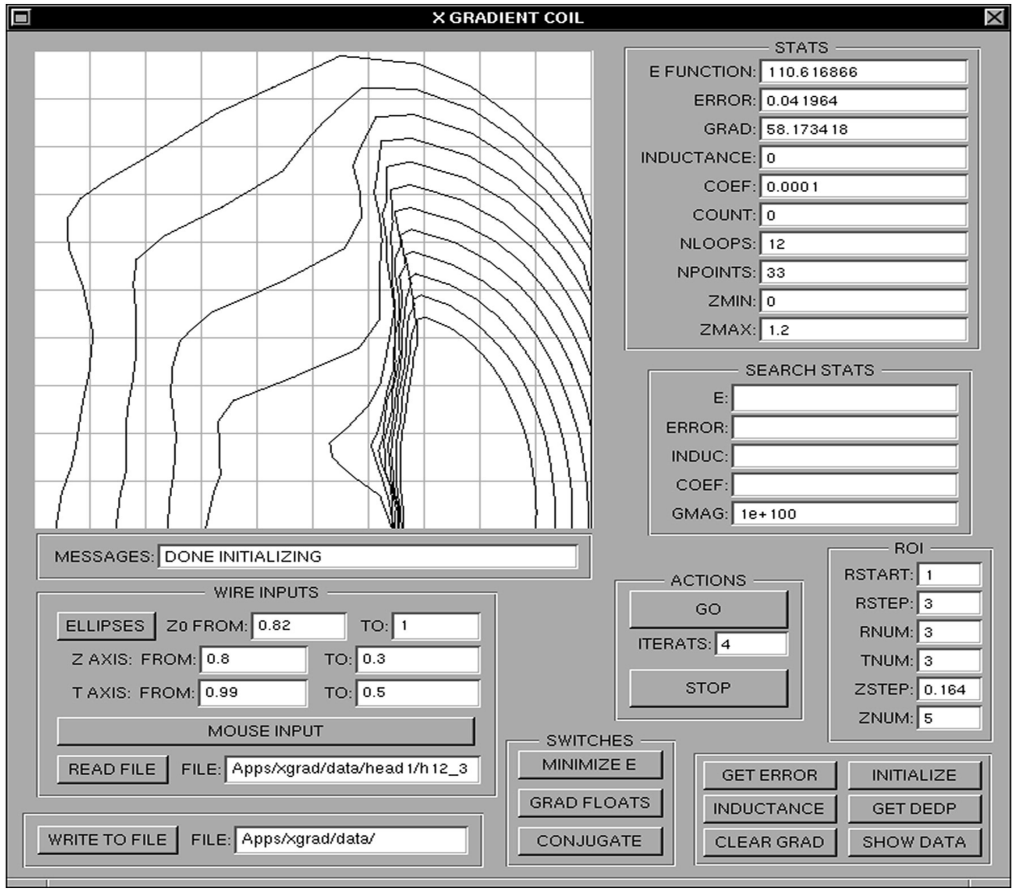

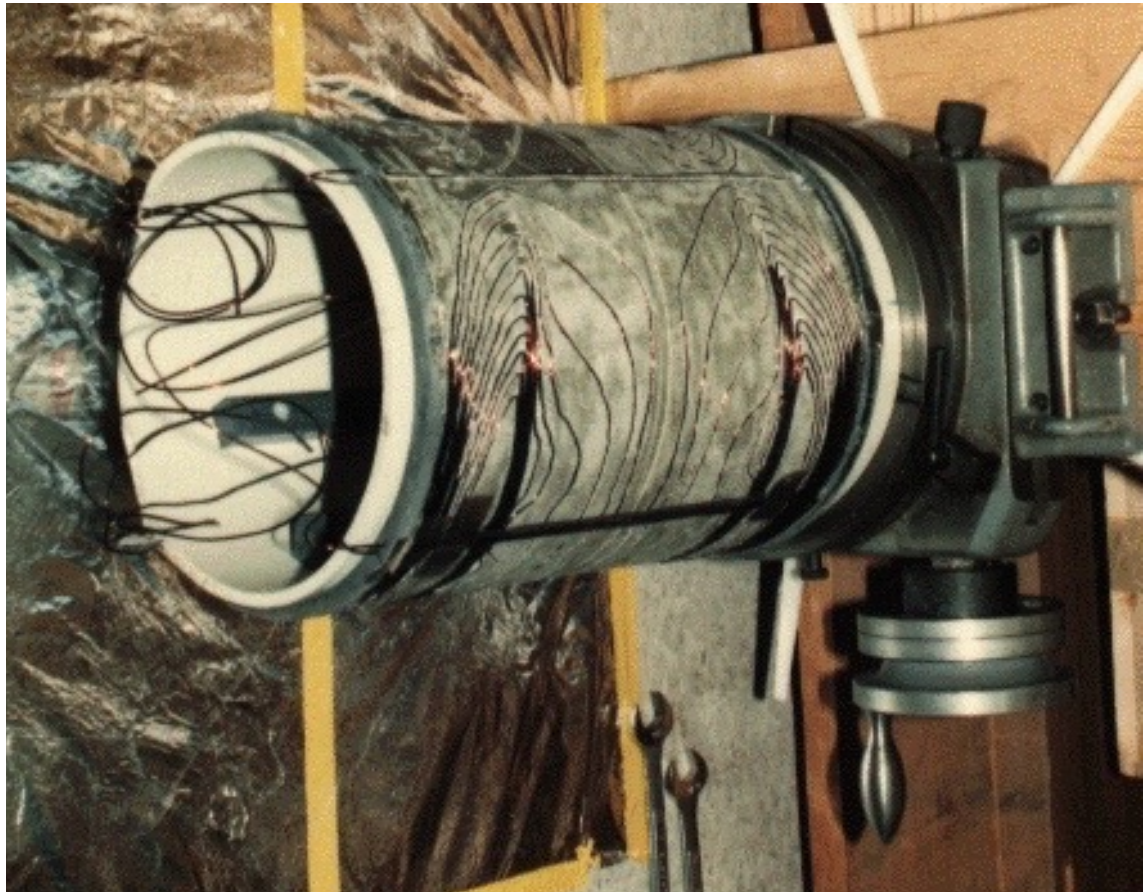

GUI for gradient descent gradient coil design tool. The design shown is one octant of the X gradient coil designed and built in August 1991. The program was written in Objective C and ran on a NeXT Cube computer.

NeuroImage, Volume 62, Issue 2, 2012, 660 - 664

http://dx.doi.org/10.1016/j.neuroimage. 2012.01.025

August, 1991

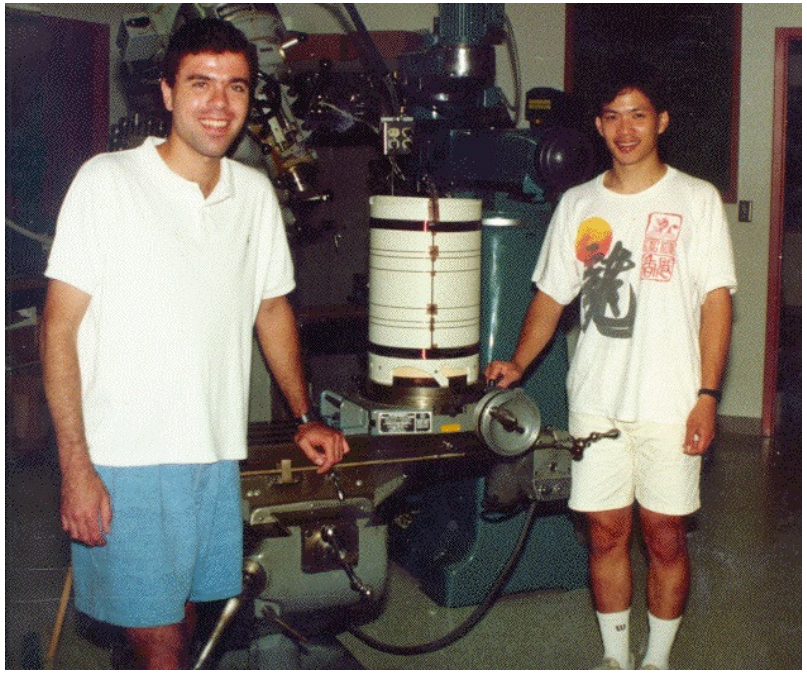

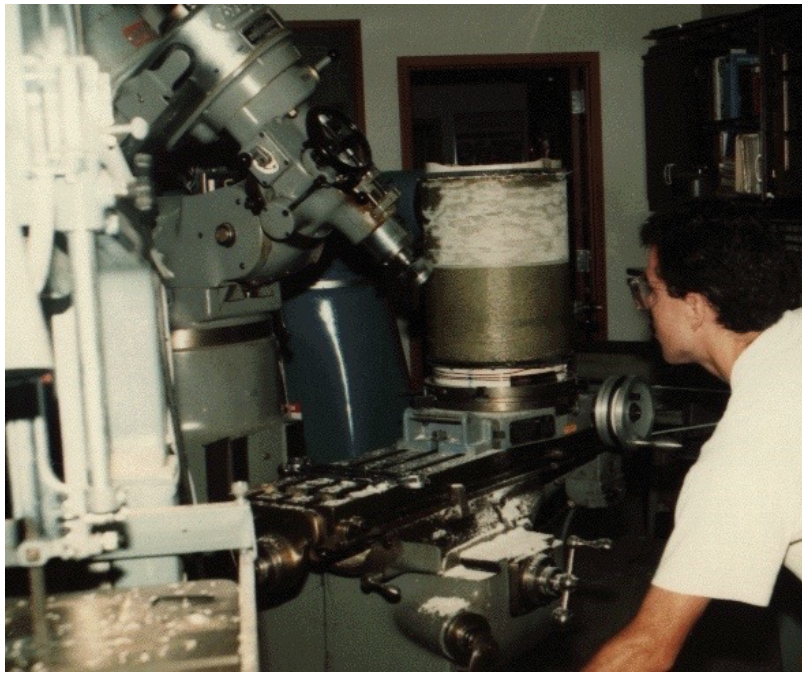

Later versions of the RF coils.

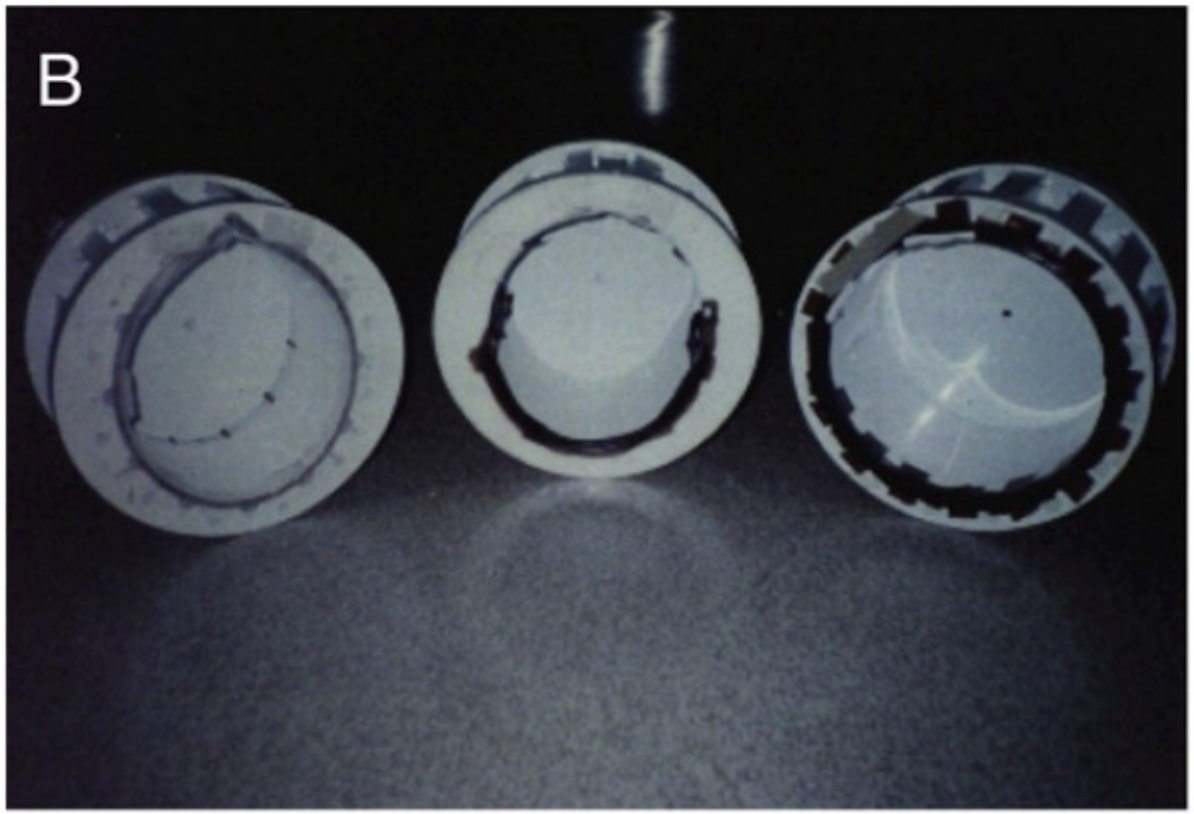

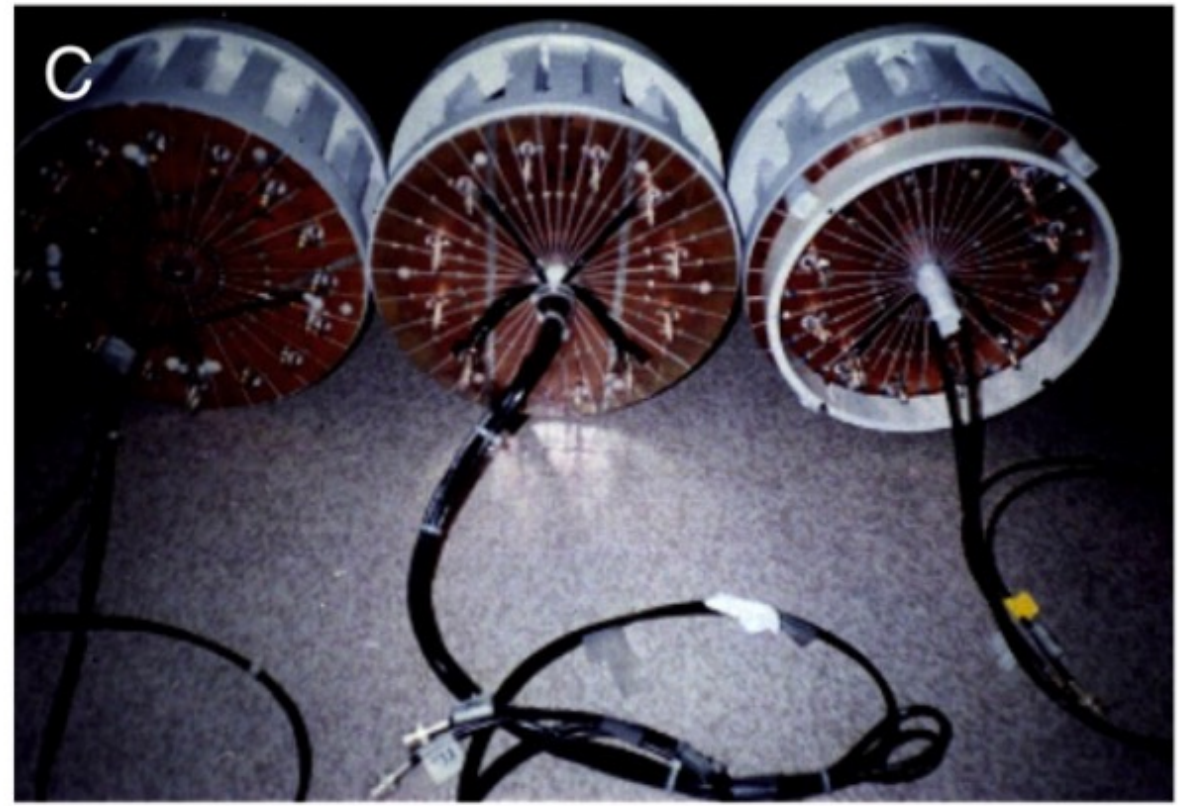

Initially could only do one slice…

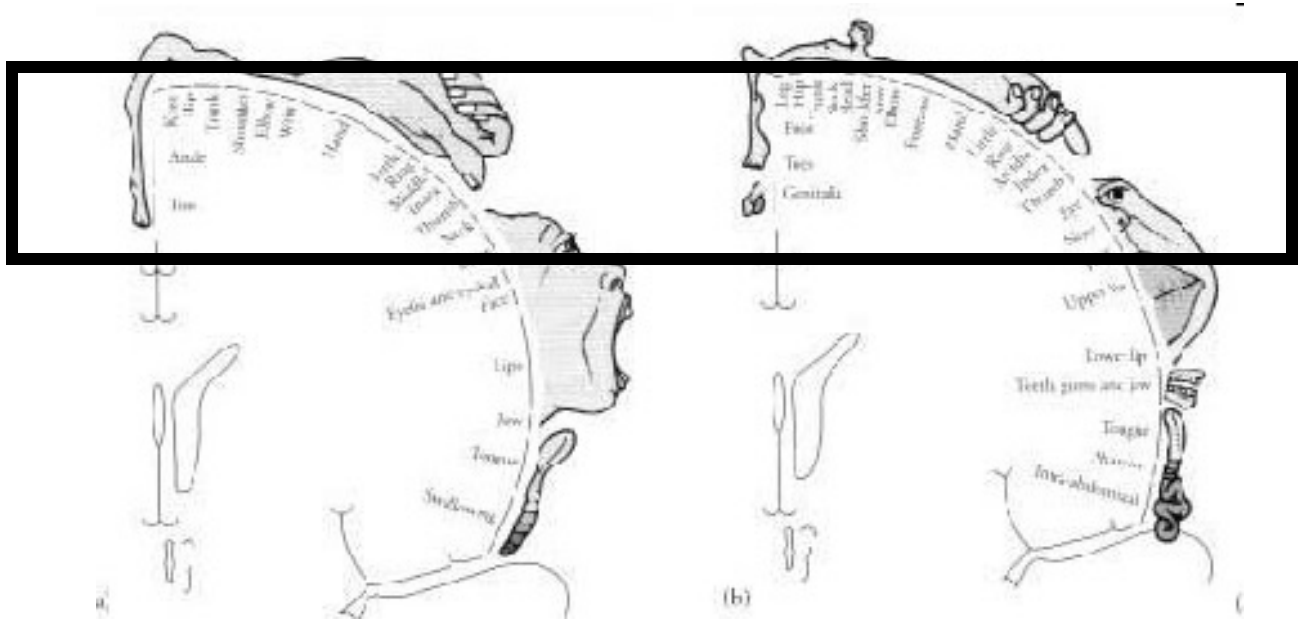

2.5 cm !

TR = 2 sec
TE = 50 ms
One slice
In plane 3.75 x 3.75

We didn't even need a gradient coil (but didn't realize this):

EPI at 5mm x 5mm x 5mm was quite possible using 100 amp gradient amplifiers and the whole body gradient coils…

Every scanner in the world in 1991 could have performed EPI-based fMRI at low resolution.

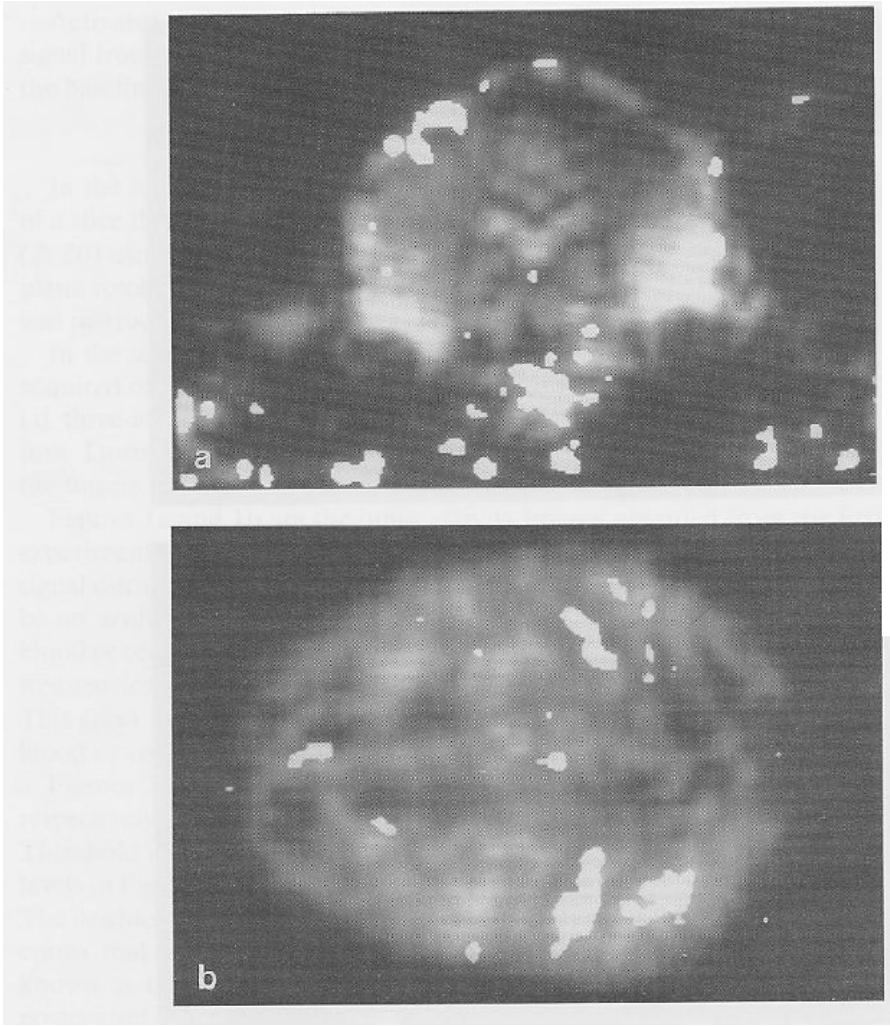

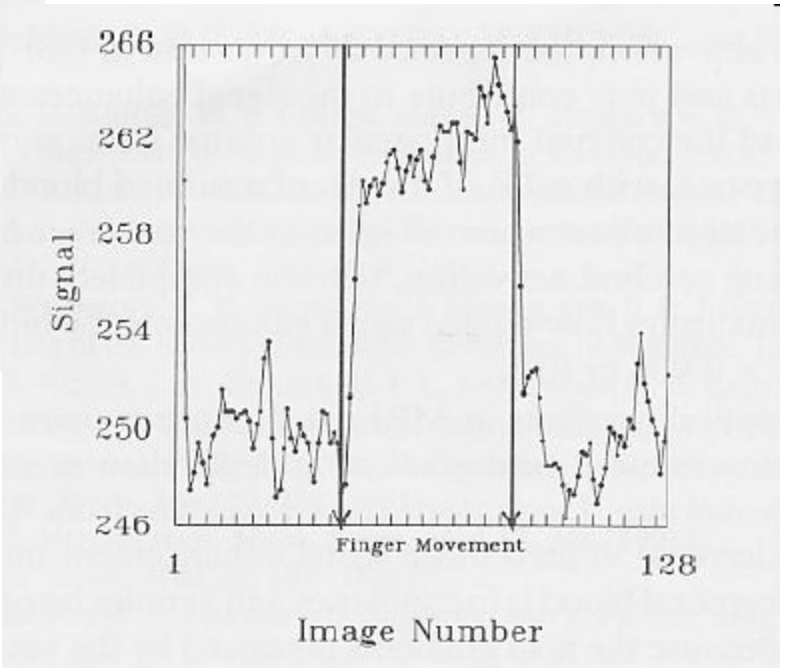

P. A. Bandettini, et al., (1992) “Time course EPI of human brain function during task activation.” Magn. Reson. Med 25, 390-397.

9-16-91 Results from dH61 (Sig ↑ upon stim?!!)

Experiment 1: Rest until 63 then move right fingers

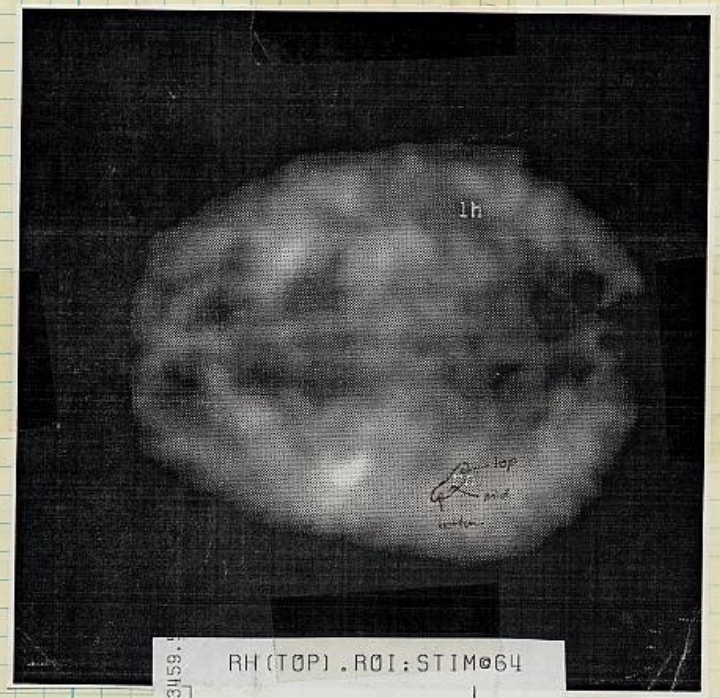

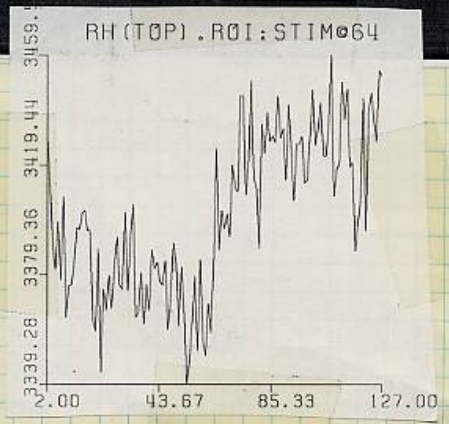

19

9-16-91

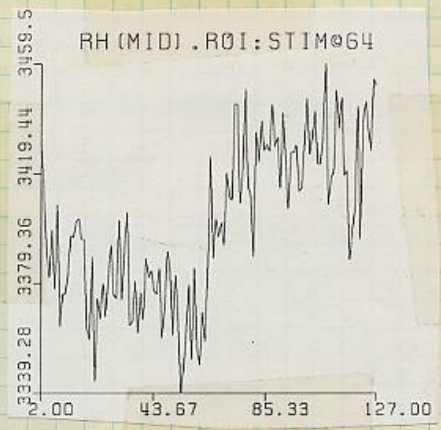

ROI's from p17

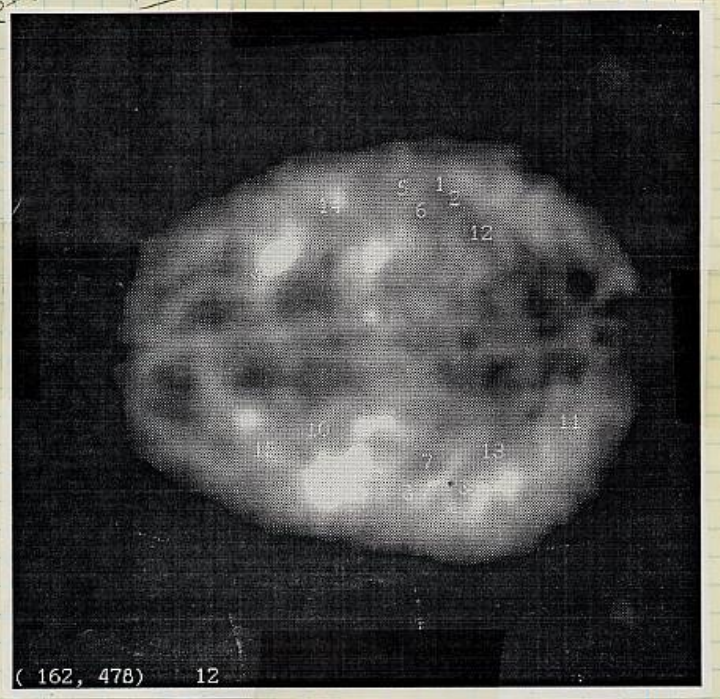

My brain: Alternating Tapping of Left Fingers then Right Fingers

1991

Brain Activity **No Brain Activity**

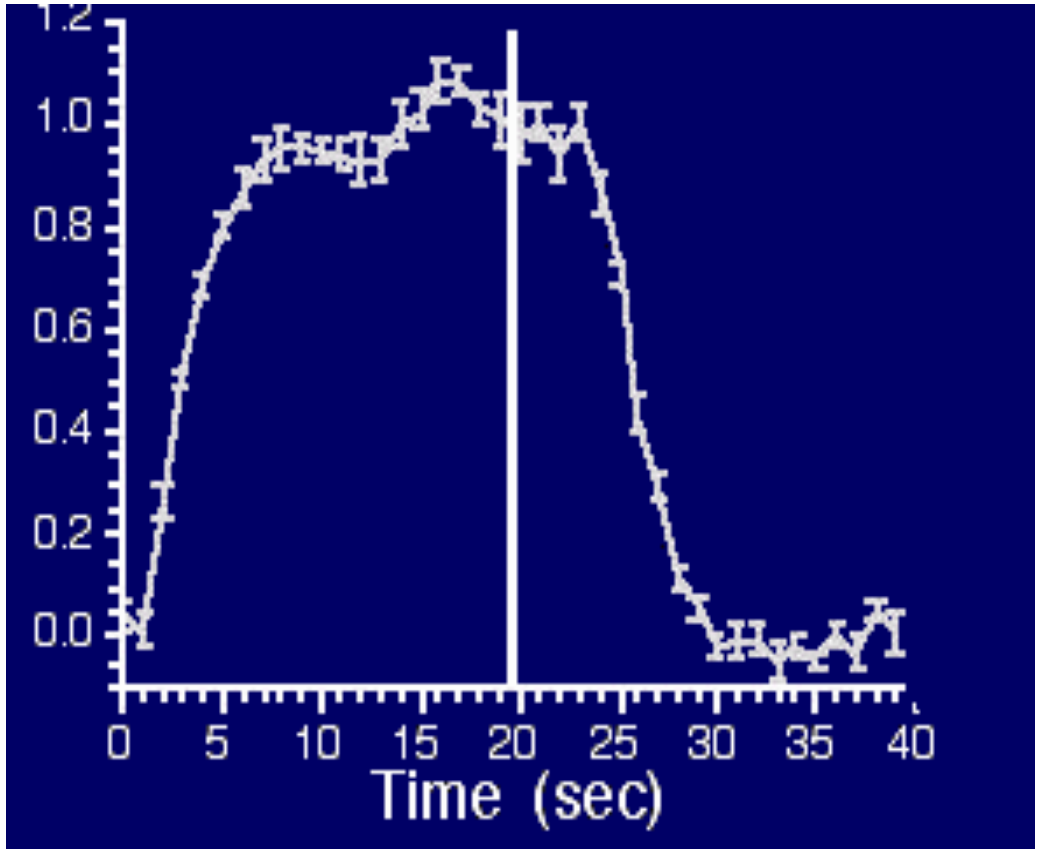

Why does BOLD signal increase?

OEF ↓

Therefore…

Blood PO_2 ↑

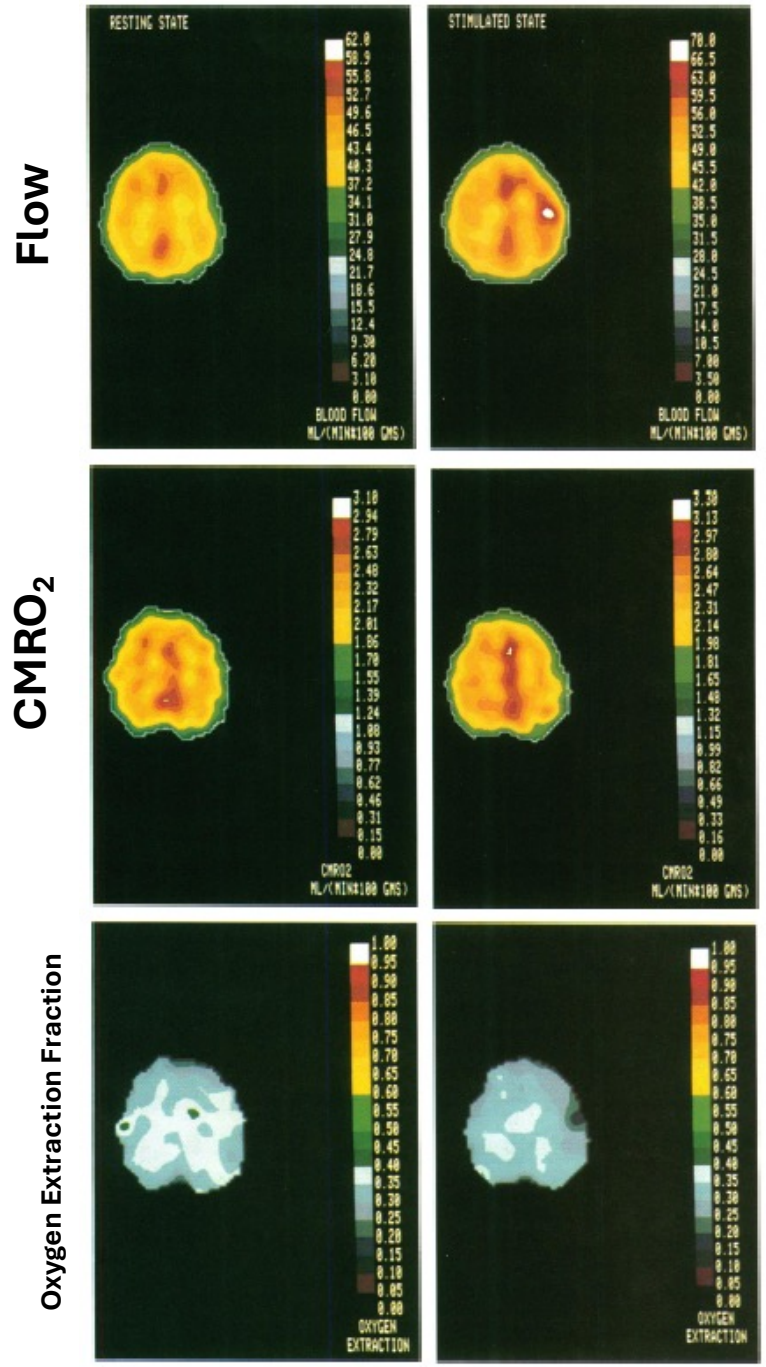

Proc. Natl. Acad. Sci. USA
Vol. 83, pp. 1140–1144, February 1986
Neurobiology

Focal physiological uncoupling of cerebral blood flow and oxidative metabolism during somatosensory stimulation in human subjects

(positron emission tomography)

PETER T. FOX*†‡ AND MARCUS E. RAICHLE*†

*Department of Neurology and Neurological Surgery (Neurology), †Department of Radiology (Radiation Sciences), and The McDonnell Center for Studies of Higher Brain Function, Washington University School of Medicine, St. Louis, MO 63110

Communicated by Oliver H. Lowry, October 7, 1985

FIG. 1. Physiological uncoupling of brain blood flow and metabolism. (*Left*) Resting-state measurements. (*Right*) Stimulated-state measurements (unilateral vibrotactile stimulation of the fingers). All images are from a single subject's scanning session and pass through the same brain plane. Color scales are linear with the maxima set at a fixed multiple (1.6) of the global average, to facilitate visual comparisons (16). During specific somatosensory stimulation a marked focal increase in CBF (29% of mean, nine subjects, three trials per subject) was produced in the contralateral sensorimotor cortex. The observed increase in the $CMRo_2$ was much smaller (5% of mean, nine subjects, three trials per subject) and failed to attain significance. This physiological uncoupling of CBF and $CMRo_2$ flow produced a highly significant decrease in the local OEF (−19% of mean), indicating that tissue Po_2 (and probably pH) rose during stimulation. Note that, although the data were analyzed as contralateral/ipsilateral ratios (see text and Tables 1–4), the disparity between blood flow and metabolism was evident from the raw data and was not dependent on a particular strategy of analysis.

UV visible spectrum used to assess blood volume and oxygenation changes

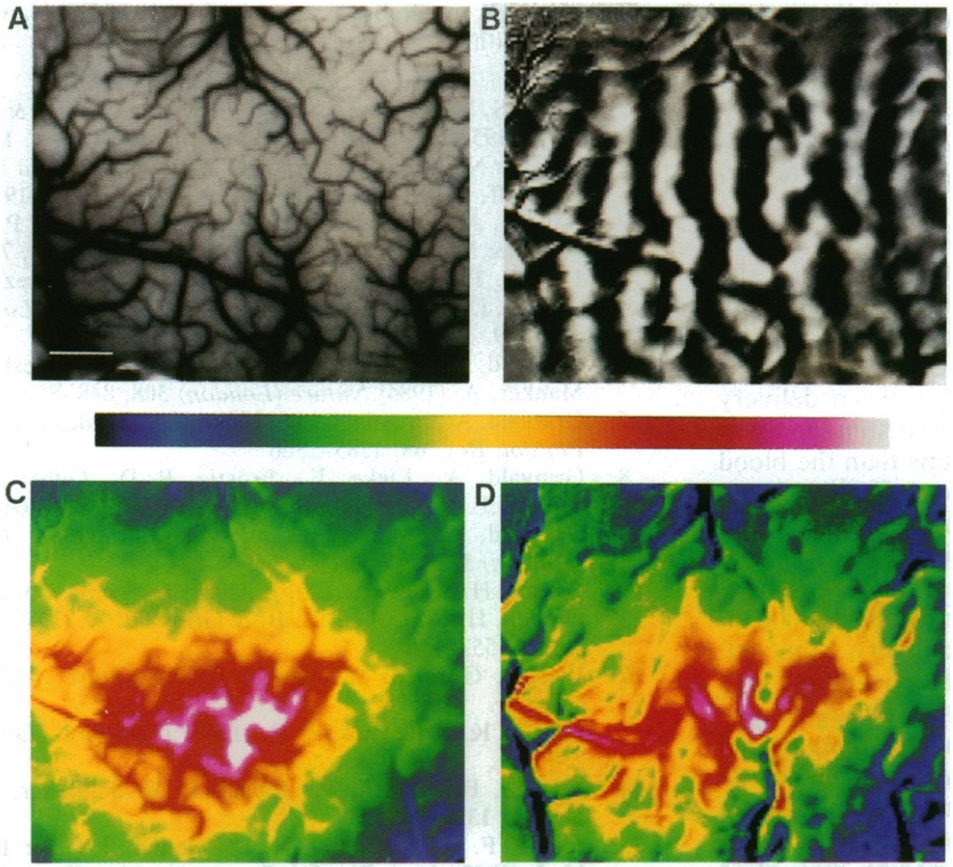

FIG. 4. Comparison of cortical maps of ocular dominance, blood volume, and the oxygen delivery changes. (*A*) Picture of the cortical surface taken at 570 nm. (*B*) Picture of the ocular dominance column. (*C*) Map of the local blood volume change (570 nm). The stimulus was a drifting bar covering only a field of 0.5 × 0.7°. Single unit recordings showed that this stimulus activated the right ocular dominance columns in a small cortical region of ≈1 × 2.5 mm. (This small visual stimulus was about half the size used to obtain the ocular dominance map in *B*.) (*D*) Map obtained at 600 nm. To facilitate the comparison, the scaling of the two pseudo-color maps was normalized to the size of the reflection signal at the two wavelengths (see text for quantitative comparison). Color scale: the white and red edge shows the largest absorption increase or reflection decrease. (Bar = 1 mm.)

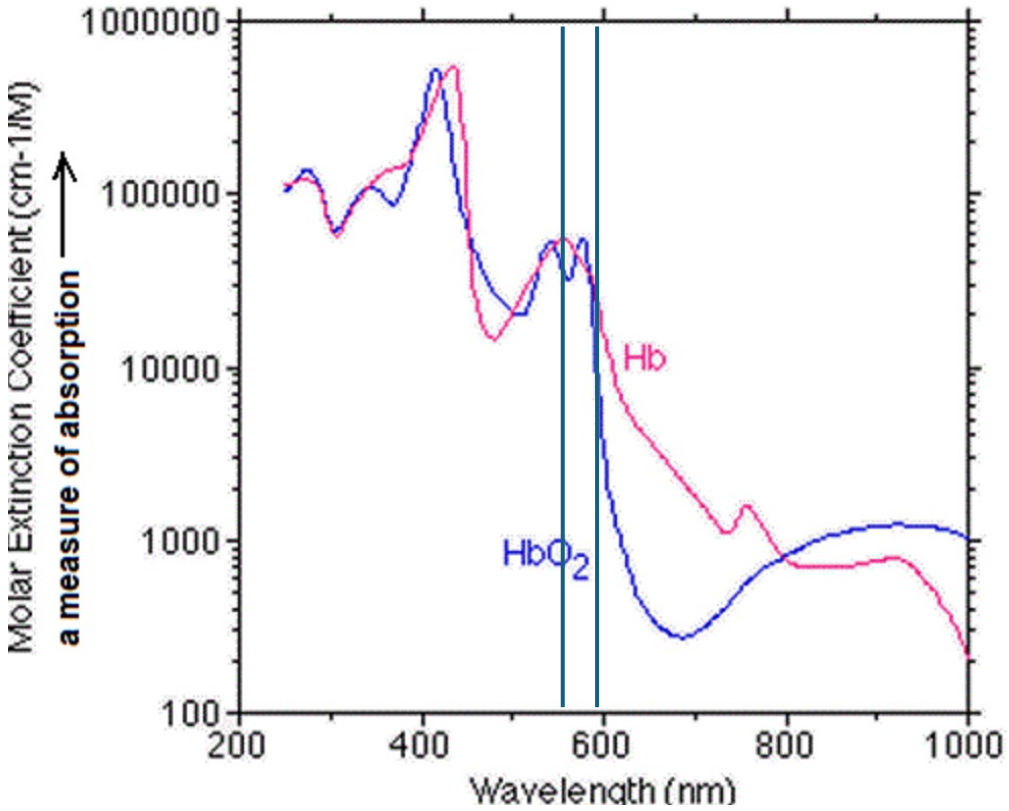

oxygenated

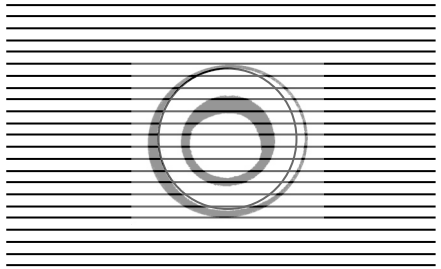

deoxygenated

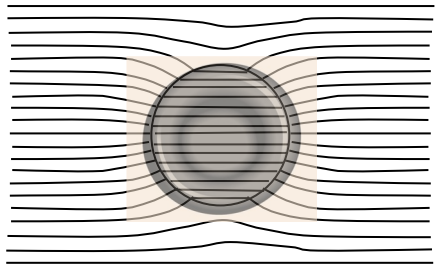

Deoxy-hemoglobin: *distorts field, short T2*,* ***low signal***

Oxy-hemoglobin: *no distortions, longer T2*,* ***higher signal***

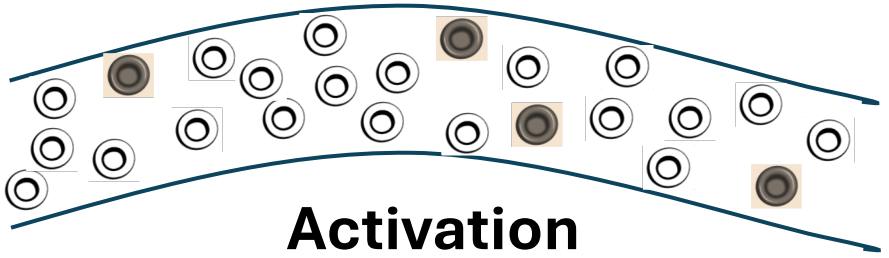

Activation

Blood volume

Blood flow

Blood oxygenation
…higher signal

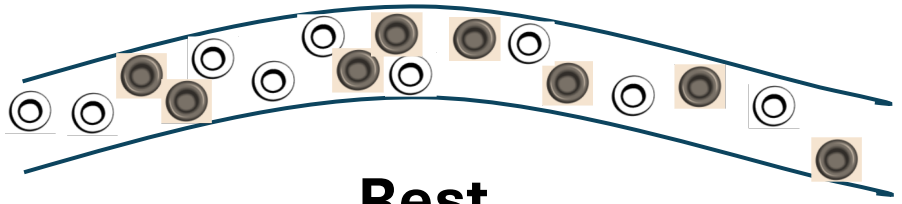

Rest

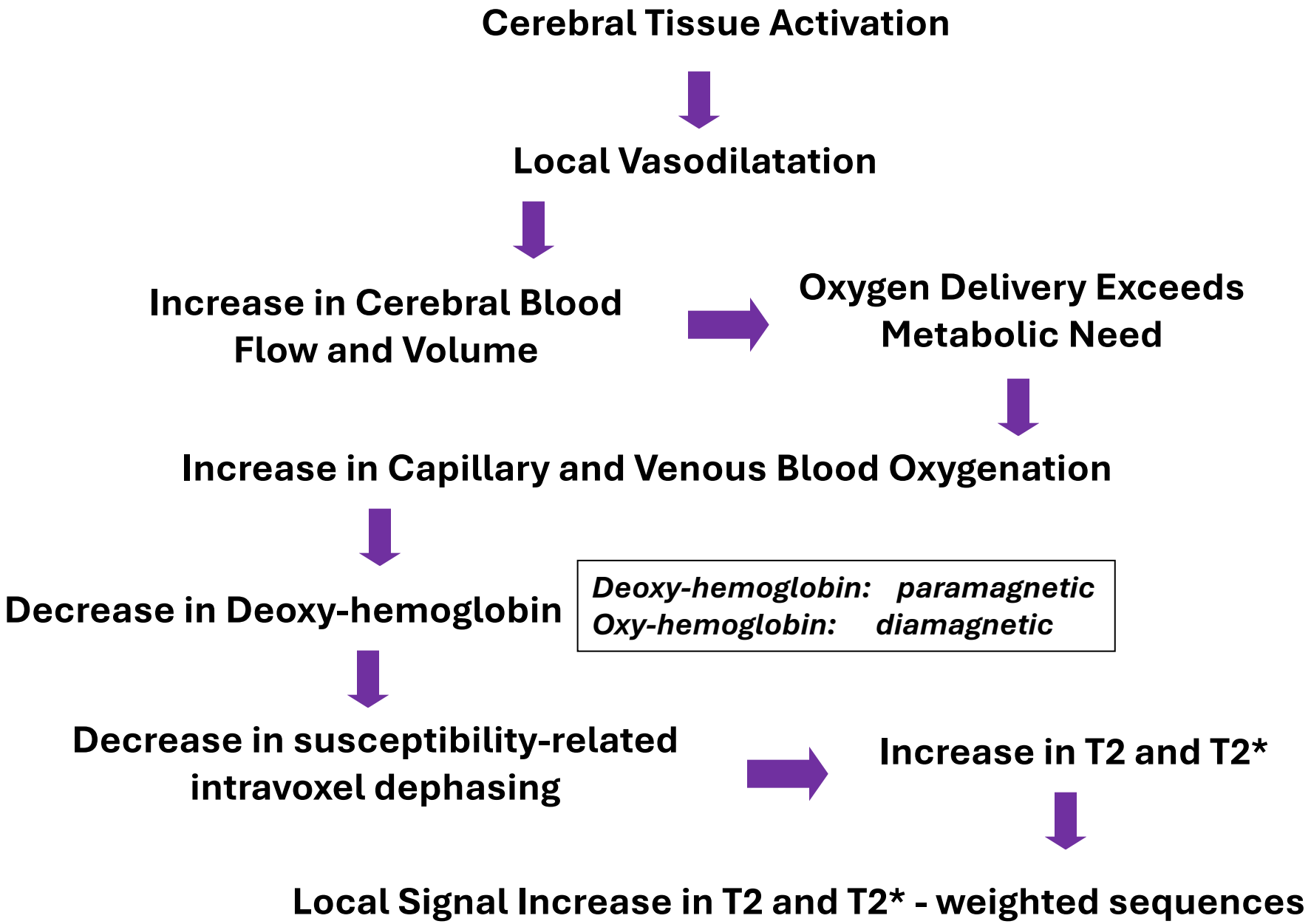
Cerebral Tissue Activation
Local Vasodilatation
Increase in Cerebral Blood Flow and Volume
Oxygen Delivery Exceeds Metabolic Need
Increase in Capillary and Venous Blood Oxygenation
Decrease in Deoxy-hemoglobin
Deoxy-hemoglobin: paramagnetic
Oxy-hemoglobin: diamagnetic
Decrease in susceptibility-related intravoxel dephasing
Increase in T2 and T2*
Local Signal Increase in T2 and T2* - weighted sequences

The ”Coupling Controversy”

Sokolof versus Fox

Sokoloff:

- Flow is coupled via metabolic demand, especially oxidative metabolism.
- Large flow increases with small measured CMRO changes likely reflect measurement issues or complex metabolic responses, not true uncoupling.

Fox:

- Activation can produce disproportionate CBF/CBV increases, with relatively smaller CMRO changes—thus a functional uncoupling between flow and oxidative metabolism.
- Flow is driven by vasoactive signals linked to neuronal activity, and these can oversupply oxygen and glucose, leading to BOLD-relevant changes in oxygenation without matching metabolic consumption.

Fox PT. The coupling controversy. Neuroimage. 2012 Aug 15;62(2):594-601. doi: 10.1016/j.neuroimage.2012.01.103. Epub 2012 Jan 28. PMID: 22306802; PMCID: PMC4019339.

1992 : first BOLD fMRI papers published

- K. K. Kwong, et al, (1992) “Dynamic magnetic resonance imaging of human brain activity during primary sensory stimulation.” Proc. Natl. Acad. Sci. USA. 89, 5675-5679.
- **1.5T EPI using ”retrofitted” gradient, Perfusion and BOLD, comparison with PET, visual, motor**

- S. Ogawa, et al., (1992) “Intrinsic signal changes accompanying sensory stimulation: functional brain mapping with magnetic resonance imaging.” Proc. Natl. Acad. Sci. USA. 89, 5951-5955.
- **4T, multi-echo, echo time comparison, high resolution. Visual**

- P. A. Bandettini, et al., (1992) “Time course EPI of human brain function during task activation.” Magn. Reson. Med 25, 390-397.
- **1.5T, local head gradient coil, motor whole brain coil, left and right motor cortex.**

- Blamire, A. M., et al. (1992). “Dynamic mapping of the human visual cortex by high-speed magnetic resonance imaging.” Proc. Natl. Acad. Sci. USA 89: 11069-11073.
- **Event-related fMRI**

- Frahm, J., et al (1992) “Dynamic MR Imaging of Human Brain Oxygenation During Rest and Photic-Stimulation.” Journal of Magnetic Resonance Imaging, 2, 501-505.
- **High resolution, multi-shot, 1.5T**

Activation Statistics

Time series of images

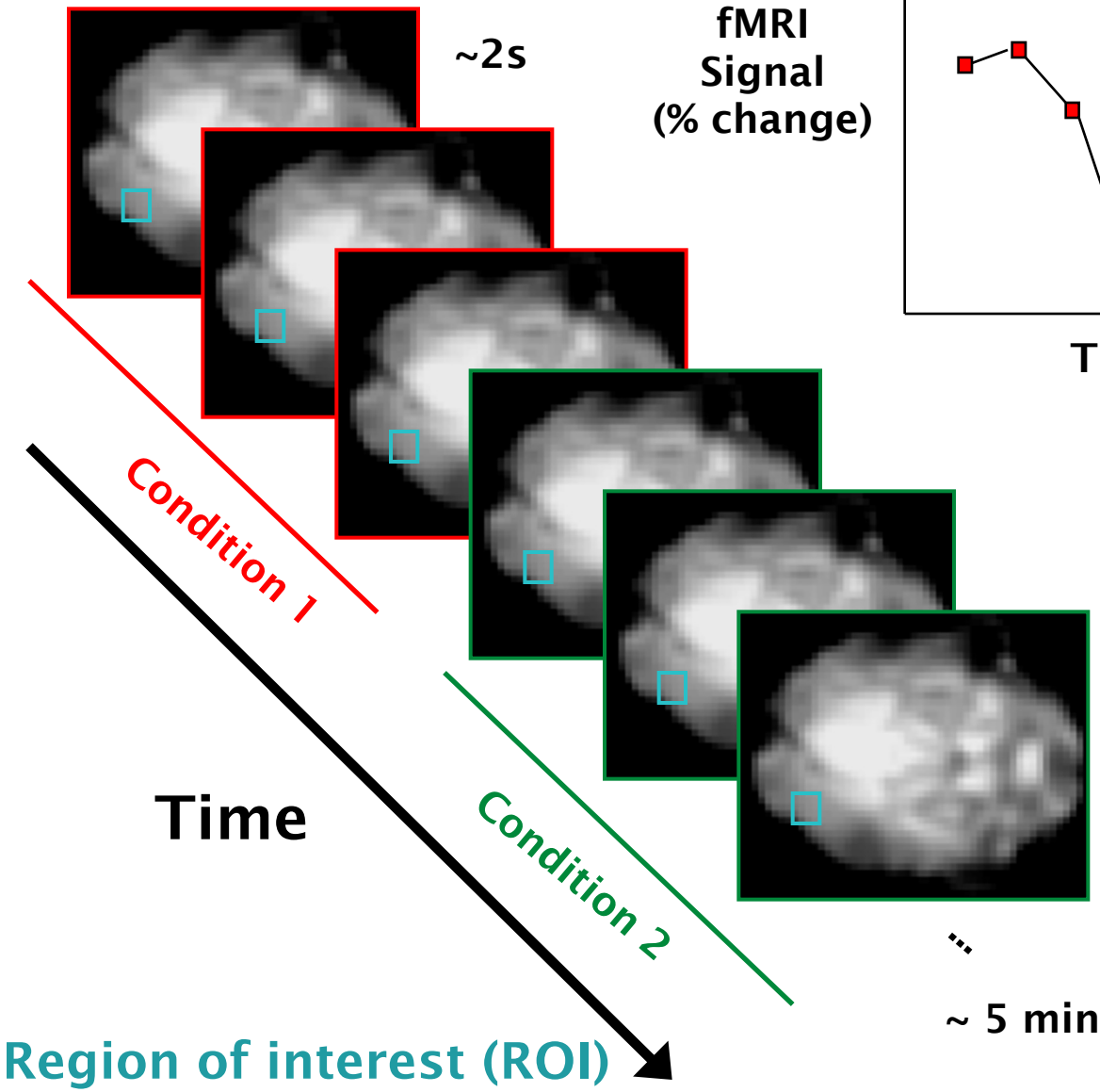

fMRI Signal (% change)

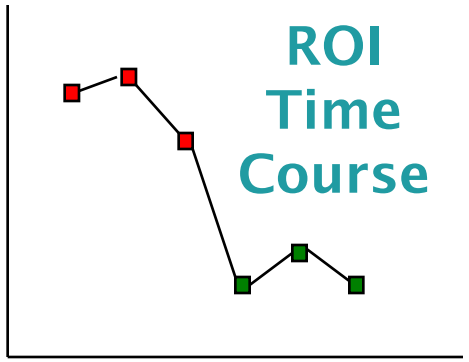

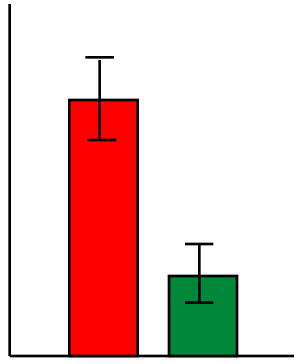

Statistical Map
superimposed on anatomical MRI image

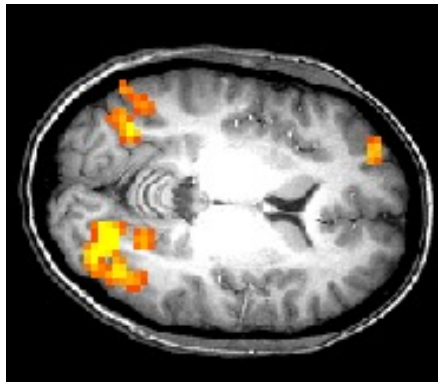

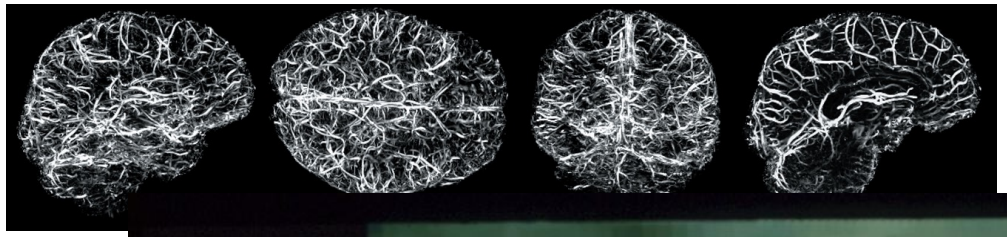

Ven

Fiber

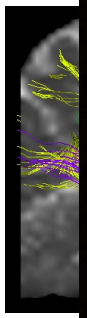

An

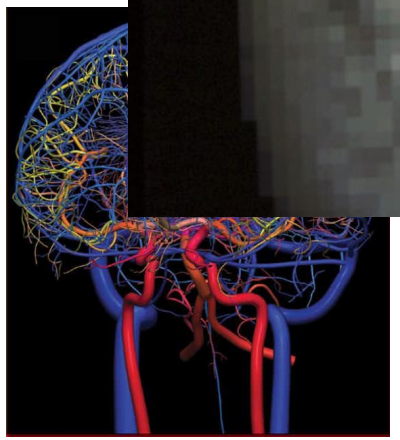

Functional MRI or fMRI

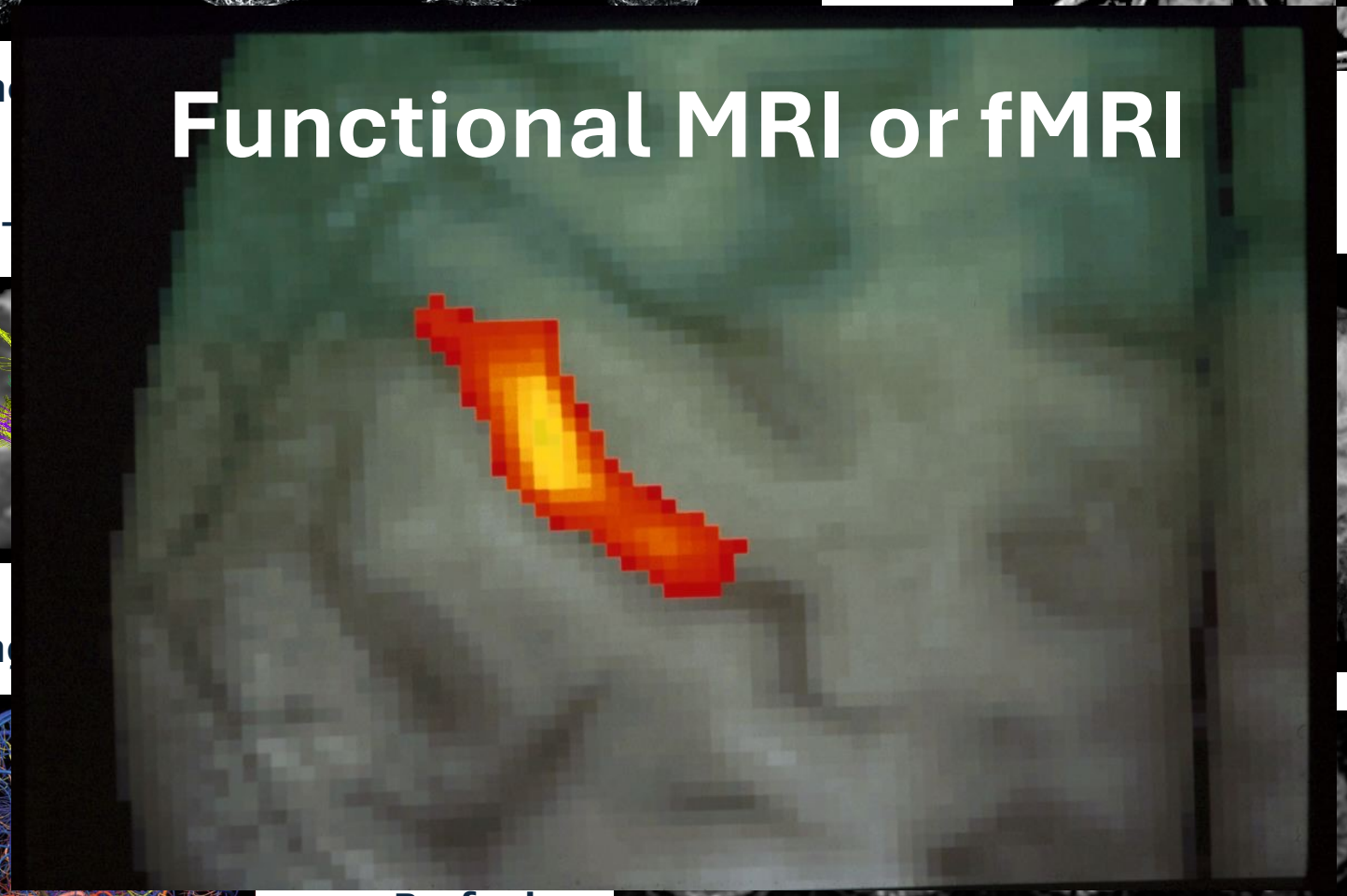

Perfusion

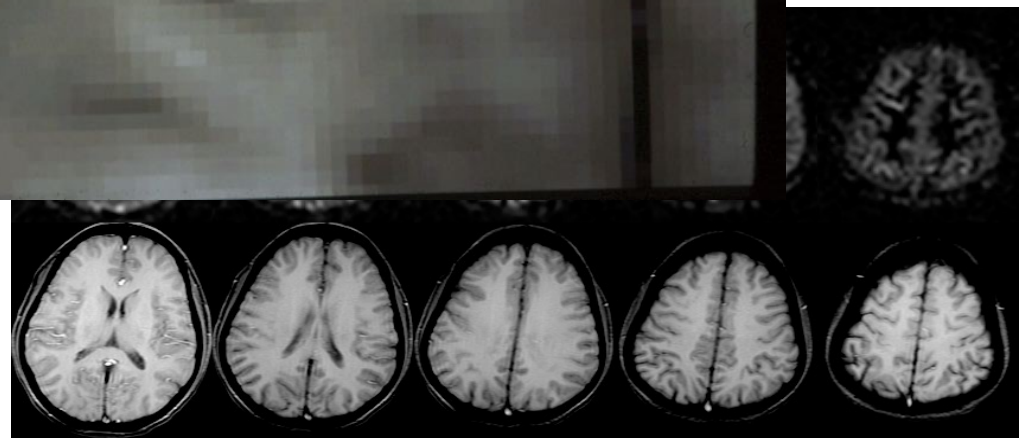

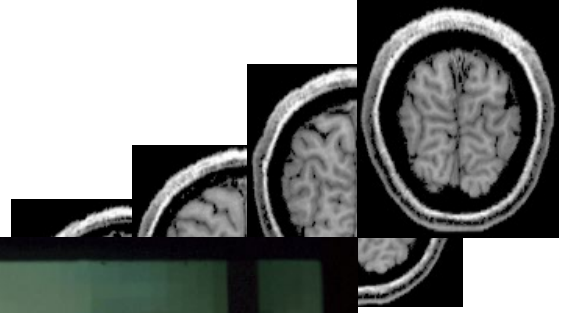

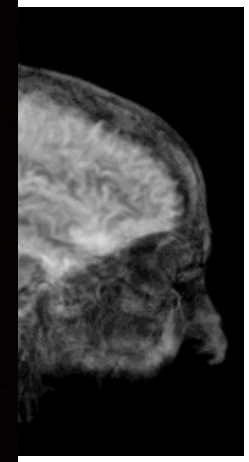

First Studies

Primary visual, auditory, motor
Dynamics: Long, Short durations, Duty cycle
Biophysical and Dynamic Modeling
Parametric variation of intensity
Comparisons with PET, MEG, etc..
Field Strength Comparisons
Pulse Sequence Sensitivity Comparisons
Resolution Comparisons
Studying the noise....leading to resting state.
Modulating the signal by CO_2, O_2, breath hold, etc..

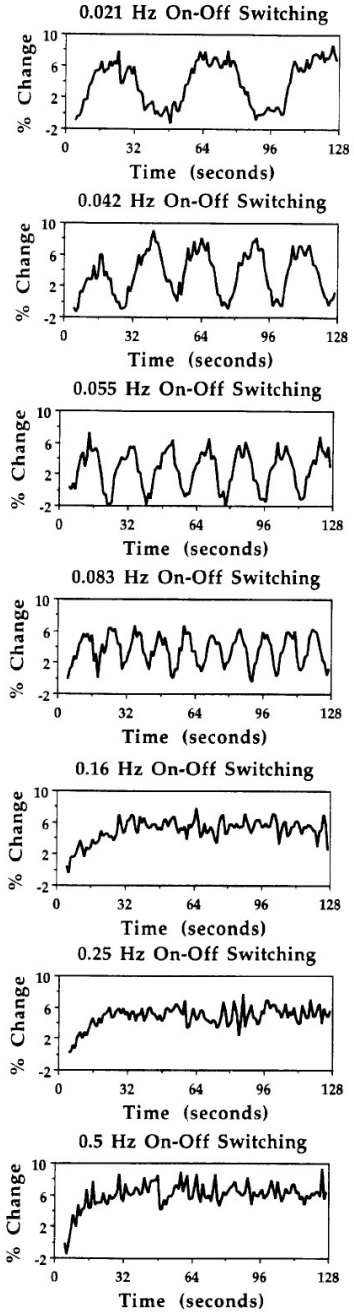
0.021 Hz On-Off Switching
0.042 Hz On-Off Switching
0.055 Hz On-Off Switching
0.083 Hz On-Off Switching
0.16 Hz On-Off Switching
0.25 Hz On-Off Switching
0.5 Hz On-Off Switching
% Change
Time (seconds)

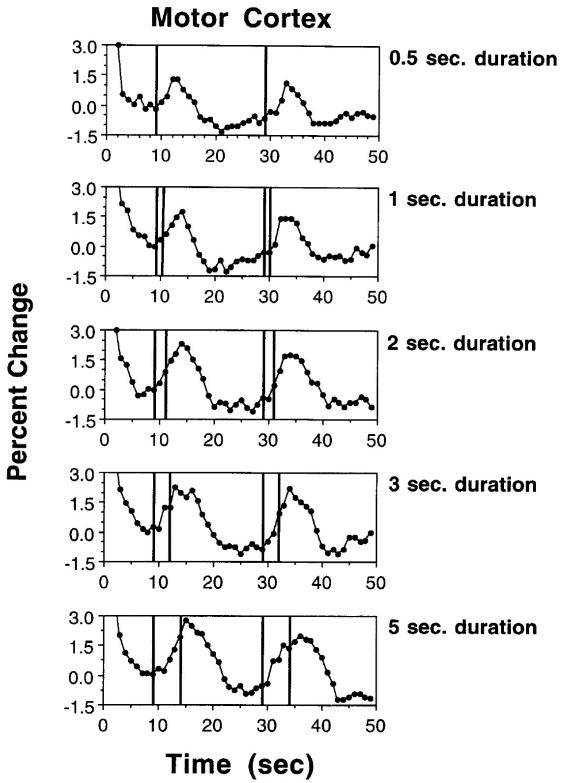
Motor Cortex
0.5 sec. duration
1 sec. duration
2 sec. duration
3 sec. duration
5 sec. duration
Percent Change
Time (sec)

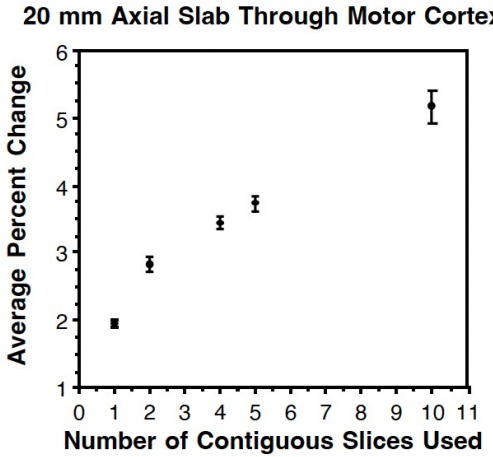
20 mm Axial Slab Through Motor Cortex
Average Percent Change
Number of Contiguous Slices Used

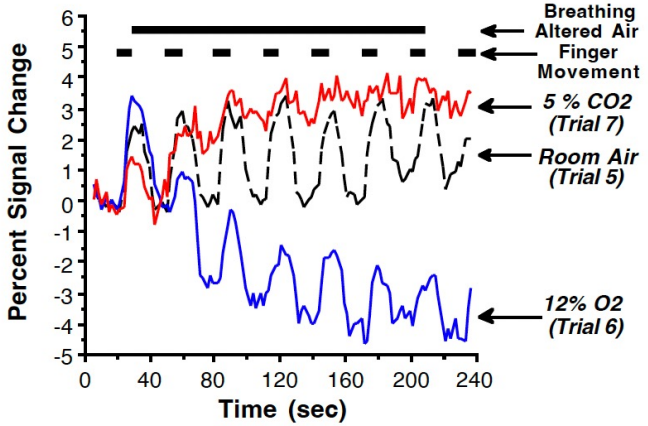
Breathing
Altered Air
Finger Movement
5 % CO2 (Trial 7)
Room Air (Trial 5)
12% O2 (Trial 6)
Percent Signal Change
Time (sec)

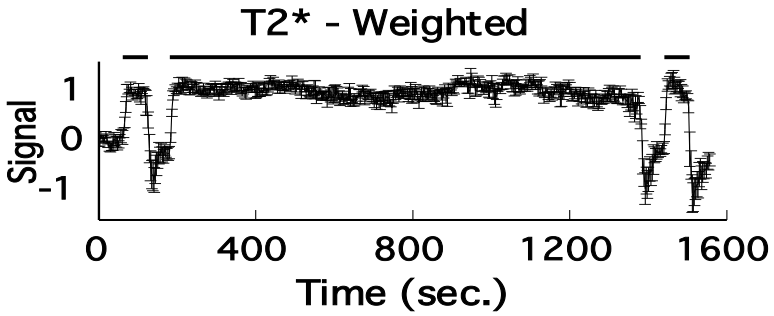
T2* - Weighted
Signal
Time (sec.)

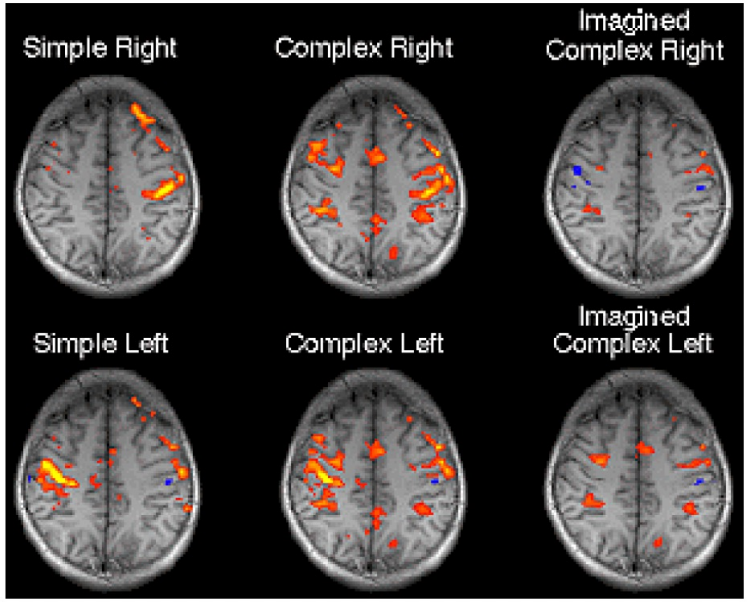
Simple Right
Complex Right
Imagined Complex Right
Simple Left
Complex Left
Imagined Complex Left

Motor Cortex

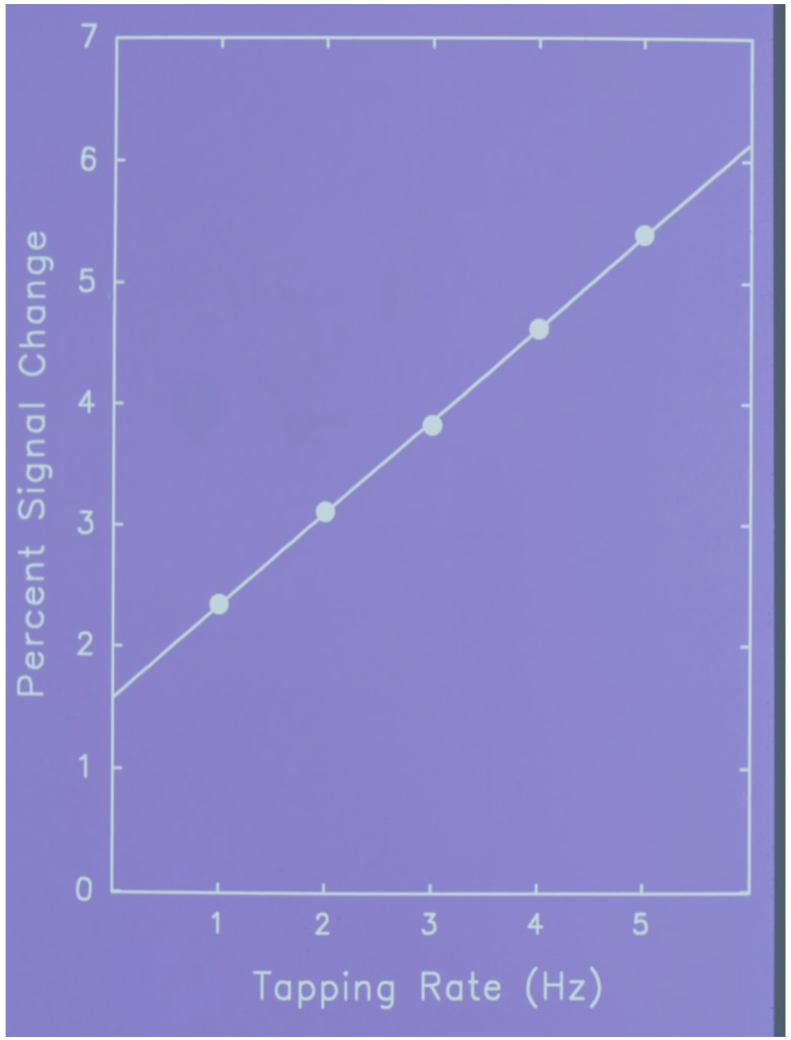

S. M. Rao et al, (1996) "Relationship between finger movement rate and functional magnetic resonance signal change in human primary motor cortex." *J. Cereb. Blood Flow and Met.* 16, 1250-1254.

Auditory Cortex

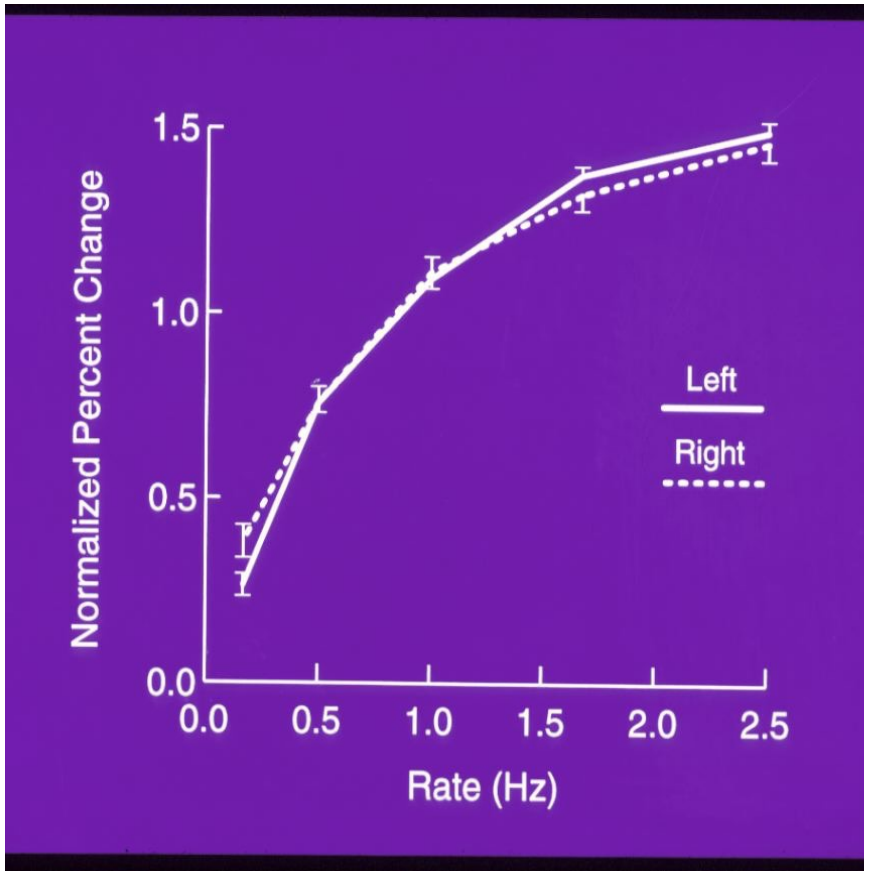

J. R. Binder, et al, (1994). "Effects of stimulus rate on signal response during functional magnetic resonance imaging of auditory cortex." *Cogn. Brain Res.* 2, 31-38

Topographical Mapping

If parametrically varied stimuli produces a varying spatial topography, then a powerful paradigm/processing approach is to cycle through a continuously varying stimuli.

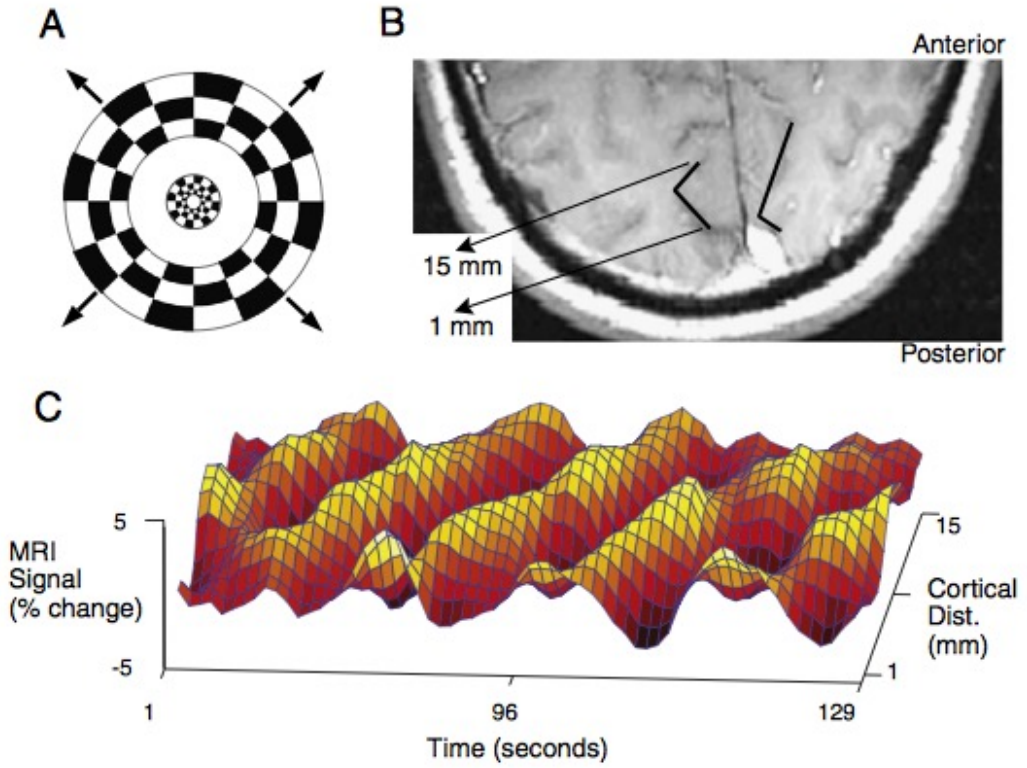

S. A. Engel, et al. Nature 369, (1994)

Differentiating Visual Areas: Retinotopy

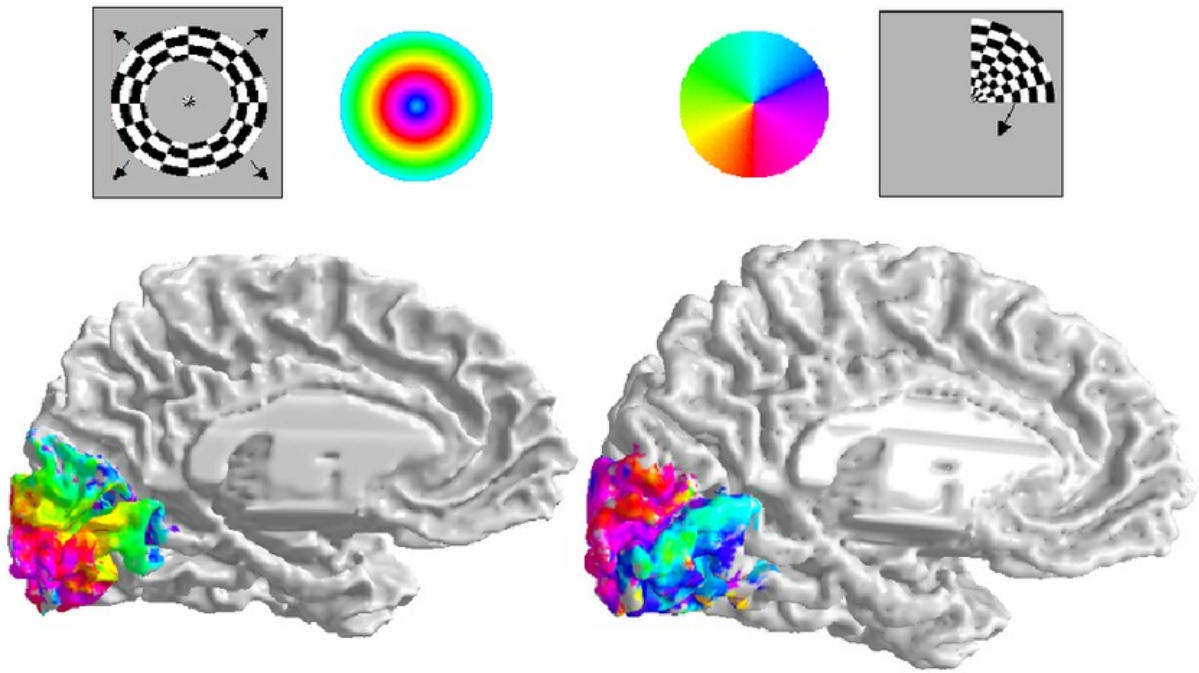

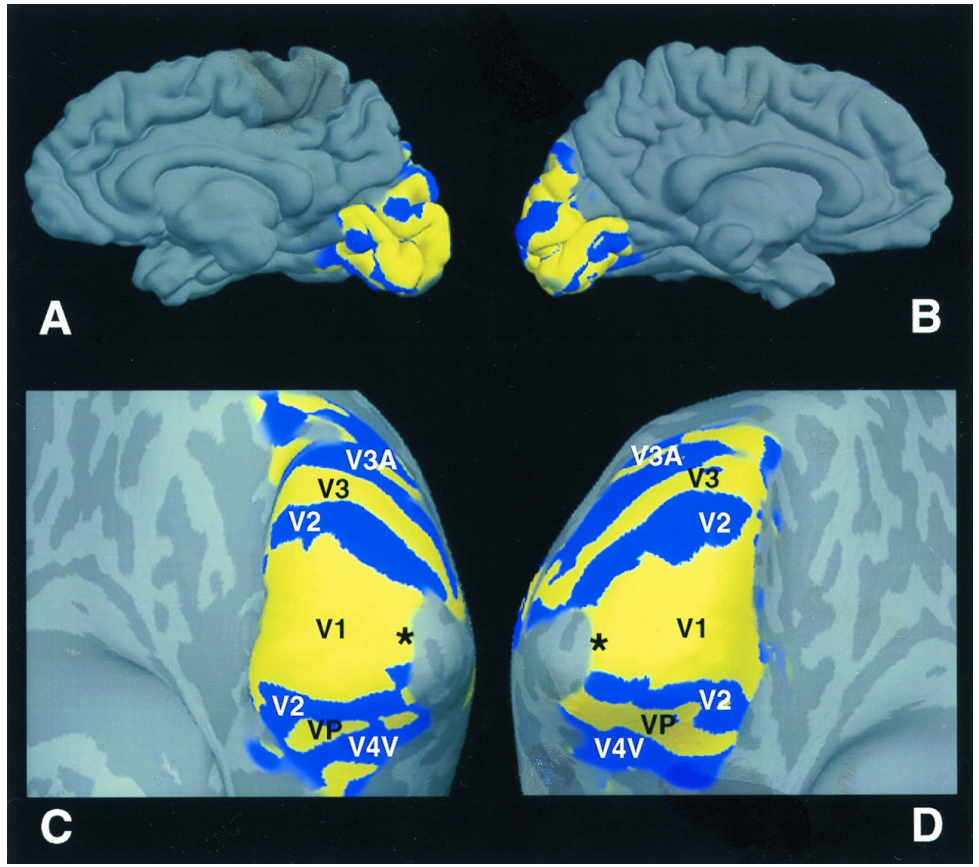

R. B. Tootell, et al. PNAS 95: 811-817, (1998)

The human brain is the most complex system known

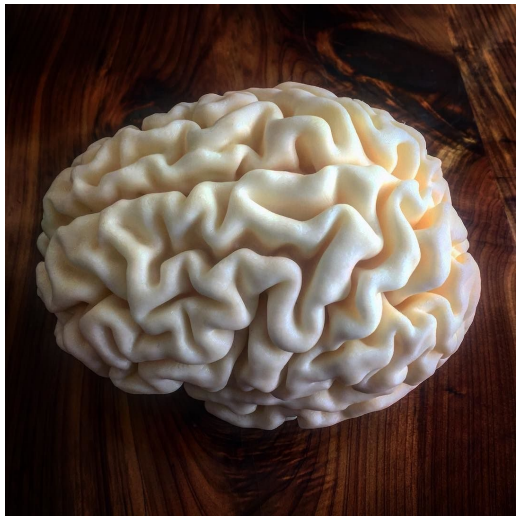

- 86 billion neurons
- 16,000 cortical neurons per mm^3
- 128,000 cortical neurons per $2mm^3$ voxel
- 1,000 trillion connections
- Impulses travel 200mph
- Weights 3 lbs
- Uses 23 Watts (1 light bulb)

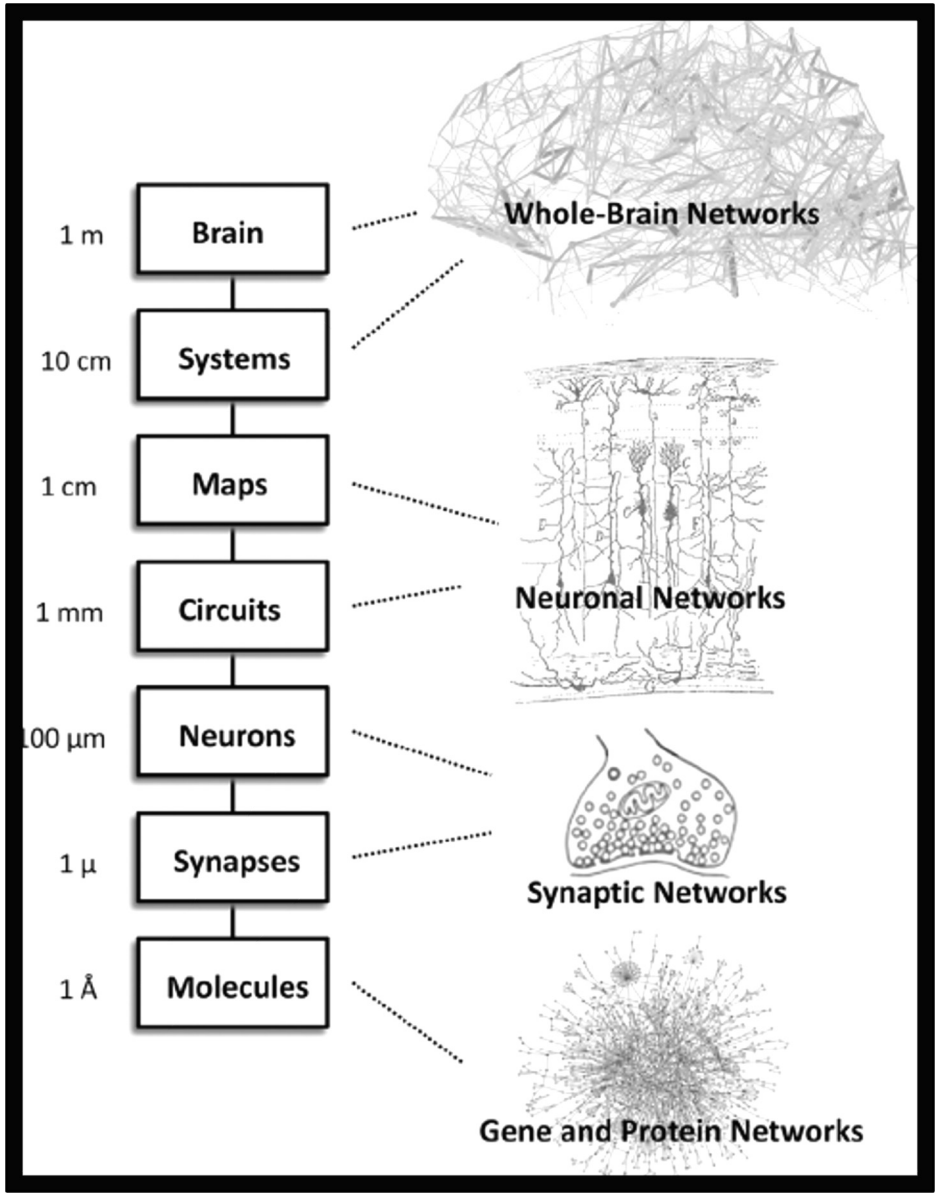

Functional Areas of the Brain[1]

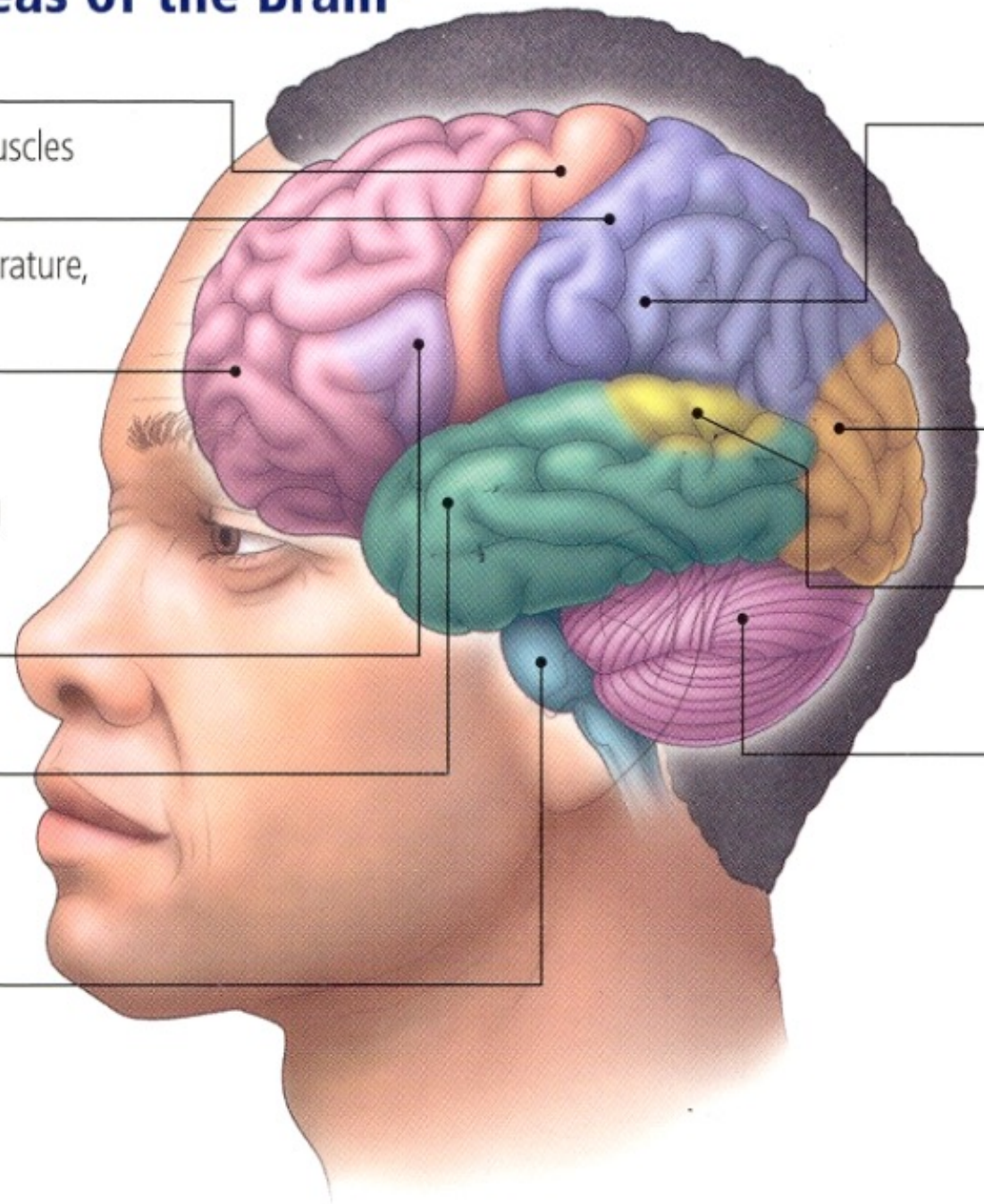

Motor Area
- control of voluntary muscles

Sensory Area
- skin sensations (temperature, pressure, pain)

Frontal Lobe
- movement
- problem solving
- concentrating, thinking
- behaviour, personality, mood

Broca's Area
- speech control

Temporal Lobe
- hearing
- language
- memory

Brain Stem
- consciousness
- breathing
- heart rate

Parietal Lobe
- sensations
- language
- perception
- body awareness
- attention

Occipital Lobe
- vision
- perception

Wernicke's Area
- language comprehension

Cerebellum
- posture
- balance
- coordination of movement

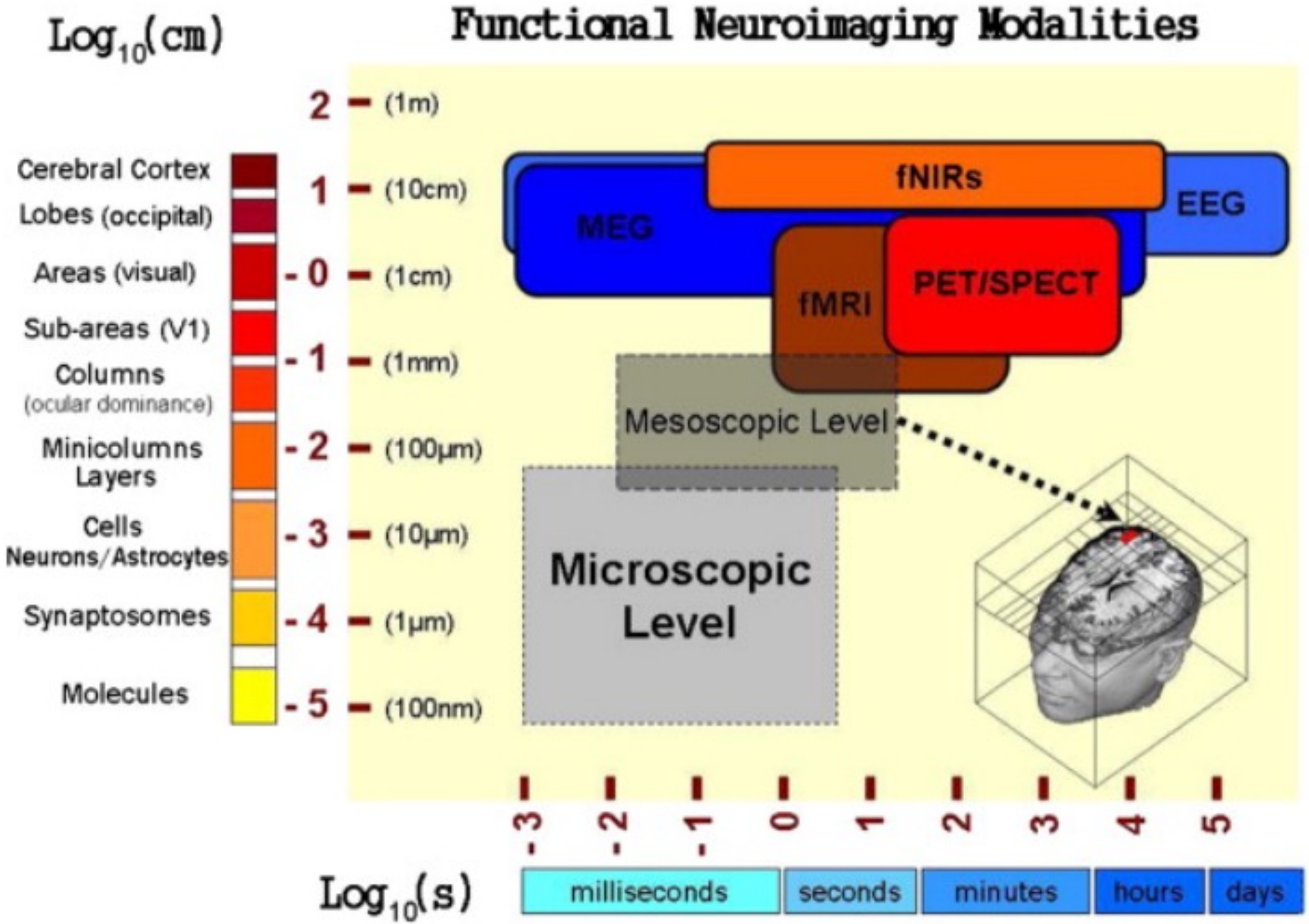

Uludag et al, NI, 2014

Most fMRI research has been towards understanding functional brain organizat

Spatial and Temporal Scales of Brain Function

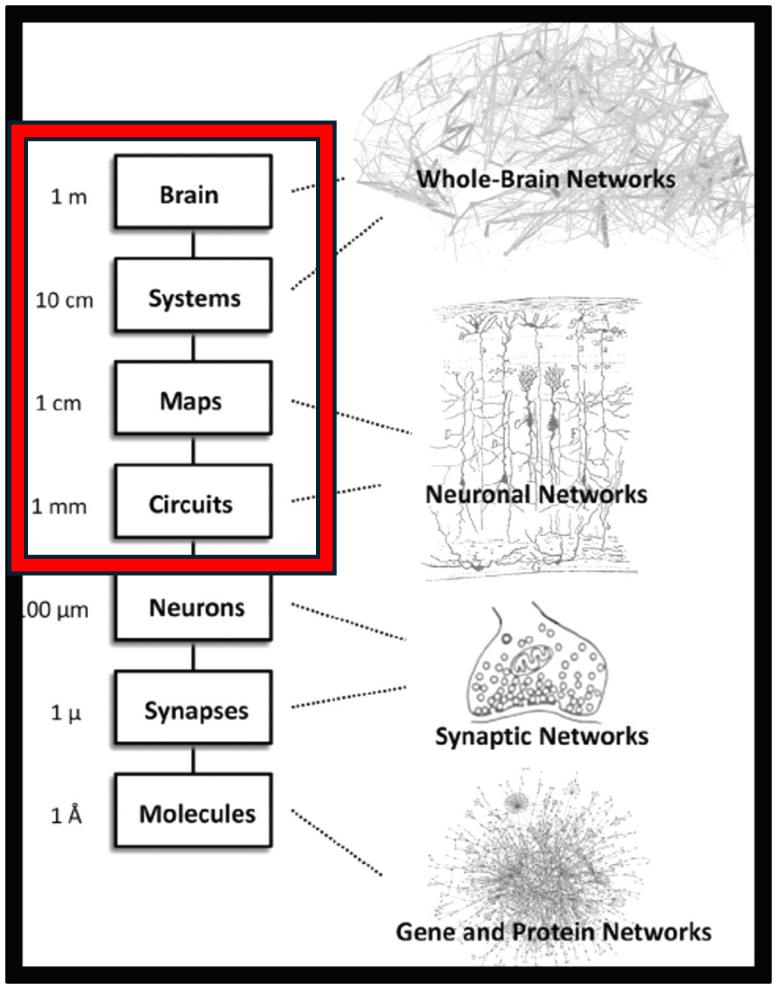

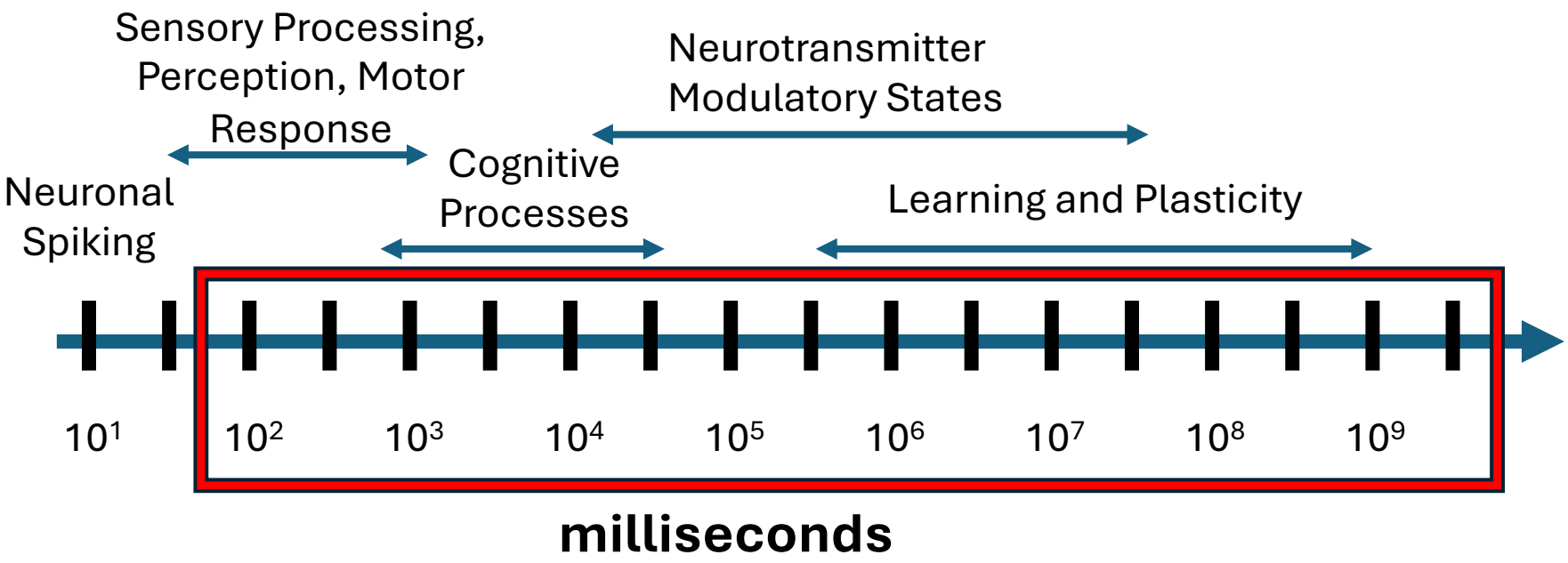

FMRI "Pillars"

- Capture neuronal activity, pattens, dynamics in time and space.
- Separate information from noise and artifact.
- Compare states, individual traits, and groups.

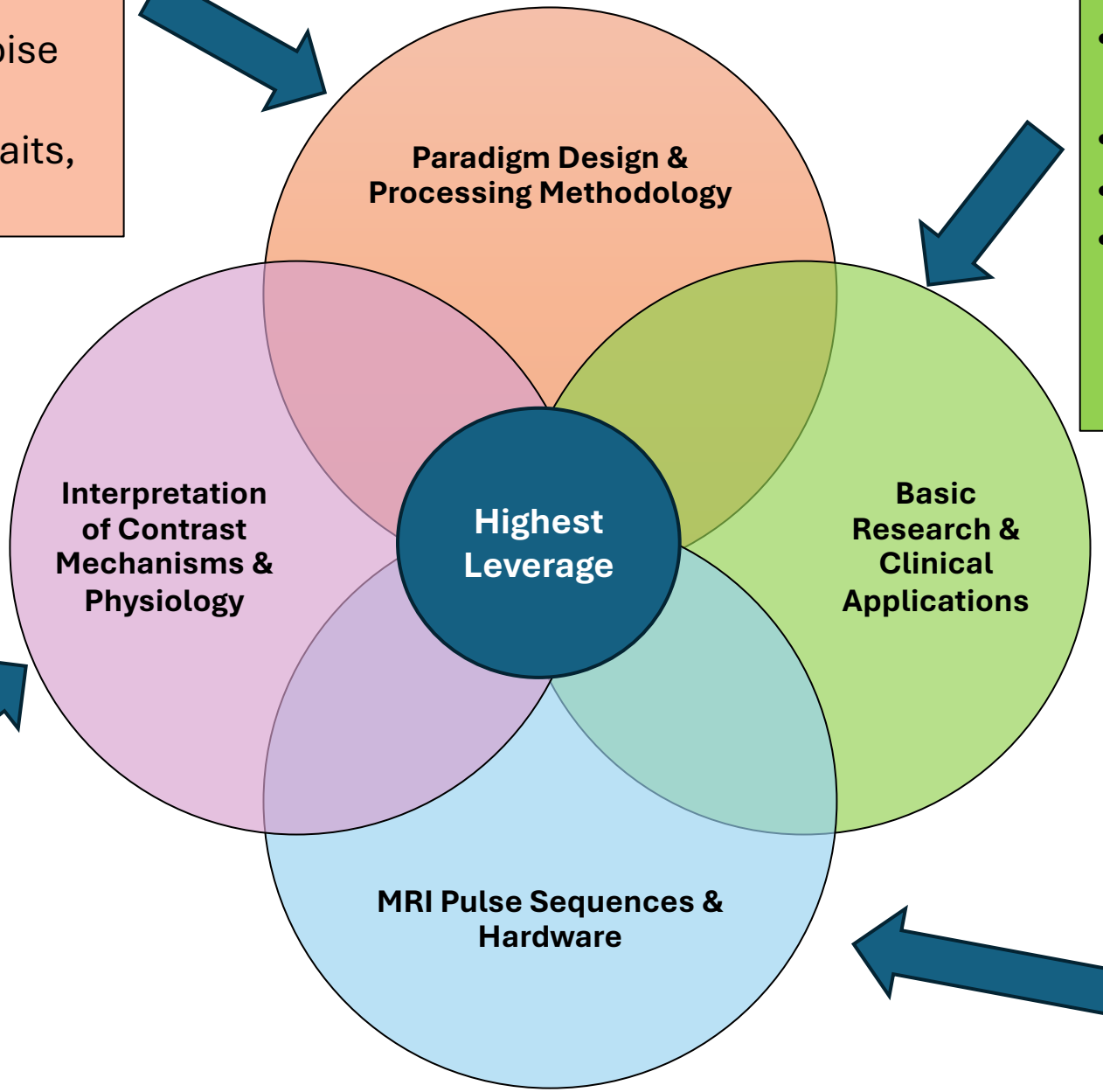

- Biomarker discovery and development
- Targets for neuromodulation
- Presurgical mapping
- Neurofeedback
- Uncover mechanisms and principles of functional brain organization.

- Identify relevant temporal and spatial structure.
- Multi-modal assessment: Relate signal to neuronal activity and non-neuronal measures.

- Speed
- Resolution
- Sensitivity
- Specificity
- Reproducibility
- Quantitation
- New Contrasts

1991 1996 2001 2006 2011 2016 2021 2026

Pulse Sequences and Hardware

- First BOLD & ASL
- EPI on most scanners
- 1.5T & 4T
- 3T
- 4 channel receive coils
- Multi-echo
- SENSE, GRAPPA
- Simultaneous EEG/fMRI
- First Commercial 3T
- 7T
- VASO
- 8 channel receive coils
- 32 channel receive coils
- Multi-echo available from vendors
- SMS or Multi-band for fMRI
- 64 channel receive coils
- 3D EPI more widespread
- VASO for layer fMRI
- FDA clearance for 7T
- pTX
- Local head gradient coil @7T "Next Gen"
- Simultaneous EEG/fMRI @7T

Interpretation, Contrast Mechanisms, and Physiology

- Location confirmation
- Resting state correlation
- Biophysical Models
- Parametric modulation
- Echo time dependence
- SE vs GE vs ASL comparisons
- BOLD relates to LFP
- CMRO2 from BOLD and ASL
- Mechanistic HRF models
- Slow QPPs found
- Gliovascular coupling
- Alpha/Beta negative correlation with BOLD
- Calcium flux coupled to BOLD
- Gamma positive correlation with BOLD

Paradigms and Processing

- Resting state correlation
- Block designs
- Event-related
- Event-related cognition
- Short/variable ISI Event-related
- "Topy" paradigms
- AFNI
- Brain Voyager
- Real-time fMRI
- FSL
- MVPA
- neurofeedback
- fMRI Adaptation
- Generative Reconstruction
- Brain Fingerprinting
- Represent. Simi. Analysis
- Human Connectome Project
- Parcellation atlases
- Open neuro
- Intersubject Correlation
- Open fMRI
- UK Biobank (5K)
- UK Biobank (100K)
- 1000 functional connectomes
- Dynamic Resting State
- Covert neurofeedback
- fMRI guided neuromodulation
- Dense Sampling

Controversies

- Brain or Vein?
- Initial dip
- Post undershoot origin
- White matter activation
- Dead Salmon
- Voodoo correlations
- Double dipping
- Global signal regression
- Diffusion changes w/activation.
- Retraction due to systematic motion
- Cluster failure
- Replication Crisis
- BWAS & >1000 subjects needed
- DIANA paper controversy
- Many analysis different results (NARPS)